Dissecting the roles of the Dectin-1R in the bladder innate defences

Andrejus Suchenko

Thesis submitted for the degree of Doctor of Philosophy

Institute for Cell and Molecular Biosciences

Newcastle University, UK

September 2018

Declaration

I certify that this thesis is my own work, except where stated, and has not been previously submitted for a degree or any other qualification at this university.

Andrejus Suchenko

2018

Abstract

Previous work using immortalised cells transfected with a NF-κB reporter and challenged with zymosan, to mimic a fungal infection, suggested possible co-operation between Dectin-1 and TLR5 receptors in urogenital tissues. These data were interesting as research describing Dectin-1R functioning relates specifically to myeloid derived cells and TLR5, classically, is known to function as a homodimer. The aim of the research reported in this thesis was therefore to focus on the Dectin-1 and TLR5 receptors in the bladder urothelium, with the objective of investigating Dectin-1 receptor functioning, Dectin1/TLR5 receptor co-operation and cell signalling events following a zymosan (β-glucan) challenge.

Western analyses of cell lysates from a bladder biopsy and immortalised RT4 bladder cells using a Dectin-1R antibody (R&D systems, AF1859) revealed the synthesis of proteins representing full-length and truncated (stalk-less) Dectin-1 receptors. These data supported the use of the immortalised RT4 cells in all subsequent analyses exploring Dectin-1R functioning in the urothelial tissues. Following challenge of the cells with the yeast cell wall extract zymosan (50ug/ml) increased synthesis of an array of host defence agents including hBD2, IL-8 and LCN2 were observed ($p<0.05$). Furthermore IL-8 effector synthesis was significantly reduced following *CLEC7A* (Dectin-1R) gene knockdown ($p<0.05$) and antibody blocking of the Dectin-1R ($p<0.01$). These data supported synthesis of the Dectin-1R in urothelial cells and a role in defending the bladder against a fungal challenge.

Knocking-down the *TLR5* gene in RT4 cells (80% knockdown) and challenging the cells with zymosan, resulted in a significant reduction in hBD2, IL8 and LCN2 synthesis ($p<0.05$). These data suggested co-operation between the Dectin-1 and TLR5 receptors in bladder cells, which was supported by immunostaining and a proximity ligation assay approach. In addition these analyses supported clustering of the Dectin-1 and TLR5 receptors following activation.

Experiments to explore roles for the encoded Dectin-1 receptor isoforms, 1, 2 and 4, in the TLR5 co-operation events involved engineering a suite of stable cell lines each over-expressing a Dectin-1 receptor isoform and either a TLR5 full-length or TLR5 truncated receptor. This approach exploited the pVitro2-neo-mcs vector, which is able to co-express two cDNA sequences simultaneously. However, the resultant cell lines did not over-express the Dectin-1 and TLR5 receptors. It was hypothesised that the increased number of receptors synthesised by the cells over-loaded the urothelial cell membranes causing gene silencing and/or cell death.

The signalling mechanisms activating the transcription of host effector genes following a zymosan challenge of RT4 bladder cells were explored using western analyses and an antibody to Syk-P (Cell Signalling, C87C1), *SYK* gene knockdown and piceatannol (100 ug/ml) a Syk inhibitor followed by ELISA to measure LCN2 and IL-8 media concentrations. No phosphorylation of Syk was observed and the knock-down/inhibition approaches had no significant effects on the media concentrations of either IL-8 or LCN2. However, knockdown of the *RAF1* gene resulted in decreased secretion of the host defence molecules LCN2 and IL-8 ($p<0.01$). Additionally western blot analyses showed phosphorylation and degradation of the NF-κB inhibitor IκBα. These data suggested that Dectin-1R activation in response to zymosan in bladder cells involved Raf-1 signalling, which supported a non-canonical signalling pathway.

In summary, Dectin-1 receptors were shown to be synthesized in RT4 bladder epithelial cells and were activated in response to zymosan (fungal) challenge resulting in the production of host defence effector molecules. Data showed potential co-operation between Dectin-1 and TLR5 receptors in mediating the bladder cell response. Dectin-1R signalling in urothelial cells was also orchestrated via a non-canonical signalling pathway involving Raf-1. These data support a novel host defence mechanism, involving Dectin-1 and TLR5 receptors functioning co-operatively, to defend urothelial from fungal infections.

Acknowledgements

I would like to thank my excellent supervisor Dr Judith Hall for guidance, enormous help and great advice during this project. I would also like to thank my co-supervisor the late Prof Robert Pickard who passed away in July 2018. He was an inspiration and gave great advice during my PhD. Additionally I would like to acknowledge the Dr William Edmund Harker Foundation for the studentship that financed my PhD and allowed me to study within ICAMB. I would also like to thank members of the research group, Dr Catherine Mowbray for her great advice, invaluable help and friendliness, Dr Sherko Subhat for all his help at the beginning of my research and colleagues Dr Anthony Moore and Dr Anna Stanton. I would like to thank Dr Git Chung for his advice, support and friendship during this entire project.

A big thank you to my parents Vladislav and Sigita for their love and support, my brother Valentin and sister Anna for friendship and great time we have together.

Especial thank you goes to my loving wife Aleksandra for all her support and encouragement, and for being my best friend.

Abbreviations

3'UTR	3 prime untranslated region
APC	Antigen presenting cells
B-cells	Bone marrow derived cells
BLAST	Basic Local Alignment Search Tool
bp	Base pair
BSA	Bovine serum albumin
cDNA	Complementary DNA
CLEC7A	C-type lectin 7a (Dectin-1)
CLR	C-type lectin receptors
Cq	Quantitation cycle used to quantitate gene expression
CRD	Carbohydrate recognition domain
CXCL	Chemokine (C-X-C motif) ligand
DEFB4	hβD-2 gene
DH5α	*E. coli* strain used for transformation
DMSO	Dimethyl sulfoxide
DNA	Deoxyribonucleic acid
DNase	Enzyme used to digest genomic DNA
dNTPs	Deoxyribonucleotide
dsRNA	Double stranded RNA
E. coli	*Escherichia coli*
EDTA	Ethylenediaminetetraacetic acid
ELISA	Enzyme-Linked ImmunoSorbent Assay
FCS	Fetal calf serum
FimH	Fimbriae H
GFP	Green fluorescent protein
HEPES	*4-(2-hydroxyethyl)-1-piperazineethanesulfonic acid*
hβD	Human β-defensin
IgG	Immunoglobulin G
IkB	Inhibitor of kappa light polypeptide gene enhancer in B-cells Interleukin
IkBα	nuclear factor of kappa light polypeptide gene enhancer in B-cells inhibitor, alpha

IL	Interleukin
IRAK	Interleukin-1 receptor-associated kinase
kbp	1000 base pairs
kDa	1000 Dalton
LL-37	Cathelicidin (mature peptide)
LPS	Lipopolysaccharide
mRNA	Messenger RNA
MyD88	Myeloid differentiation primary response gene 88
NF-κB	Nuclear factor kappa B
NK-cells	Natural killer cells
Opti-MEM	Medium used for transfection
p	Probability
PAMP	Pathogen associated molecular patterns
PBS	Phosphate buffered saline
PCR	Polymerase chain reaction
PFA	Paraformaldehyde
PI	Propidium Iodide
PLA	Proximity ligation assay
PRR	Pattern recognition receptors
Raf-1	Proto-Oncogene, Serine/Threonine Kinase
RNA	Ribonucleic acid
RNase	Enzyme used to digest RNA
RT-qPCR	Reverse transcription quantitative real time PCR
RT4	Bladder uroepithelium cell line
scr	scrambled siRNA
SDS	Sodium dodecyl sulfate
SDS-gel	Sodium dodecyl sulfate containing gel for protein separation
SNP	Single-nucleotide polymorphism
SYK	Spleen tyrosine kinase
T-cells	Thymus cells
TIR	toll-interleukin 1 receptor

TIRAP	Toll-interleukin 1 receptor (TIR) domain containing adaptor
TLR	Toll-like receptor
TNF-α	Tumour necrosis factor alpha
UPEC	Uropathogenic *Escherichia coli*
UT	Urinary Tract
UTI	Urinary Tract Infection
VK-2	Immortilized vaginal epithelium cell line

CONTENTS

I. Figures

II. Tables

Chapter 1. Introduction

The urinary tract comprises the kidneys and ureters (upper urinary tract) and bladder and urethra (lower urinary tract) and its key function is to remove metabolites and toxic waste products from the body, which it does through urine [1]. Urine is produced in the kidneys, of which nephrons are the key functional units, and on entering the ureters is devoid of essential metabolites including glucose and amino acids, but high in organic waste materials including urea, creatinine and uric acid.

Ureters are tubes, 20-30 cm in length, comprising smooth muscle material lined by a specialised layer of epithelial cells called the urothelium. The function of the ureters is to act as a conduit that allows the continuous removal of urine from its site of production, the kidney, to the bladder. A typical human bladder, which is tetrahedral in shape when empty but ovoid on filling can hold 300 – 500 ml of urine so it acts as a collecting vessel storing urine, until its expulsion from the body. The periodic release of urine or flushing of urine from the bladder plays a key role in protecting the urinary tract from microbial infection. This is particularly important as the opening of the urinary tract to the exterior of the body is sited close to the anus, which means the urinary tract is constantly challenged by significant populations of gut and skin microbes.

The urinary tract from ureters to urethra is lined by a specialised epithelium called the urothelium, although there is data to suggest differences between the urothelia lining the ureters and the bladder [1]. In fact results of tissue culture analyses support the ureteral urothelium to contain reduced amounts of cell surface proteins called uroplakins and apically located membrane vesicles, called fusiform vesicles, compared to bladder [2, 3]. This difference most likely relates to the embryological origin of these tissues with the ureteral urothelium being derived from mesoderm and the bladder, and urethra urothelia being derived from the endoderm [4, 5].

Studies involving electron microscopy and immune-histochemical analyses indicate the urothelium to be composed of distinct layers including basal, intermediate and superficial/umbrella layers (Figure 1.1). It is a slow cycling

epithelium with turnover rates of up to 200 days, which probably relates to its functioning as a highly efficient permeability barrier that protects the body against any toxic materials in urine [6]. A trans-epithelial resistance of up to 75,000 Ω/cm^2 has been reported making it a more efficient barrier than skin epidermis [6]. Although the turnover rate of the urothelium is slow it is quick to regenerate when damaged. For example following the loss of umbrella cells due to infection and/or senescence the underlying intermediate cells differentiate into umbrella cells a process, which is also accompanied by tight-junction formation [7].

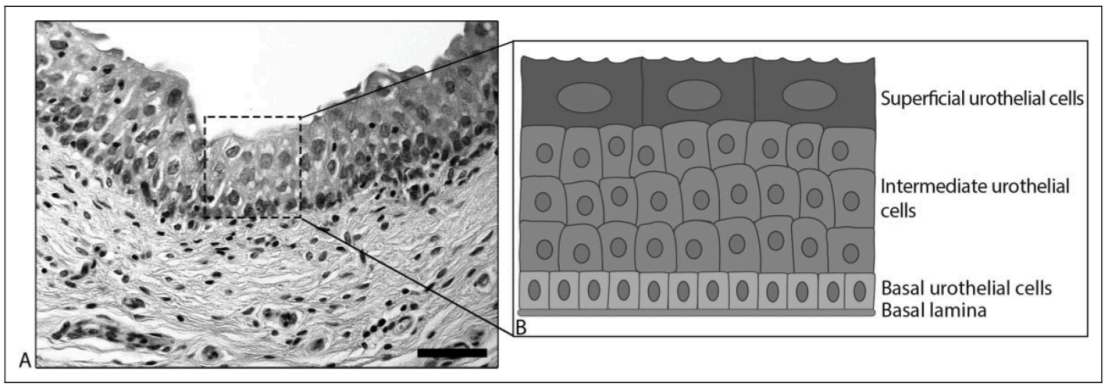

Figure 1.1 Structure of urinary bladder.
Urinary bladder is composed of basal urothelial cell, intermediate urothelial cells and superficial urothelial cells [8].

The urothelium also needs flexibility so it can increase and decrease its surface area during the micturition cycle. Flexibility is achieved through the presence of urothelial plaques, which are concave structures that cover approximately 90% of the urothelial apical surface (Figure 1.2) and are present in fusiform vesicles in the cytoplasm of superficial umbrella cells. The plaques themselves are composed of four uroplakin building blocks comprising uroplakin 1a (27kDa), uroplakin 1b (28kDa), uroplakin II (15kDa) and uroplakin IIIa (47kDa). Ion exchange chromatography and transfection studies suggest these proteins to form two heterodimers, UPIa/II and UPIb/IIIa [9]. The importance of these heterodimers in the urothelium has been shown through mice transgenic studies where UPII or UPIIIa gene knock-outs were associated with the loss of urothelial

plaques [10]. In addition their roles in permeability were confirmed by Ussing chamber experiments that revealed urothelia taken from knock-out mice showed increased permeability to ^{14}C-urea and ^{3}H water [6].

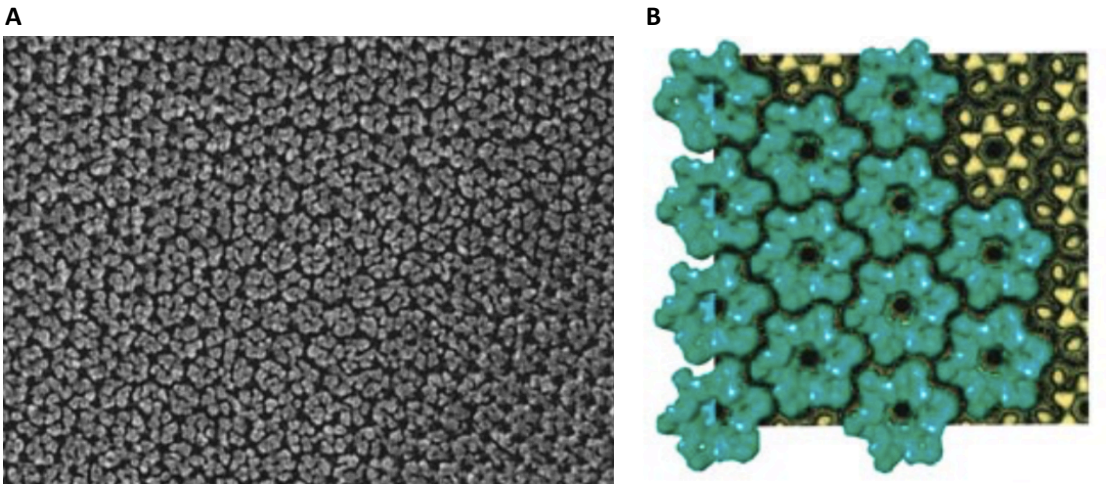

Figure 1.2 Urothelial plaques.
A: Electron microscopy image of bladder showing urothelial surface; B: reconstruction of urothelial plaque. Taken from [11].

It is also known that a glycosaminoglycan (GAG) layer lines the luminal surface of the urinary tract. GAGs are polysaccharide molecules that contain repeating disaccharide units and are reported to function in creating an impermeable barrier to charged and uncharged molecules present in urine, and inhibiting bacterial attachment [12, 13]. There are four families of GAGs including the chondroitin and dermatan sulphate family, heparin and heparan sulphate family, the keratan sulphate family and hyaluronate. The presence of sulphur is associated with anti-proliferative effects suggesting that the presence of sulphated GAGs in urothelia helps maintain a quiescent cell phenotype [14]. Interestingly, GAG instillations have been found to be linked to fewer episodes of urinary tract infections in women and longer periods between infections [15].

1.1 Urinary microbiome

Historically the urinary tract was considered to be sterile in healthy individuals. However, the use of molecular techniques including 16S RNA sequencing have revealed the urinary tract to be colonised and carry a *natural* microbiota. Microbes identified in healthy men and women include *Lactobacillus spp*, *Streptococcus* spp, *Prevotella* spp, *Sneathia* spp, *Mycoplasmas*, *Ureaplasmas*, and *Gardnerella* spp [16, 17]. As expected a change in diversity of microbiota can correlate with some diseases [18] with key example being the loss of *Lactobacilli* during the menopause associated with increased infections of the urinary tract by *Escherichia coli* [19], although more recent work has challenged this relationship [20]. While, lately, significant research has focussed on the gut microbiota and its roles in health and disease there is in comparison little work exploring the role(s) of the microbiota in the urinary tract. It is possible to speculate however, that the urinary microbiome functions similarly to the gut microbiota including priming the innate immune system and creating a barrier to potential pathogenic microbes from the faeces contaminating the urethra and ascending the urinary tract.

Initial characterisations of the human mycobiome have utilised culture based systems mainly to identify pathogenic species including *Candida albicans*, *Aspergillus fumigatus* and *Coccidiodes* spp. Again however, new non-culture-based techniques including next generation sequencing are being used to identify fungal species or the mycobiome colonising the urinary tract [21]. To date, a significant diversity of fungi including *Dothideomycetes*, *Eurotiomycetes*, *Saccharomycetes,* which includes *Candida* spp, and *Orbiliomycetes* (actually 16 classes relating to 12 women with no reported urinary issues were recorded) has been revealed in clean–catch mid-stream urine samples, of which no one taxa showed dominance.

1.2 Urinary tract infections

As stated a diverse variety of microorganisms can colonise the urinary tract and many do so without causing infection. However, infections of the urinary tract are common with statistics indicating that 25 to 50 % of women will suffer an urinary tract infection at least once in their lifetime [22]. Female susceptibility is linked primarily to the female anatomy and shortness of the urethra, which is 4-5 cm in women compared to approximately 20 cm in males [23]. Additionally 20 to 50 % of women reporting an UTI will develop recurrent UTI (rUTI), which is characterized as three or more infections in 12 months or two infections in six months [24]. UTIs in men and children are observed, but these are much less prevalent at 0.1 % and up to 6.4 % respectively. These infections are often a consequence of some anatomical disorder of the urinary tract [22] and as such are described as complicated UTIs.

In the majority of uncomplicated UTI cases the predominant infecting microbe is *Escherichia coli,* which originates from the gastro-intestinal tract and contaminates the urinary tract (UT) via the faecal material. In the urinary tract it is known as uropathogenic *E. coli* (UPEC).

Figure 1.3 demonstrates the mechanism by which *E. coli* infects the urinary tract. Essentially *E. coli* (UPEC) from the anus colonise the urethra and infect the bladder resulting in cystitis [25]. These bacteria can, in certain individuals, also migrate through ureters to the kidney where they cause pyelonephritis and blood sepsis, which can result in death [26].

UPEC are generally flagellated and work in mice has shown that flagella are key virulence factors that allow the bacteria to ascend and infect the urinary tract [27]. UPEC also use surface adhesins, called FimH proteins, to interact with uroplakins UPIa/Ib on the urothelium, which prevents them from being flushed out during micturition. Murine studies have suggested UPEC can actually invade the urothelial cells and form intracellular bacterial communities (IBC). These IBC contain metabolically-active bacteria that are either able to infect adjacent cells or form non-replicating quiescent intracellular reservoirs (IQR) [6]. It is proposed that in response to a stimulus, potentially weeks or months after the

initial infection and probably involving cell turnover these bacterial reservoirs emerge to start a new acute infection. Interestingly although the IBC/QIR model has been demonstrated in multiple mouse backgrounds there is limited evidence to support its functioning in humans [28-30].

E. coli accounts for up to 80% of non-complicated UTIs [22]. Other common species of bacteria linked to UTIs are *Enterococcus faecalis*, *Klebsiella pneumonia* and *Proteus mirabilis* [31], although many of these infections are classed as complicated and involve catheters or a pathology such as diabetes.

Antibiotic treatment is the most common method to treat UTIs. However, the constant use of antibiotics is known to promote antimicrobial resistance. This is supported by data that shows 35 to 75 % of uropathogenic *E. coli* strains are resistant to the antibiotic trimethoprim, which is commonly used to treat UTIs [32-34]. In the UK and Europe antibiotic stewardship and reduction of antibiotic prescriptions are key political targets [35]. This means there is a desperate need to further understand the defences of the urinary tract to help develop new therapies to either replace or work alongside antibiotics in the treatment of UTIs.

Candida albicans is the most common cause of fungal infections of the uro-genital tract [36], and, interestingly is often associated with long-term antibiotic therapies. This yeast often exists in the uro-genital tract as a commensal, but can become a pathogen especially in immunocompromised individuals [37]. In fact a one day surveillance in 228 hospitals from 29 European countries indicated that 9.4% of UTIs were caused by a *Candida* fungal infection [38]. However, these cases mainly included a mix of immunocompromised, diabetes and renal transplant patients, neonates, the elderly, those in burn and intensive care units as well as those on long-term antibiotic therapies.

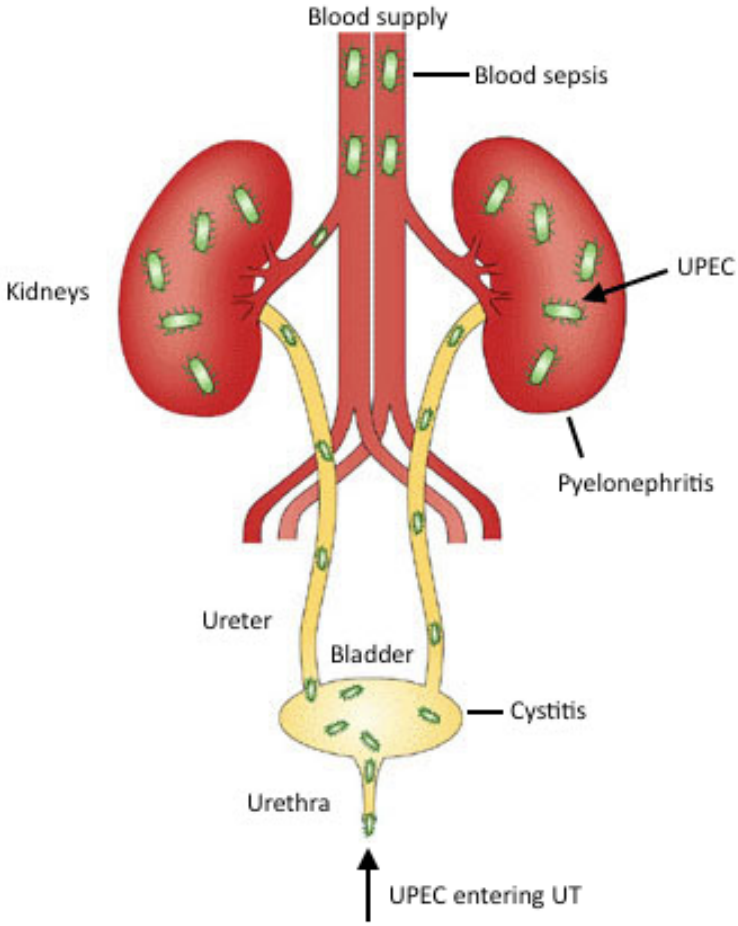

Figure 1.3 Anatomy of the urinary tract and sites of infection.
Diagram adapted from Kaper et al. (2004) [39].

1.3 The innate defences of the Urinary Tract

Protection of the urinary tract is through innate defence mechanisms. These include the flushing action of urine and the constitutive and regulated synthesis of host defence peptides and proteins including β-defensin-1 (HBD1), β-defensin-2, lipocalin 2 (LCN2), RNase 7, cathelicidin and Tamm-Horsfall protein, all of which function to limit bacterial growth [40, 41]. In addition urothelial detection of potential pathogens also triggers the secretion of cytokines and chemokines, including IL-8, which is associated with the migration of macrophages and neutrophils to the infected site [42, 43], and which function to facilitate bacterial clearance [44, 45].

1.4 Defensins

Beta-defensins are a family of hydrophobic, cationic host peptides (3 to 5 kDa in size) that function by forming pores in prokaryote membranes that causes cell lysis. Their effectiveness as killing agents relates specifically to their charge and hydrophobicity, which allows them to target and kill gram-negative and gram-positive bacteria, fungi as well as enveloped viruses [46-49]. Their positive charge reflects a high number of arginine and lysine amino acids, which interact, through electrostatic interactions, with the negatively charged membranes of bacteria. Their hydrophobicity then allows the peptides to insert into the bacterial membranes creating pores that result in bacterial killing [50, 51]. However, membrane disruption is not the only role of defensins; it has been shown that defensins can kill fungi by promoting ROS production and apoptosis [49].

The defensin family of peptides are characterised by six conserved cysteine residues, which form three di-sulfide bridges. The family in humans includes α-defensins and β-defensins, which differ in their di-sulfide (C-C) bridges [52]. Alpha-defensins are characterised by C1-C6, C2-C5 and C3-C4 bridges while β-defensins are characterised by C1-C5, C2-C6 and C3-C4 bridges (Figure 1.4). It is known that the urothelium synthesises human β-defensins 1, 2 and 3 [41, 53], with data from clinical and *in-vitro* studies identifying human β-defensin-2 (hBD-2), which is induced in response to infection, as a key antimicrobial factor in the protection of the urogenital tract [54, 55].

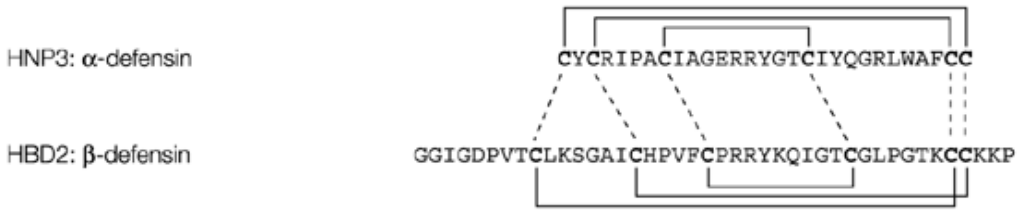

Figure 1.4 Di-sulfide bridges in α-defensin and β-defensin peptides.
Di-sulfide bonds are showed as solid lines. Diagram adapted from Ganz et al. (2003) [56].

1.5 Other antimicrobial molecules in the urinary tract

Another key molecule protecting the urinary tract is lipocalin 2 (LCN2) also known as NGAL. This molecule limits bacterial growth by sequestering iron [57], which is a key microbial growth factor. Microbes sequester iron through synthesis of siderophores [58] and LCN2 synthesised by the host binds to bacterial siderophores preventing iron uptake and limiting bacterial infection. A specific role for LCN2 in protecting against fungal infections has, to date, not been investigated extensively. However, upregulation of LCN2 has been demonstrated following *Candida* infection [59].

Cathelicidin is a linear antibacterial peptide secreted by epithelial cells. It is encoded by the *CAMP* gene as a pro-peptide also known as pro-LL-37. Once secreted it is cleaved into cathelin and LL-37, both of which have antimicrobial and antifungal properties [60-62]. Like the defensins cathelicidin prevents bacterial and fungal infection by pore formation [63] although it has also been shown to function by inhibiting bacterial division [64]. More recently cathelicidin has been described as a potent immunomodulatory agent, including functioning to amplify TLR9 and TLR3 activation [65]. Although suggested to be a significant protector of the urinary tract from bacterial infection [66] laboratory investigations using RT4 bladder cells have failed to identify expression of the *CAMP* gene (unpublished data).

RNases are another family of cationic molecules, functioning to defend the urinary tract from infection and one member RNase 7 is synthesised by the urothelium [67]. As with other cationic molecules RNase 7 is proposed to kill bacteria through targeting and disrupting their microbial membrane [68, 69].

Tamm-Horsfall protein or uromodulin is an abundant glycoprotein found in urine and also a key defender of the urinary tract. While Tamm-Horsfall proteins are found in urine, they result from the expression of the *UMOD* gene and protein synthesis in the kidney tissues. They are known to function by preventing bacterial adhesion to uroplakin receptors Ia and Ib on urothelial cells [70].

1.6 Pathogen recognition receptors

Secretion of host defence peptides and proteins in the urinary tract is stimulated through the activation of pathogen recognition receptors (PRRs) including Toll-like receptors (TLRs) and C-type lectin receptors [71, 72]. PRRs are part of the host innate defences and recognise components of microbes called pathogen-associated molecular patterns (PAMPs). These PPRs are expressed by epithelial cells as well as antigen presenting cells, including dendritic cells, monocytes, macrophages and neutrophils, involved in the innate response [71, 73].

1.7 Toll-like receptors

In humans ten functional Toll-like receptors (TLRs) have been identified to date [74] although in mice this number is 13 with TLRs 11, 12 and 13 unique to the mouse [75]. TLRs are located on the plasma membrane and in the cytoplasm of epithelial and antigen presenting cells, and function to detect potential pathogens and activate a host response. Receptor recognition and binding of different bacterial, viral and fungal molecules or PAMPS including lipopolysaccharides, flagellin, nucleic acids and peptidoglycans activates signalling pathways resulting in the expression of genes encoding an array of host defence molecules including antimicrobial peptides such as the β-defensins and pro-inflammatory proteins such as IL-8 [75].

Table 1.1 lists the 13 TLRs and the microbial components recognised by each. Toll-like receptors assemble into homo- or heterodimers to bind ligands and initiate signalling cascades that result in the host response. It has been shown that while TLR-1, TLR-2, TLR4 and TLR-6 operate as heterodimers [76, 77], TLR-5 functions only as a homodimer [78, 79].

Table 1.1 Toll-like receptors and their ligands.

Receptor	Localisation	Ligand
TLR-1	Plasma membrane	Lipoproteins and peptidoglycans
TLR-2	Plasma membrane	Peptidoglycans
TLR-3	Endosome	Double-stranded RNA
TLR-4	Plasma membrane	Lipopolysaccharides
TLR-5	Plasma membrane	Flagellin
TLR-6	Plasma membrane	Diacyl lipoprotein
TLR-7	Endosome	Single-stranded RNA
TLR-8	Endosome	Single-stranded RNA
TLR-9	Endosome	Double-stranded DNA
TLR-10	Plasma membrane	Unknown
TLR-11	Endosome	Flagellin and profilin
TLR-12	Endosome	Profilin
TLR-13	Endosome	Ribosomal RNA

The TLRs 1 and 2, and TLRs 4 - 6 signal via the intracellular MyD88 protein (Figure 1.5). TLR5, TLR2/TLR1 and TLR2/TLR6 bind MyD88 directly following their activation, while TLR4 induces signalling through the adaptor molecule TIRAP. Activated MyD88 promotes complex formation, which involves the IRAK4 (Interleukin-1 receptor-associated kinase 4), IRAK1 and IRAK2 proteins. A consequence of the signalling cascade is the phosphorylation and degradation of IκB, and the release of NF-κB, which translocates to the nucleus and induces the expression of genes encoding cytokines, chemokines and host defence peptide molecules.

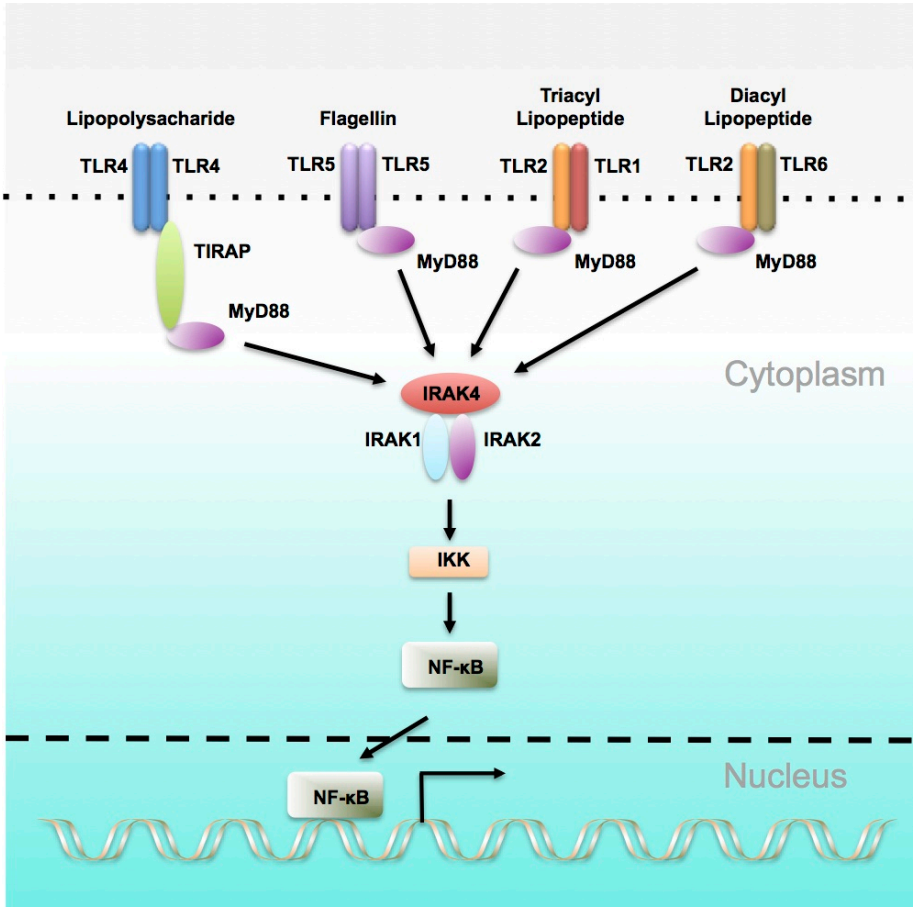

Figure 1.5 Toll-like receptor signalling pathways.
Stimulated Toll-like receptors initiate a signalling cascade involving MyD88 protein, IRAK and NF-κB activation.

Using a murine model, including TLR4$^{-/-}$ mice, TLR4 has been reported as a key protein in defending the bladder from uropathogenic *E. coli* infections [80-82]. However, *in vitro* data has demonstrated that in the human, TLR5 and not TLR4 receptors function to protect tissues of the lower urinary tract from infection [83, 84]. As [84][84][84][84][83][82][81]TLR5 receptors recognise flagellin proteins, which are the major components of the flagella that facilitate uropathogenic *E.coli* motility, this detection system allows the host urothelial tissues to quickly orchestrate a defence response (Figure 1.6A). Importantly the TLR5 polymorphism TLR5_C1174T, carried by 10 % of population, results in the synthesis of a truncated TLR5 protein lacking its cytoplasmic signalling apparatus [40, 85] (Figure 1.6B) and carriers of this polymorphism are more susceptible to recurrent urinary tract infections [40, 86]. *In vitro*, *in vivo* and clinical data from our laboratory have also shown that this polymorphism is

linked to a reduction in the production of HBD2, which illustrates that the reduced signalling significantly impacts host defence mechanisms [40].

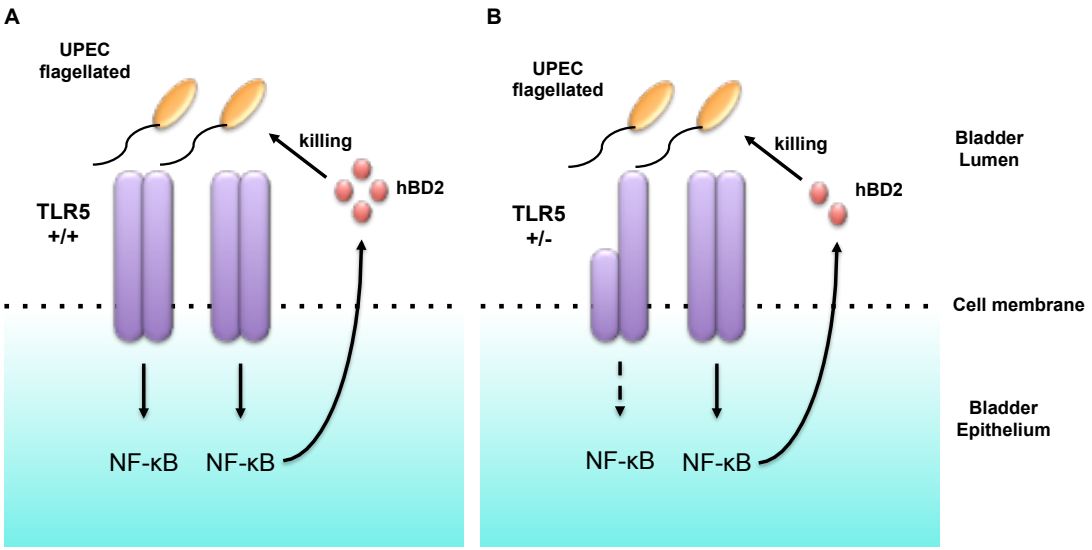

Figure 1.6 Normal and defective TLR5 signalling.
Flagellated bacteria activate TLR5, which results in HDP production including hBD2 synthesis (A). Polymorphism TLR5_C1174T leads to reduced signalling and reduced innate defences (B).

Essentially individuals carrying the TLR5_C1174T polymorphism are unable to clear UTIs efficiently and suffer from recurrent UTIs. These patients are prescribed prophylactic antibiotic treatments to help clear the infections, but because of their genetic defect the treatment does not cure the problem and contributes to the development of antibiotic resistant bacterial strains. One idea to help address this problem is to develop therapies that boost their urogenital innate immune defences and therefore reduce the number of infections and their use of antibiotics.

1.8 C-type Lectin Receptors

C-type lectin receptors are another group of membrane bound receptors that recognise pathogen-associated molecular patterns (PAMPs) and whose activation results in a host response. These receptors, namely Dectin-1, Dectin-2,

Mincle and DC-SIGN (Figure 1.7), each have a carbohydrate-recognition domain (CRD) and play important roles in antifungal immunity [87].

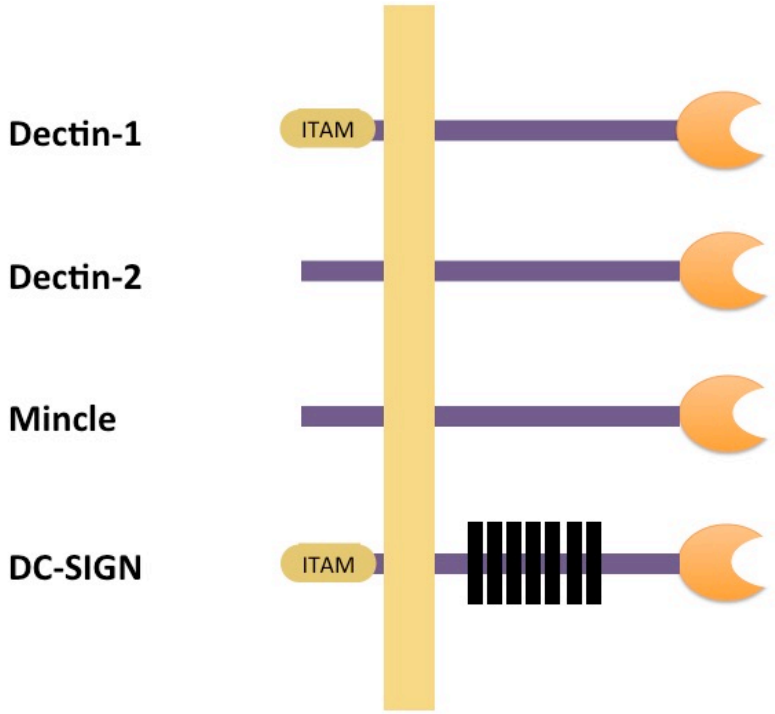

Figure 1.7 Family of C-type lectin receptors.
Taken from [88]. Orange: Carbohydrate binding domain; Purple: stalk region; Black: neck region; ITAM and Y are intracellular signalling domains.

The Dectin-1R recognises β-1,3-glucans, which are synthesised as part of the fungal cell wall (Figure 1.8A & B). The receptor is synthesised and known to function in myeloid derived cells including monocytes, macrophages and dendritic cells [87], and there are reports of Dectin-1 receptors in epithelial cells of the lung, cornea and intestine [89-91]. Interestingly previous work in our laboratory suggested that the Dectin-1R is also synthesised in bladder (RT4) and vaginal (VK2 E6/7) cells [83]. Moreover, data from studies in which vaginal VK2 E6/7 cells were challenged with zymosan, representing the 1-3 β-glucan component of the fungal cell wall, supported *DEFβ4* expression and hBD2 synthesis [83].

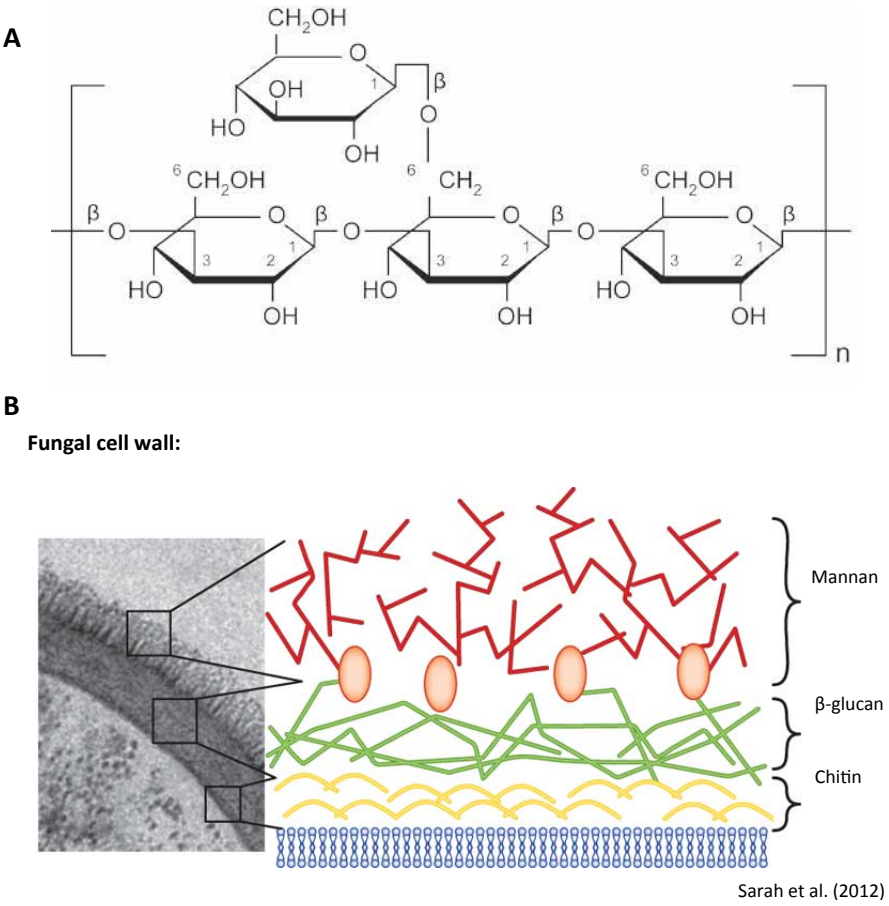

Figure 1.8 β-glucans as components of the fungal cell wall.
A: (1,3)-β-D-glucan B: Fungal cell wall components. Taken from [87].

The Dectin-2 receptor is also found in myeloid derived cells, namely monocytes and macrophages, and recognises mannose-capped structures. It does not appear to have an unique signalling motif (Figure 1.7), but associates with the Fc receptor γ subunit, which has an ITAM signalling motif [92]. Similarly the Mincle receptor, synthesised in macrophages, dendritic cells, neutrophils and B cells, and which recognises glycolipids also associates with the Fc receptor γ subunit [93].

The fourth member of the group, the DC-SIGN receptor, binds carbohydrates containing mannose sugar units and is commonly found in dendritic cells and macrophages. Its known functions include intercellular adhesion, antigen uptake and signalling [94], and it has also been shown to modulate the immune response of Toll-like receptors TLR3, TLR4 and TLR5 [95]. It binds ligands through a

carbohydrate recognition domain (CRD) [94] and its intracellular domain exhibits a YXXF signalling motif [96].

1.9 Structure of the Dectin-1 Receptor

The Dectin-1R is a Type II transmembrane receptor, with the extracellular region composed of a C-type lectin-like (CTLD) domain and a stalk region, although some isoforms synthesised lack this stalk region. The intracellular components include ITAM-like and DED domains (Figure 1.9) [97]. The ITAM-like domain has only one tyrosine (Y) residue, while the classical ITAM domain found in the Fc receptor γ subunit has two tyrosine (Y) residues, which are both required to activate signalling. DED is a tri-acidic domain, which can participate in intracellular signalling independently of the ITAM-like domain. Ligand binding to the Dectin-1R promotes receptor dimerisation, phosphorylation of the tyrosine residues and activation of an intracellular signalling cascade.

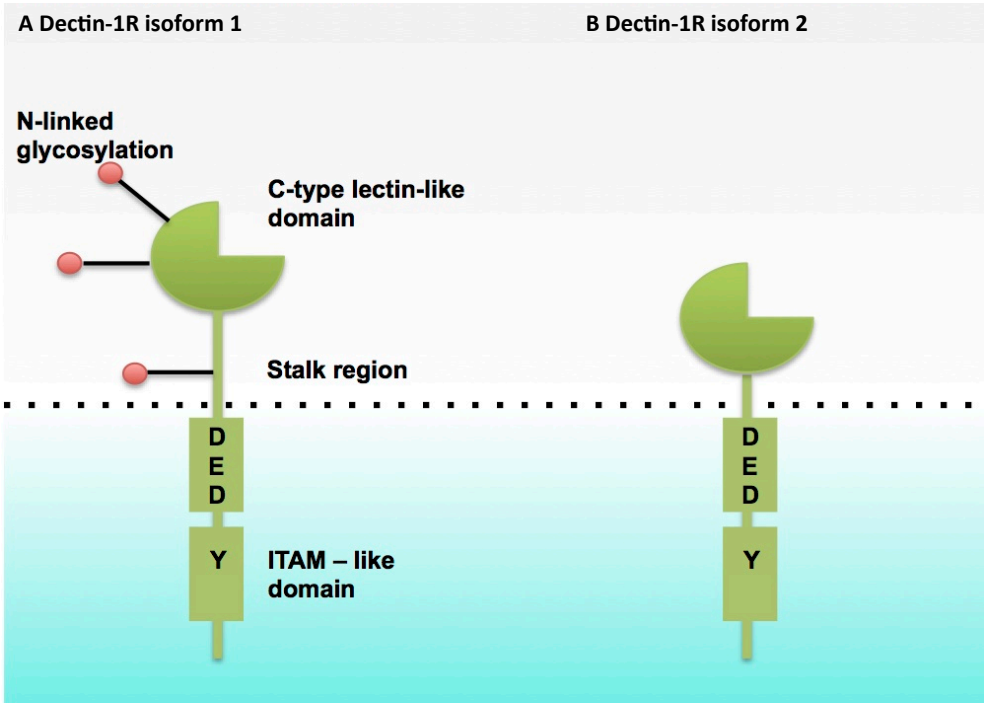

Figure 1.9 Structure of Dectin-1 receptor.
Full-length Dectin-1R (A) and truncated Dectin-1R (B).

The gene encoding the Dectin-1 receptor is *CLEC7A*, which has six exons and is transcribed as eight different mRNA isoforms (Figure 1.10). The main variants synthesised in humans are a full-length isoform 1 and a short isoform 2 that lacks a stalk region [98-100]. Mice macrophages have similarly been shown to synthesise full-length and stalk-less isoforms [101]. Importantly it has been shown that only isoforms A and B (isoform 1 and 2) can bind β-glucans [102].

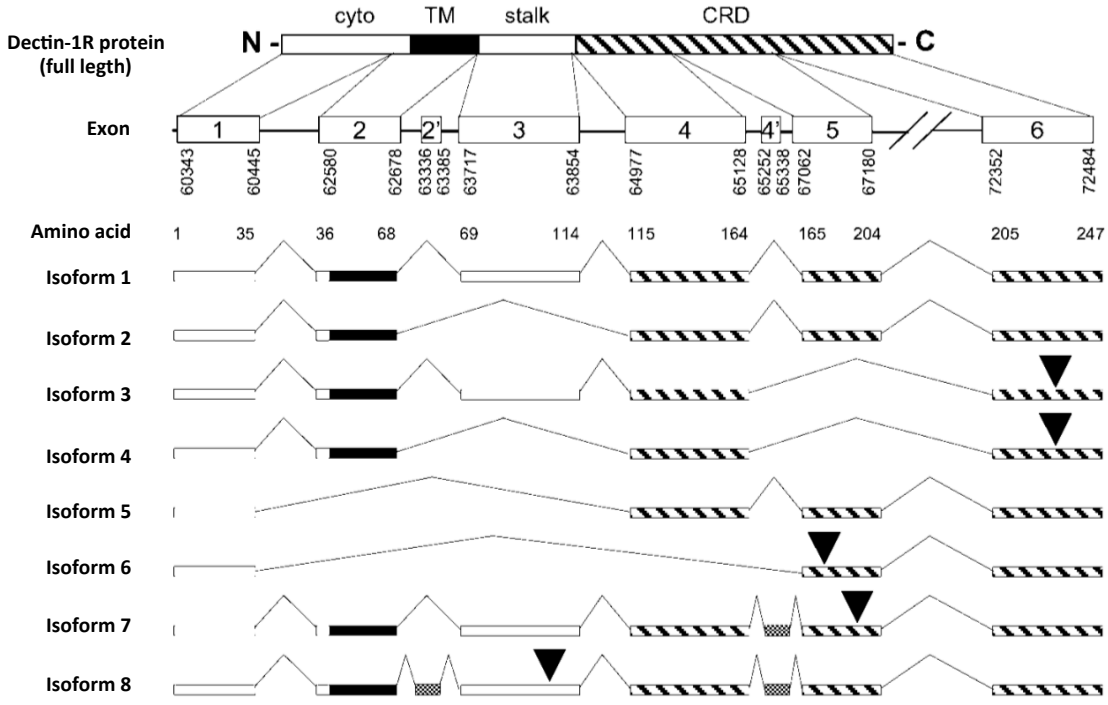

Figure 1.10 *CLEC7A* gene and mRNA isoforms.
CLEC7A gene encoding the Dectin-1R has 6 exons and can be spliced into 8 mRNA isoforms. Taken from [102].

1.10 Dectin-1R activation and signalling pathways

The research related to Dectin-1R activation and signalling has been performed using myeloid derived cells specifically macrophages, monocytes and dendritic cells. Using macrophages, receptor activation has been shown to result in a number of outcomes including phagocytosis, cell autophagy, inflammatory lipid

production and the expression of various cytokines and chemokines including TNFα, IL-2, IL-8, IL-10 and IL-12 [103-106]. The signalling cascades following activation have been determined and it is established that Dectin-1R signalling functions via either the canonical spleen tyrosine kinase (Syk) dependent or non-canonical Syk independent pathways (Figure 1.11).

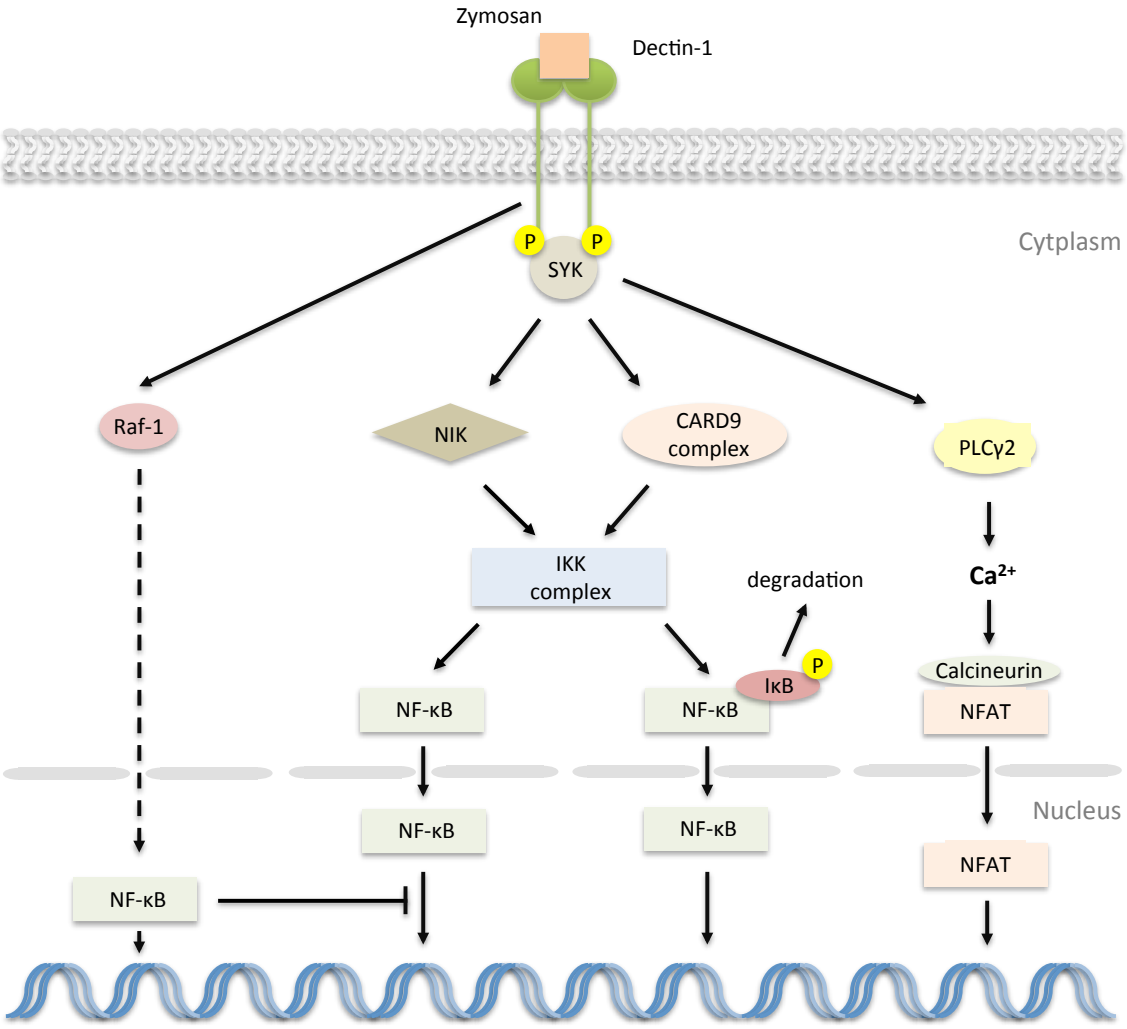

Figure 1.11 Dectin-1 signalling pathways.
Dectin-1R signalling can trigger Syk dependent or Syk independent pathways. Syk dependent pathways involve activation of the CARD9 complex, NIK and PLCγ2. The Syk independent pathway activates Raf-1 protein. All pathways result in NF-κB activation.

In the Syk dependent pathway the ITAM-like motif phosphorylates Syk, which activates the CARD9 complex and leads to IKK complex activation. This promotes phosphorylation and degradation of IκBα, which in turn releases NF-κB allowing

it to translocate into the nucleus and activate gene transcription (Figure 1.11). Phosphorylation of Syk can also activate an NF-κB-inducing kinase (NIK) [107, 108], which in turn activates the IKK complex although this pathway appears specific to the development of secondary lymphoid organs and lymphocyte survival [109]. Additionally, Syk activation can also result in the phosphorylation of PLCγ2, causing an influx of Ca^{2+} ions into the cytoplasm, which through calcineurin promotes NFAT translocation to the nucleus and gene transcription. In dendritic cells this pathway is associated with the transcription of cytokines IL-2, IL-10 and IL-12 [110].

The non-canonical pathway is the Dectin-1R Syk-independent pathway. In this signalling cascade it is proposed that the Raf-1 signalling protein is phosphorylated following Dectin-1R activation, and the consequence is NF-κB activation and gene transcription. It has been shown that activation of this pathway by curdlan in dendritic cells is associated with IL-12 expression and differentiation of T-helper cells [111]. To date the intracellular signalling components of the Dectin-1R/Raf-1 signalling pathway have not been identified. It has however, been reported that stimulation of DC-SIGN with mannosylated lipoarabinomannan activates Raf-1 signalling and that the cascade also involves Ras [95].

1.11 Co-operation of the Dectin-1R and TLRs

Cross-talk between receptors is an important mechanism to integrate and amplify signals as well as induce a specific response [112]. Previous studies in macrophages have shown the Dectin-1R to interact with Toll-like receptors including TLR2 and TLR4 [104, 113]. In fact it has been demonstrated that the Dectin-1R, in mouse macrophages and dendritic cells, in response to β-glucan challenge co-operates with TLR-2 to stimulate production of pro-inflammatory molecules including TNF and IL-12 [103, 104]. Other studies involving macrophages have also shown Dectin-1R and TLR-2 to co-operate in response to either mycobacteria or *C. albicans* challenges [113, 114]. Additionally, the co-operation of Dectin-1R with TLR4 was demonstrated by stimulating of murine

dendritic cells with curdlan, an agonist of Dectin-1R, and lipopolysaccharide, resulting in the potentiation of IL-6 and TGF-α production [115]. Further evidence of Dectin-1R synergy with TLR-2 and TLR-4 has been demonstrated in human primary peripheral blood mononuclear cells and in human monocyte-derived macrophages where co-operation was necessary for IL-10 and TNF-α production [116].

1.12 Dectin-1R /TLR5 co-operation

Previous work by Lanz suggested possible co-operation between the Dectin-1R and TLR5 receptor in immortalised vaginal VK2 E6/E7 and bladder RT4 epithelial cells [83]. In these experiments, which used cells transfected with a NF-κB reporter and challenged with zymosan, NF-κB reporter activity was decreased in cells incubated with a monoclonal antibody to TLR5 (Figure 1.12). These data suggested synergy of the TLR5 and Dectin-1R receptors in the response to zymosan, used to mimic a fungal challenge.

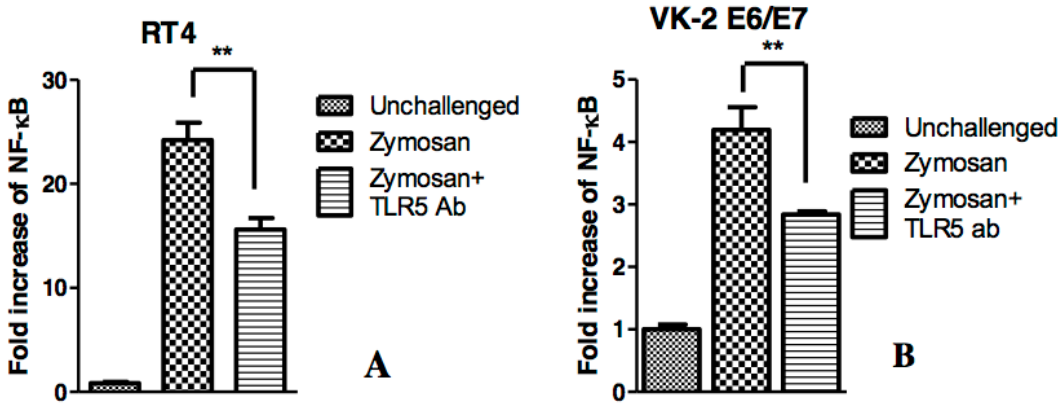

Figure 1.12 Inhibition of TLR5 receptor decreased zymosan activated NF-κB production in RT4 (A) and VK2 (B) cells.
Figure is taken from Lanz (2013) [83]. The TLR5 receptor was blocked with antibody in RT4 and VK2 E6/E7 cells, the cells challenged with the Dectin-1R ligand, zymosan and NF-κB reporter activity measured.

To further investigate possible co-operation of the Dectin-1 and TLR5 receptors immunocytochemistry (ICC) of RT4 bladder cells following a zymosan challenge was performed [117]. These ICC data, shown in Figure 1.13, confirmed the

epithelial presence of the Dectin-1R and TLR5 proteins, and the cyan colouration observed in panel C suggested co-localisation and potential co-operation of the two receptor proteins following a zymosan challenge.

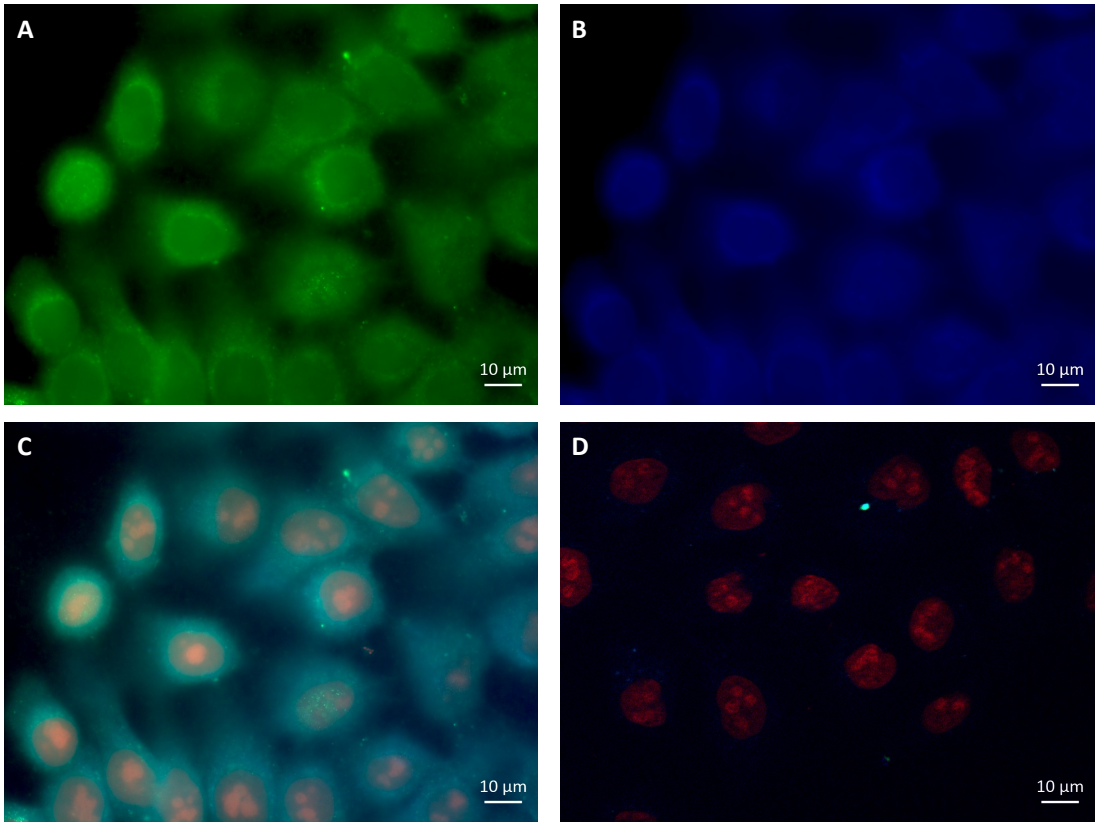

Figure 1.13 Dectin-1R and TLR5 staining in RT4 cells following zymosan challenging.
A: Dectin-1R – green colour; B: TLR5 – blue colour; C: merged green and blue channels. Nuclei are stained in red; D: RT4 cells were incubated with secondary antibodies only. Images were taken using Zeiss Axioimager II fluorescent microscope with apotome and 400x magnification [117].

Dectin-1R is classically linked to antifungal defence while TLR5 is associated with an antibacterial defence. These data therefore suggested that in the urogenital tissues, where the presence of fungi and bacteria linked to the gut-faecal cycle is common co-operation between the Dectin-1 and TLR5 receptors has evolved.

Classically the TLR5 receptor is reported to function as a homodimer [118] and receptor co-operation with another and none TLR was potentially novel and

exciting. The aim of the research reported in this thesis was therefore to focus on the Dectin-1 and TLR5 receptors in the bladder urothelium with the objective of investigating receptor co-operation following a zymosan challenge used to mimic a fungal infection.

Using an *in vitro* model namely the RT4 bladder cell line the project attempted to:

1. Investigate the gene expression and synthesis of the Dectin-1R in bladder epithelial cells.
2. Explore and demonstrate co-operation between the Dectin-1 and TLR5 receptors in bladder epithelial cells following β-glucan challenges.
3. Engineer novel bladder cell lines to further investigate co-operation between different Dectin-1R isoforms and TLR5 receptors.
4. Investigate the Dectin-1R signalling pathway in bladder epithelial cells.

Chapter 2. Materials and methods

2.1 Pathogen-associated molecular pattern s (PAMPs)

Zymosan, curdlan, scleroglucan and flagellin diluted in water described in Table 2 were used to stimulate inflammatory response in cells.

Table 2 PAMPs used to challenge the RT4 cells

PAMP	Source	Challenge conc.	Stock conc.	Supplier
Zymosan	*S. cerevisae*	50 µg/ml or 200 µg/ml	1 mg/ml	Sigma Aldrich
Curdlan	*A. faecalis*	50 µg/ml or 200 µg/ml	1 mg/ml	Invivogen
Scleroglucan	*S. rolfsii*	50 µg/ml or 200 µg/ml	1 mg/ml	Invivogen
Flagellin	*E. coli*	70 ng/ml or 250 ng/ml	670 µg/ml	Lanz (2013) [83]

2.2 Chemicals

Phosphate buffered saline (PBS) tablets, TRIS, sodium chloride, paraformaldehyde (PFA), dimethyl sulfoxide (DMSO), Tween 20, acrylamide, tetramethylethylenediamine (Temed), APS, Tris Base, sodium dodecyl sulphate (SDS) and bovine serum albumin (BSA) were purchased from Sigma-Aldrich.

2.3 Antibodies

Antibodies for Western blot included primary anti-human Dectin-1R (R&D systems, AF1859), TLR2 (Abcam, ab68159), Syk (Cell Signalling, D3Z1E), phospho-Syk (Cell Signalling, C87C1), IκBα (Abcam, ab32518), and β-actin (Santa Cruz, SC-1616). Secondary antibodies were donkey anti-goat IRDye 800CW (Li-Cor, 925-32214), goat anti-rabbit Alexa Fluor 680 (Thermo Fisher, A-21109) and rabbit anti-mouse Alexa Fluor 750 (Abcam, ab175743) .

Primary antibodies used in immunocytochemistry were anti-human Dectin-1R (R&D systems, MAB1859), anti-human TLR5 (Abcam, ab37071), anti-TLR2, anti-MPR1. Secondary antibodies were Alexa Fluor 350 (Life technologies, A-11046) and Alexa Fluor 488 (Life Technologies, A-11059). Working concentrations are shown in Tables 3.2 and 3.3.

Table 3 Primary antibodies used in western blot (WB) and immunocytochemistry (ICC).

Protein	Cat No	Type	Conc.	Procedure	Supplier
Dectin-1	AF1859	Goat polyclonal IgG	0.4 µg/mL	WB	R&D Systems
Dectin-1	MAB1859	Mouse monoclonal IgG2B	20 µg/mL	ICC/blocking	R&D Systems
TLR5	ab37071	Rabbit polyclonal IgG	20 µg/mL	ICC	ABCAM
TLR2	ab68159	Rabbit monoclonal IgG	1: 250/1:500	ICC/WB	Abcam
MPR1	ab32574	Mouse monoclonal IgG1	1:25	ICC	Abcam
β-actin	SC-1616	Goat polyclonal IgG	1:1000	WB	Santa Cruz
Syk	D3Z1E	Rabbit monoclonal IgG	1:1000	WB	Cell Signalling
Phospho-Syk	C87C1	Rabbit monoclonal IgG	1:1000	WB	Cell Signalling
IκBα	ab32518	Rabbit monoclonal IgG	1:1000	WB	Abcam

Table 4 Secondary antibodies used in western blot (WB) and immunocytochemistry [ICC].

Probe	Cat No	Type	Conc.	Procedure	Supplier
Alexa Fluor 750	ab175743	Rabbit anti-Mouse IgG	1:5000	WB	Abcam
IRDye 800	925-32214	Donkey anti-Goat IgG	1:5000	WB	Li-Cor
Alexa Fluor 680	A-21109	Goat anti-Rabbit	1:5000	WB	Thermo Fisher
Alexa Fluor 488	A-11059	Rabbit anti-Mouse IgG	1:2000	ICC	Life Technologies
Alexa Fluor 350	A-11046	Goat anti-Rabbit IgG	1:1000	ICC	Life Technologies
Mouse IgG2b Control	02-6300	Mouse IgG2b	3 – 20 µg/mL	Blocking	Invitrogen

2.4 Cell culture

Immortalised bladder epithelial RT4 cells (ATCC-HTB-2, LGC Standards, UK) were maintained in RPMI 1640 (Sigma) growth medium with 2 % of HEPES buffer, 2 mM L-glutamine and 10 % foetal calf serum (FCS). The cells were cultured in 75 cm^2 culture flasks (Corning, UK) with 25 ml of media and passaged weekly. Passaging included cell trypsinisation for 10 minutes at 37°C and 5 % CO_2, cell counting and dispensing the appropriate volume of cell suspension so that $4x10^5$ of cells were seeded into 25 ml of fresh growth media. Cells were used at passage numbers 15 to 25.

Chinese hamster ovary (CHO) cells were cultured from in house stocks and maintained in DMEM (Sigma), 2 mM L-glutamine supplemented with 10 % FCS. The cells were cultured, passaged and counted as described for RT4 cells. Cells were used at passage numbers 1 – 17, where 1 was the first passage in this laboratory.

2.5 Challenging of RT4 cells with PAMPs

RT4 cells were seeded into six well or twelve well plates (Corning) (10^5 cells/ml), grown for 48 h to confluence and 1ml of fresh media added 24h before challenging with zymosan (50 µg/ml or 200 µg/ml), flagellin (70 ηg/ml or 250 ηg/ml) or curdlan (50 µg/ml or 200 µg/ml) for 6, 16 or 24 hours.

2.6 RNA isolation

RNA was isolated using SV Total RNA Isolation System (Promega) as directed by the manufacturer's instructions. Briefly 175 µl of RNA lysis buffer was added to each well in 12 well plate containing about 2 million cells. The cells were scraped, transferred to a 1.5ml microfuge tube and RNA dilution buffer, 350 µl, added to each sample. The content in the tubes was mixed by inverting and then the tubes were centrifuged for 10 minutes at 13000 x g at room temperature. The supernatant was diluted using 200 µl of 95 % ethanol, centrifuged for 1 minute at 13000 x g in a spin basket and washed with 600 µl of RNA wash solution. To remove residual DNA the sample was treated with 50 µl of DNase incubation mix and the reaction stopped with 200 µl of DNase stop solution. After washing and centrifugation the RNA was eluted with 100 µl of nuclease-free water and the concentration measured using NanoDrop 2000 (Thermo Scientific).

2.7 Isolation of genomic DNA

Genomic DNA was isolated using the PureLink Genomic DNA Mini Kit (K1820-00, Invitrogen). Medium bathing cells grown in 12 well plates, was removed, the cells harvested by scraping with a pipette tip, the cells resuspended in 200 µl of PBS and transferred to the tube containing Proteinase K. The sample was briefly vortexed with 20 µl of RNase A and following a 2 minute incubation 200 µl of Lysis/Binding buffer was added. The sample was again vortexed and following a further 10 min incubation at 55°C, 200 µl of 96-100% of ethanol was added and the lysate transferred to a spin column. The column was centrifuged at 10000 x g

for 1 minute at room temperature. The spin column was washed with 500 µl of Wash Buffer 2 at 16000 x g for 3 minutes. The DNA was eluted with 50 µl Elution Buffer and stored at -20°C.

2.8 cDNA synthesis

To quantify mRNA in samples cDNA had to be synthesised. Complementary (c) DNA was synthesised using MMLV RT enzyme (Promega) as shown below:

0.5 µg	Isolated RNA
1 µl	Hexamers [0.5 mg/ml (Roche)]
12.5 µl	Volume adjusted using MilliQ water

The samples were incubated in at 65°C for 5 min, the mix left on ice for 2 minutes, the following reagents added and incubated at 42°C for 2 hours:

5 µl	MMLV Buffer (Promega)
6.25 µl	dNTPs [2mM] (Promega)
0.25 µl	RNasin (Promega)
0.5 µl	MMLV RT enzyme (Promega)

The reaction was stopped by incubating at 70°C for 5 minutes and cDNA stored at -20°C.

2.9 End-Point PCR

End-point PCR was used to analyse expression of genes or to clone genes of interest. GoTaq G2 polymerase (Promega) was used to synthesise DNA fragments of interest. The reaction mix was as follows:

5 µl	5x green GoTaq reaction buffer (Promega)
2.5 µl	dNTPs [10 mM] (Bioline)
2.5 µl	Primers (mix of forward and reverse primers, 10 µM each; IDT DNA)
0.2 µl	GoTaq G2 DNA polymerase (Promega)
1.5 µl	cDNA
20 µl	Volume adjusted using MilliQ water

The reaction mix was added to a 0.2 ml PCR tube (I1402-8100, StarLab). The reaction conditions were as shown below:

Polymerase activation	95 °C	2 min	
Denaturation	95 °C	30 sec	35 cycles
Annealing	T_m	30 sec	
Extension	72 °C	30 sec	
Final extension	72 °C	10 min	

Genes for cloning were amplified using KOD Hot Start DNA Polymerase kit (71086-3, Novagen). All the components except primers and water were contained within the kit. The reaction mix was as follows:

5 µl	10x Buffer for KOD Hot Start DNA Polymerase
3 µl	Mg_2SO_4 [25 mM]
5 µl	dNTPs [2 mM]
1.5 µl	Forward Primers [10 µM] (IDT DNA)
1.5 µl	Reverse Primers [10 µM] (IDT DNA)
2 µl	DNA template
1 µl	KOD Hot Start DNA Polymerase (1 U/ µl)
50 µl	Volume adjusted using PCR grade water

The PCR conditions:

Polymerase activation	95 °C	2 min	
Denaturation	95 °C	20 sec	30 cycles
Annealing	T_m	10 sec	
Extension	68 °C	25 sec	
Final extension	72 °C	10 min	

Primers designed for qRT-PCR showed in Table 5:

Table 5 Primers designed for End-Point PCR.

Gene	Direction	Sequence	Product size
Human *CLEC7A* (full length)	Forward	ATGGAATATCATCCTGAT	744, 626, 606, 507 and 487 bp
	Reverse	TTACATTGAAAACTTCTTCTC	
Human *CLEC7A* (isoform 1)	Forward	TGGAGATCCAATTCAGGAAGCAA	372 bp
	Reverse	GAGCCATGGTACCTCAGTCT	
Human *CLEC7A* (isoform 2)	Forward	TGGGTACCATGGGGGTTCTT	228 bp
	Reverse	GCCGAGAAAGGCCTATCCAA	
Human *DEFB4*	Forward	CAGCCATCAGCCATGAGGGT	83 bp
	Reverse	CCACCAAAAACACCTGGAAGAGG	
Human *LCN2*	Forward	CAAAGACCCGCAAAAGATGT	126 bp
	Reverse	GGCAACCTGGAACAAAAGTC	
Human *IL6*	Forward	GGCACTGGCAGAAAACAACC	85 bp
	Reverse	GCAAGTCTCCTCATTGAATCC	
Human *CXCL8*	Forward	ATGACTTCCAAGCTGGCCGTGGCT	292 bp
	Reverse	TCTCAGCCCTCTTCAAAAACTTCTC	
Human *IL10*	Forward	GGTTGCCAAGCCTTGTCTGA	101 bp
	Reverse	AGGGAGTTCACATGCGCCT	
Human *IL1A*	Forward	CTTCTGGGAAACTCACGGCA	162 bp
	Reverse	GTGAGACTCCAGACCTACGC	
Human *IL1B*	Forward	TGAGCTCGCCAGTGAAATGA	552 bp
	Reverse	AACACGCAGGACAGGTACAG	
pVitro2 MCS2/*CELC7A* (Primer 1)	Forward	CCTCATCCGTCGCTTCATGT	399 bp
	Reverse	TCCTGGTATTGCTTTGAGAGTCG	
pVitro2 MCS1/*TLR5* (Primer 2)	Forward	TCGGGCTTCTTAGCGGTTCA	347 bp
	Reverse	CAAGGGGGTATACTGGCTCC	

Agarose gel electrophoresis was used to separate and analyse amplified DNA fragments. Gels (1%) were prepared by dissolving 1g of agarose in 100 µl Tris-buffer (50 mM Tris-Cl, pH 7.5 and 150 mM NaCl) and 5 µl of Sybre Safe stain was added (Thermo Fisher). Samples and DNA markers were loaded on the gel and ran using electrophoresis for 1 hour at 100 V.

2.10 qRT-PCR

Quantitative PCR (qRT-PCR) was used to investigate relative gene expression. RNA was isolated from cells and reverse transcribed into cDNA as described (Section 2.6). The cDNA was diluted 1:3 with water for housekeeping genes and 1:2 for other genes. The diluted DNA and primers were mixed with reaction mix SYBR Green (04887352001, Roche) as follows:

	x1 (µl)
SYBR Green	5
Primers	0.5
Water	2.5

Eight (8) µl of master mix was pipetted into each well in LightCycler 480 96 well plate (04729692001, Roche) and 2 µl of diluted cDNA added per well. Samples were analysed in duplicate using a Lightcycler 480 (Roche). Primers designed for qRT-PCR are shown in Table 2.

Table 6 Primers designed for qRT-PCR.

Gene	Direction	Sequence	Product size
Human *CLEC7A*	Forward	GGGGCTCTCAAGAACAATGGAA	113 bp
	Reverse	CTGAAACAACAGCTATCCTGGT	
Human *TLR5*	Forward	AGCATCCCTGGTTTGGTGAC	91 bp
	Reverse	TGATGTTCATGTTCCTGACACT	
Human *DEFB4*	Forward	CAGCCATCAGCCATGAGGGT	83 bp
	Reverse	CCACCAAAAACACCTGGAAGAGG	
Human *SYK*	Forward	TTTTGGAGGCCGTCCACAAC	222 bp
	Reverse	ATGGGTAGGGCTTCTCTCTG	
Human *RAF1*	Forward	TTTCCTGGATCATGTTCCCCT	153 bp
	Reverse	ACTTTGGTGCTACAGTGCTCA	
Human *CXCL8*	Forward	ATGACTTCCAAGCTGGCCGTGGCT	292 bp
	Reverse	TCTCAGCCCTCTTCAAAAACTTCTC	
Human *IL1A*	Forward	CTTCTGGGAAACTCACGGCA	162 bp
	Reverse	GTGAGACTCCAGACCTACGC	
Human *LCN2*	Forward	CAAAGACCCGCAAAAGATGT	126 bp
	Reverse	GGCAACCTGGAACAAAAGTC	
Human *GAPDH*		Unknown (commercial primers)	
Human *ATP5B*		Unknown (commercial primers)	

Commercial primers were used for the reference genes: GAPDH and ATP5B HK-SY-hu-1200 (Primerdesign).

Relative gene expression calculations were performed using standard curve. A serially diluted plasmid with a gene of interest was amplified by qRT-PCR. Obtained cycle numbers were plotted against concentrations of serially diluted plasmid and a standard curve was produced. Then this curve was used to calculate relative concentrations in samples.

2.11 Protein extraction from RT4 cells

Proteins were extracted from RT4 bladder cells for western blot analyses. Media was removed from the well and washed with 1 ml of PBS twice. Then 100 µl of RIPA buffer (R0278-50ML, Sigma) was added per well in a 12 well plate and the cells were scraped. The lysate was transferred to a 1.5ml microfuge tube and centrifuged at 13000 x g at 4°C for 15 minutes, the supernatant was then collected and stored at -80°C.

2.12 Determination of protein concentration

Total protein concentrations were measured using the Bradford assay. Briefly 10 µl of diluted sample in water (1:6) or standards (bovine serum albumin, Sigma) were analysed in duplicate using a 96 well plate (Thermo Fisher). To each sample 100 µl of Coomassie Plus assay reagent (1856210, Thermo Fisher) was added and the absorbance of the samples read at 595 nm using a plate reader (FLUOstar Omega, BMG Labtech) right away. Readings from the standards were used to plot a standard curve and this was used to determine the sample protein concentrations.

2.13 SDS PAGE electrophoresis

Reducing SDS PAGE (sodium dodecyl sulfate–polyacrylamide gel electrophoresis) was used to separate proteins by mass. Proteins were separated using 4 -12 % polyacrylamide gels. Recipes for separating and stacking parts of the gel were as follows:

Separating gel 12%	
40% Acrylamide/Bis Acrylamide (37.5:1)	1.75 ml
4x Separating Buffer	1.7 ml
Distilled Water	3.48 ml
TEMED	6 µl
10% APS	65 µl

Stacking gel 4%	
40% Acrylamide/Bis Acrylamide (37.5:1)	0.3 ml
5x Stacking Buffer	0.6 ml
Distilled Water	2 ml
TEMED	3.75 µl
10% APS	27 µl

4x Separating Buffer	**5x Stacking Buffer**
1.5M Tris Base pH 8.9	0.3 M Tris Base pH 6.7
0.25% SDS	0.5% SDS

Acrylamide, TEMED, APS, Tris Base and SDS were purchased from Sigma.

Protein samples were mixed with 4X NuPAGE LDS (lithium dodecyl sulphate) sample buffer (Thermo Fisher), 10X NuPAGE sample reducing agent (Thermo Fisher) and incubated at 70°C for 10 minutes. The samples were electrophoresed at 200 V for 50 minutes in 1x running buffer. When the electrophoresis was completed the gels were either stained using commassie brilliant blue G250 (Pierce) or used for western blot analyses. The recipe of the running buffer was as follows:

Running buffer 5x 1L	
Tris Base	60.6 g
Glycine	144.1 g
SDS	5 g

2.14 Western blot

Proteins separated by SDS PAGE were transferred to a nitrocellulose membrane (Bio-Rad) using a semi-dry transferring system Atto AE-6675 (Atto) set at 15 V for 50 minutes and transfer buffer.

Transferring buffer 50 ml	
Running buffer 1x	40 ml
Methanol	10 ml

The resulting membrane was blocked for 1 hour or overnight at room temperature using Odyssey blocking buffer (Li-Cor Biosciences) diluted in equal parts with PBS-Tween 20 (0.1%) (PBST) or TBS-Tween (TBST) 20 (0.1%), The membrane was incubated with appropriately diluted primary antibody in the same blocking buffer for either 1 hour or overnight at room temperature or 4°C respectively. Following this step the membrane was washed three times in either PBST or TBST and then incubated with appropriately diluted secondary antibody for 30 minutes at room temperature. This incubation step was followed by three PBST or TBST washes and then the membrane was scanned using an Odyssey CLx infrared scanner (Li-Cor Biosciences).

2.15 ELISA

Sandwich ELISAs were used to quantitate the protein concentrations in the media bathing the RT4 cells. IL8 and LCN2 were measured using BD ELISA kits (DY208 and DY1757, R&D Systems). For both analyses a 96 well plate (Thermo Fisher) was coated, 100 µl per well, with capture antibody diluted in PBS to the recommended working concentration. The plate was sealed, incubated overnight at room temperature then each well aspirated and washed three times with 400 µl of buffer (Tween 0.05% in PBS). The wells were blocked with 300 µl of 1% BSA in PBS for 1 hour at room temperature and the washing steps repeated. 100 µl per well of standards and samples were added in duplicate and incubated 2 hours at room temperature. After washing 100 µl of detection antibody diluted in 1% BSA in PBS was added to each well and incubated 2 hours at room temperature. The washing steps were repeated, 100 µl of Streptavidin-HRP antibody diluted in 1% BSA in PBS added to each well for 20 minutes at room temperature and the plate washed again. Finally, 100 µl of a mixture of Colour reagent A/reagent B (1:1) was added to each well. The reaction was stopped after 20 minutes with 50 µl of 1N sulphuric acid. Absorbance was read with plate reader (FLUOstar Omega, BMG Labtech) set at 450 nm. The readings were corrected by subtraction reading at 540 nm from the readings at 450 nm as said in the instruction manual of the plate reader.

Human BD2 protein was measured by ELISA using a capture antibody (ab109570, Abcam), detection antibody (ab83509, Abcam) and Streptavidin-HRP antibody (N504, Thermo Fisher) and standards (G2815, PeproTech) at concentration recommended by manufacturer. The protein was detected using 100 µl of TMB-ELISA substrate solution (34028, Thermo Fisher). All steps were same as described before.

2.16 Immunocytochemistry

RT4 cells were cultured to confluence on 13 mm coverslips (Deckglaser) and fixed with 4 % paraformaldehyde (PFA) (Sigma-Aldrich) for 15 min. The cells were washed three times with 20 mM NH_4Cl, three times with PBS and with 1 % BSA in PBS-Tween 20 (0.1 %) blocking buffer for 1h at room temperature. The cells were incubated with either primary antibodies or appropriate control antibodies diluted in 1 % BSA in PBST overnight at 4 °C. After incubation the cells were washed three times in PBST and incubated with secondary antibodies for 30 min at room temperature. After washing five times in PBST and three times in PBS, the coverslips were mounted on microscope slides and the nuclei stained using Vectashield with propidium iodide or DAPI (Vectorlabs) mounting medium. Images were taken using Zeiss Axioimager II fluorescent microscope with ApoTome and ZEN software.

2.17 Proximity ligation assay (Duolink)

Protein-protein physical interaction was investigated using a Duolink proximity ligation assay kit (Sigma-Aldrich). Cells were fixed with 4% paraformaldehyde (PFA) for 15 min at room temperature, washed three times with PBS and blocked using 1% BSA in PBS Tween 0.1% for two hours. Following blocking, the cells were incubated with appropriately diluted ICC primary antibodies or appropriate control antibodies overnight. The cells were then washed in PBST 2x5 minutes. Two PLA probes were diluted 1:5 in 1% BSA in PBS Tween 0.1%, incubated at room temperature for 20 min and 25 µl of this solution added to the

cells on each coverslip. Following incubation of the cells plus probes in a humidity chamber for 1h at 37 °C, the cells were washed in 1x Wash Buffer A 2 x 5 min using a rocker. Ligation solution comprising 1:5 ligation stock and 1:40 ligase diluted in water was added to each of the coverslips (25 µl per coverslip), incubated 30 min at 37 °C and then washed in Wash Buffer A for 2 x 2 min on a rocker. Amplification stock and polymerase were diluted 1:5 and 1:80 respectively in water and 25 µl of the amplification solution was added to each of the coverslips for 100 min at 37 °C. In the dark coverslips were washed in Wash Buffer B for 2 x 10 min and then with 0.01 x wash Buffer B for 1 min, dried and mounted on slides with Duolink mounting medium. Imaging of the cells was using a fluorescent microscope Zeiss Axioimager with Apotome.

2.18 Fluorescent microscopy

Cells in immunocytochemistry and proximity ligation assay were visualised using Zeiss Axioimager microscope with Apotome. The images were obtained and analysed with Zeiss Zen Blue software.

2.19 DNA Cloning

Dectin-1 and TLR5 cDNA material was cloned into plasmid pVitro2-neo-msc (Invitrogen) to co-express the proteins in RT4 cells (Figure 2.1). This plasmid contains two multiple cloning sites (MCS) and two promoters hFerH and hFerL. The *neo* gene provides resistance to kanamycin in *E. coli* and to G418 in mammalian cells.

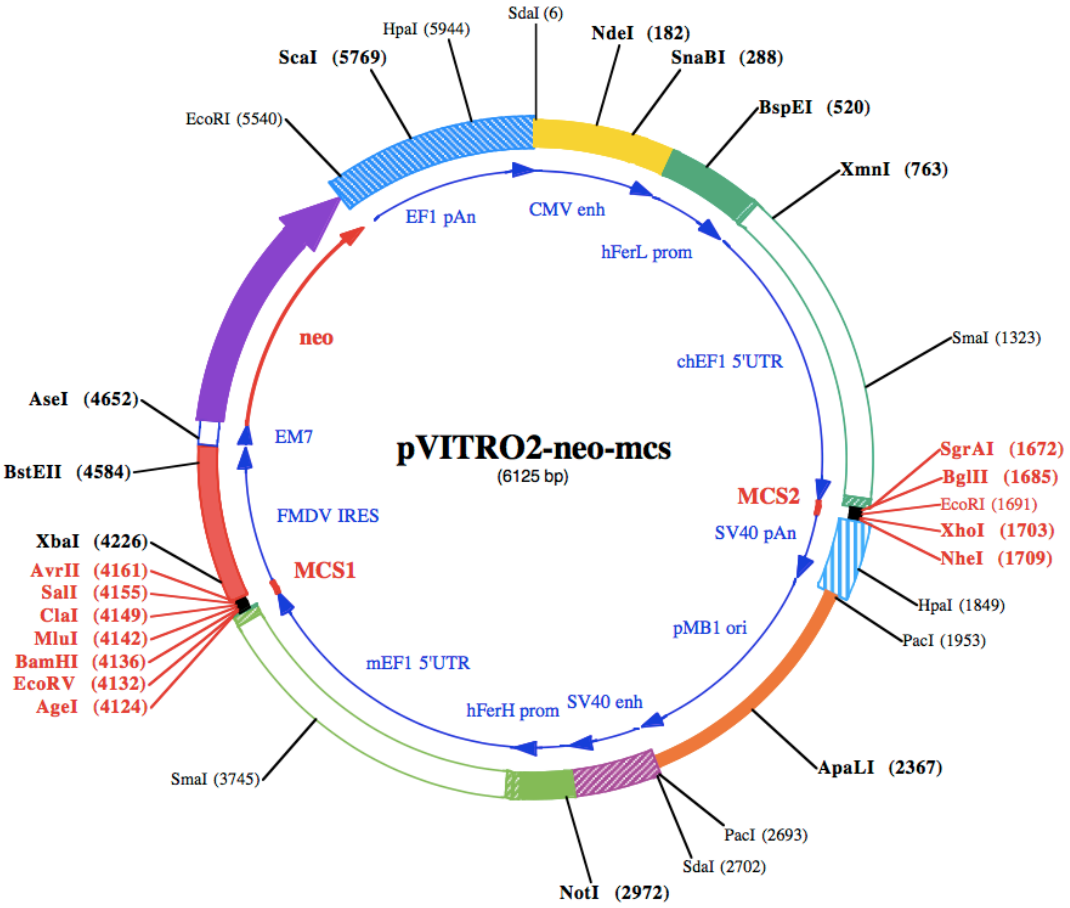

Figure 2.1 pVitro2-neo-mcs plasmid was used to overexpress Dectin-1 and TLR5 proteins in RT4 cells.
The plasmid possesses two multiple cloning sites (MCS1 and MCS2) and two promoters (hFerH and hFerL). The figure taken from [88].

Primers to amplify *CLEC7A* and *TLR5* genes were designed and included restriction fragment sites (BglII and XhoI or SalI and BamHI respectively) at their termini to allow insertion of the products into the plasmid. The genes of interest were amplified using KOD Hot-Start End-Point PCR and purified as described in the Section 2.21 and restricted as described in the Section 2.20. DNA was separated on a 1% agarose gel, the bands of interest were excised from the gel with a razor blade and purified (Section 2.21) and ligated into the plasmid pVitro2-neo-mcs as described in the Section 2.22 overnight. The recombinant plasmid was transformed into *E. coli* DH5α bacteria (Section 2.24), and the bacteria were plated on a LB plate with antibiotic kanamycine overnight. A single colony was picked, grown in LB with kanamycine overnight and the plasmid isolated as described in the Section 2.25.

Table 7 Primers designed for cloning.

Gene	Direction	Sequence	T_m, °C	Product size
Dectin-1 all isoforms	Forward	TAA GCA AGA TCT ATG GAA TAT CAT CCT GAT	55	772, 654, 630, 531, 511 bp
	Reverse	TGC TCA CTC GAG TTA CAT TGA AAA CTT CTT CTC		
Dectin-1 all isoforms	Forward	CGA GCA GGA TCC ATG GAA TAT CAT CCT GAT	55	772, 654, 630, 531, 511 bp
	Reverse	TGC TGC GTC GAC TTA CAT TGA AAA CTT CTT CTC		
TLR5 WT	Forward	CGA GCA GGA TCC ATG GGA GAC CAC CTG GAC C	61	2601 bp
	Reverse	TGC TGC GTC GAC TTA GGA GAT GGT TGC TAC		
TLR5 SNP C1174T	Forward	CGA GCA GGA TCC ATG GGA GAC CAC CTG GAC C	62	1197 bp
	Reverse	TGC TGC GTC GAC TCA GAG ATC CAA GGT CTG		

2.20 DNA digestion

The purified Dectin-1 and TLR5 DNA fragments and pVitro2 plasmid were restricted with enzymes in preparation for ligation. Dectin-1 fragments were restricted with BglII and XhoI (Promega) and TLR5 with Sall and BamHI (Promega). While pVitro2 plasmid was restricted with either BglII and XhoI or Sall and BamHI. The following reaction mix was prepared:

Sterile water	17.3 µl
Restriction Enzyme buffer 10x	2 µl
Acetylated BSA, 10 µg/µl	0.2 µl
DNA. 1 µg/µl	1 µl
Restriction Enzyme, 10 u/µl	1 µl

The reaction mix was incubated for 1 hour at room temperature and then loaded on 1% agarose gel for DNA separation. All enzyme pairs were compatible and no double digestion was used.

2.21 DNA purification from agarose gel and PCR reaction mixture

DNA from an agarose gel, and where appropriate PCR mixture, was purified using the Wizard SV Gel and PCR Clean-Up System (Promega). Briefly a DNA band was excised from agarose gel, deposited in to a microcentrifuge tube, and 10 µl of Membrane Binding Solution per 10 mg of gel slice was added. The mixture was incubated at 60°C for 15 minutes with occasional vortexing. For PCR mixtures an equal volume of Membrane Binding Solution was added. The dissolved gel or PCR mixture was transferred to the SV Minicolumn, inserted a into collection tube and incubated for 1 minute. Then the Minicolumn was centrifuged for 16000 g for 1 minute. The flowthrough was discarded, 700 µl of Membrane Wash Solution was added to the Minicolumn and centrifuged at 16000 g for 1 minute. The previous step was repeated with 500 µl of Membrane Wash Solution and centrifuged at 16000 g for 5 minutes. The flowthrough was discarded and empty Minicolumn was centrifuged at 16000 g for 1 minutes. The Minicolumn was transferred into clean 1.5 ml minicentrifuge tube. 50 µl of nuclease-free water was added into Minicolumn and incubated for 1 minute at room temperature. Then the Minicolumn was centrifuged at 16000 g for 1 minute and the eluted DNA stored at -20°C.

2.22 DNA ligation into plasmid

cDNA fragments after restriction digestion were ligated into appropriately restricted plasmid vectors using Promega T4 DNA Ligase (M180A). Generally a molar ratio of 1:3 of vector:insert was used. The following reaction mix was prepared and incubated overnight at 4°C in a cooling water bath:

T4 DNA Ligase	0.1-1 u
Ligase buffer 10x	1 µl
Vector DNA	100 ng
Insert DNA	X ng
Nuclease Free Water to final volume of	10 µl

2.23 Preparation of competent cells

E. coli DH5α bacteria were used in transformation procedures. A single colony was picked from a fresh plate of *E. coli* DH5α bacteria and grown overnight in 10 ml of LB medium at 37°C in shaking incubator. 1 ml of overnight culture was transferred into a 1L conical flask containing 100 ml of LB medium. The bacterial culture was grown at 37°C in a shaking incubator set to 200-250 rpm to an absorbance at 600 nm of between 0.3-0.4. The bacterial culture was centrifuged at 4000g at 4°C for 5 minutes, the supernatant discarded and the pellet resuspended in 10-20 ml of 0.1M $MgCl_2$. After recentrifugation and removal of the supernatant the pellet was resuspended in 4 ml 0.1M $CaCl_2$ and kept on ice for 2 hours. Competent cells were used fresh. For freezing 4 ml of these bacteria were mixed with 4 ml of 50% glycerol stock, 500 µl volumes aliquoted into microfuge tubes and stored at -80°C.

2.24 Plasmid transformation into bacteria

Following ligation the recombinant plasmids were transformed into the competent bacterial cells. The ligation mix was centrifuged briefly and 2 µl transferred to a new 1.5 ml microfuge tube pre-cooled on ice. Competent cells, 50 µl, were added to the ligation mix and after a gentle mix the tube was left on ice for 20 minutes. The bacterial mix was heat shocked for 50 seconds at 42°C, returned to ice for 2 minutes and then diluted using 950 µl of LB. This mix was then incubated for 1 hour in at 37°C with shaking (200 rpm). Following this incubation 100 µl aliquots of the mix were plated onto LB plates containing the appropriate antibiotic and incubated overnight at 37°C. Recombinant bacterial colonies were selected for further analysis.

2.25 Purification plasmid from bacteria

To purify plasmid DNA from the recombinant bacteria a PureYield Plasmid Miniprep System (Promega) was used. A single bacterial colony was selected and

grown in 3 ml of LB plus appropriate antibiotic overnight. This volume was transferred into tube and centrifuged at maximum speed (17000 g) for 30 seconds to pellet the bacteria, the supernatant discarded, the pellet resuspended in 600 µl of double distilled (dd) sterile water and 100 µl of Cell Lysis Buffer added. The sample was mixed by inverting the tube six times. Then 350 µl of cold 4°C Neutralisation Solution was added and the sample again mixed by inverting. The mixture was microfuged at maximum speed (17000 g) for 3 minutes. The supernatant was transferred to a Minicolumn that was placed into a Collection Tube and again microfuged at maximum speed for 15 seconds. The flowthrough was discarded, 200 µl of Endotoxin Removal Wash added to the minicolumn, which was microfuged as previously described. 400 µl of Column Wash Solution was added to the minicolumn and the centrifugation step repeated. The minicolumn was then transferred to clean microcentrifuge tube and 30 µl of nuclease free water was added. After 1 minute the minicolumn was centrifuged (17000 g) for 15 seconds to elute plasmid DNA solution. The plasmid DNA was stored at -20°C.

2.26 Transfection of plasmid into mammalian cells

Plasmid was transfected into mamalian cells using the transfection agent attractene (301005, QiGen). The plasmid in the amounts/volumes highlighted below was mixed with attractene and serum free media Opti-Mem (Gibco) and incubated for 20 minutes at room temperature. The mix was then added to the media bathing the RT4 cells (10^6 cells/ml) grown on the well of 12 well plate. Amounts/volumes of each component were as follows:

Plasmid	1000 ηg
Attractene	1.5 µl
Optimem	245 µl
Media	750 µl

70 µg/ml of antibiotic G418 (Geneticin) (200049, Agilent Technologies) or 100 µg/ml of antibiotic zeocin (Invivogen) was used to select cells transfected with pVitro2-neo-mcs or psiRNA-Dectin-1/Luciferase plasmids respectively. G418

concentration Cells without plasmid died while transfected cells survived and produced colonies. The survived colonies were tripsinised and were grown in 75 cm^3 culture flasks (Corning, UK). When the cells were confluent they were tripsinised and frozen for storage in liquid nitrogen (Section 43).

2.27 Freezing cells in liquid nitrogen

Transfected RT4 cells were stored in liquid nitrogen. Confluent cells were trypsinised and 8 ml of cells, 10^6 cells/ml, were gently mixed with 1 ml of foetal calf serum and 1 ml of DMSO (D8418, Sigma). One ml aliquots were frozen in liquid nitrogen.

2.28 siRNA Gene knockdown

Knockdown of Dectin-1 gene expression was performed with psiRNA-hDectin-1 plasmid (InvivoGen), while knockdown of other gene expression was performed using siRNA primers: TLR5 –S14199 (Ambion), TLR2 S168 (Ambion), TLR4 S14196 (Ambion), TLR6 S20215 (Ambion), SYK S13679 (Ambion), RAF-1 103578 (Ambion).

Plasmid psiRNA-hDectin-1 was transfected into RT4 cells using the transfection protocol described in the Section 2.26. To select stably transfected cells 100 µg/ml of antibiotic zeocin (ant-zn-1, InvivoGen) was used.

To transfect RT4 cells with siRNA 10^5 cells/ml were grown to 20 % confluence in each well of a 12 well plate. A 10-20% mix of transfection agent Lipofectamine RNAiMAX (Thermo Fisher), siRNA and serum free Optimem media was prepared and incubated for 20 minutes at room temperature. The reaction mix was as follows:

Lipofectamine RNAiMAX	2 µl
siRNA	2 µl
Optimem	196 µl

200 µl of this mix was added to each well and the cells challenged 48 hours later.

2.29 Blocking Dectin-1 receptor (R) with antibody

Dectin-1R was blocked using anti-Dectin-1 antibody MAB1859 (R&D Systems). To facilitate this 1 ml of 10^5 cells/ml were seeded in to each well of a 12 well plate. When the cells were 100% confluent 6 or 3 µg/ml of anti-Dectin-1R antibody solution was added and after two hours the cells were challenged with zymosan ligand. As a control 6 µg/ml solution of IGG_{2B} antibody was added (026300, Invitrogen).

2.30 Syk Inhibition using piceattanol

Syk protein signalling was inhibited using piceattanol (SC-200610, Santa Cruz) diluted in DMSO. RT4 cells were seeded in to 12 well plate. When 100% confluent 0 µM, 10 µM, 20 µM, 30 µM and 100 µM, of piceattanol solution were added to each well. After 20 minutes incubation the cells were challenged with 50 µg/ml of zymosan for 6 h.

2.31 Statistical analysis

Statistical analyses were performed using Prism 6.0 (GraphPad Software). Data are shown as mean ± SD. One-way ANOVA with post-hoc Tukey's test was used to determine significance of the observed differences. P values of <0.05 were considered significant.

2.32 Ethical approval

Research Ethics (09/H0905/15) and Newcastle upon Tyne Hospitals NHS Trust (ID 4841) allowed the collection of biopsy materials. Written informed consent was obtained from all participants and all methods were performed in accordance with relevant guidelines and regulations.

Chapter 3. Dectin-1 receptor and RT4 cells

The expression and synthesis of Dectin-1 receptor (Dectin-1R) isoforms were explored previously *in vivo* using male and female murine bladder tissues [117]. Using tissue RNA and molecular analyses cDNA bands of 450bp (strong) and 550bp (weak) were detected indicative of two major transcripts, encoding proteins of 23 and 27kDa respectively. DNA sequencing and BLAST analyses revealed the 450bp cDNA transcript sequence encoded the 23 kDa mouse isoform B, Dectin-1R protein, which is predicted to be stalk free (Figure 1.9). Importantly these data supported Dectin-1R synthesis in the murine bladder, hence urinary tract tissues. However, probable contamination of the murine epithelial tissues by antigen presenting cells, such as macrophages meant it was not possible to localise the observed receptors specifically to the urothelia.

To explore whether Dectin-1R is also expressed and synthesised in human bladder epithelia *in vitro* analyses were performed. Initial analyses utilised bladder biopsy material and these were followed by further experiments exploiting an in vitro bladder cell model, the immortalised RT4 human bladder epithelial cell line.

3.1 Expression of Dectin-1R isoforms in human bladder biopsy

To explore *CLEC7A* (Dectin-1R) expression and synthesis in the human urogenital tract a human bladder biopsy sample (female) was used. A section of the tissue was homogenised, RNA extracted (Section 2.6), transcribed into cDNA and the Dectin-1 gene, *CLEC7A*, amplified by end-point PCR using isoform specific primers (Table 5). Data in Figure 3.1A (lane 1) shows a strong band at 330 bp representing Dectin-1R isoform 1 (predicted to encode 25 kDa protein) and two weaker bands at 250 bp and 180 bp. These smaller bands represented DNA fragments amplified due to non-specific binding of primers.

To investigate Dectin-1R protein synthesis the tissue was homogenised, cells lysed with RIPA buffer, proteins separated by SDS-PAGE, blotted onto nitrocellulose and analysed using anti-Dectin-1R abtibody (R&D systems,

MAB1859) (Table 2). Data in Figure 3.1B demonstrated bands relating to proteins of 20kDa, 25kDa, 42kDa and 54kDa respectively. These relate to the Dectin-1R isoform 1 monomer (25 kDa) and isoform 2 monomer (20 kDa) and potentially an isoform 1 dimer (54 kDa) and isoform 2 dimer (42 kDa). The isoform 2 Dectin-1R protein lacks a stalk region, which is present in isoform 1, although the function of the stalk region is not known.

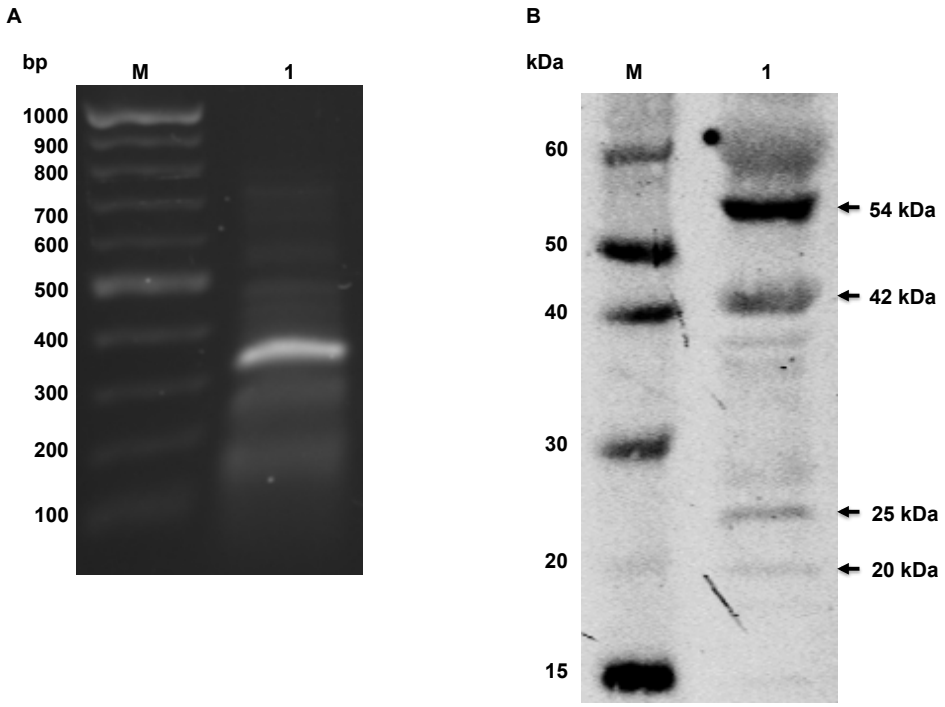

Figure 3.1 Dectin-1R mRNA expression and protein synthesis in human bladder.
A: Bladder RNA was analysed using end-point PCR and Dectin-1R primers. Lane 1 – the band of 330 bp represents Dectin-1R isoform 1, bands at 250 bp and 180 bp were amplified due to nonspecific primers binding; M – base pairs markers. B: Western blot analyses of bladder proteins using anti-Dectin-1R antibody diluted 1:50. M- protein markers; Lane 1 – bands representing Dectin-1R isoforms. The gels represent two independent experiments.

3.2 Expression of Dectin-1R isoforms in human bladder epithelial cells

While these data confirmed *CLEC7A* (Dectin-1R) gene expression and synthesis in human bladder tissue again contamination of the tissue with myeloid derived cells could not be guaranteed. To focus therefore on epithelial tissues a human

bladder epithelial cell line was used for all further experiments. The RT4 bladder cell line was chosen as it represents a robust urothelial cell model [119].

The Dectin-1R gene, *CLEC7A*, was amplified using cDNA prepared from confluent RT4 cells and primers designed to amplify the *CLEC7A* gene sequence (Table 5). PCR products were analysed on a 1% agarose gel and the results are shown in Figure 3.2. A number of cDNA bands were observed indicating the synthesis of a number of different Dectin-1R protein isoforms. Fragment sizes 1, 2, 3, 4, 5 with sizes of 744, 626, 606, 507 and 487 bp respectively align to the Dectin-1R isoforms 1, 2, 3, 4, and 5 [120]. It was noted however, that the intensity of fragment (cDNA band) 4 was much stronger compared to those of the other four cDNA bands.

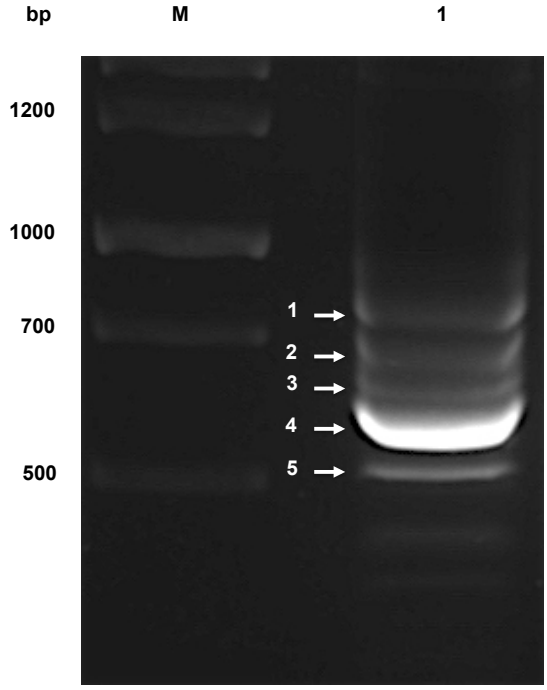

Figure 3.2 End-Point PCR showing mRNA expression of Dectin-1 isoforms in RT4 cells.
M- base pairs markers; Lane 1 cDNA bands amplified from cDNA of RT4 cells with *CLEC7A* primers. The sizes of the bands 744, 626, 606, 507 and 487 bp relate to the Dectin-1R isoforms 1, 2, 3, 4 and 5. The gel represents two independent experiments.

To confirm these cDNA bands related to Dectin-1R expression the DNA fragments were excised from the gel, purified, sequenced and BLAST analyses performed. Sequencing and BLAST results are shown in Figure 3.3 A-E. The obtained sequences (Query) were aligned with the predicted sequences of Dectin-1 gene CLEC7A (Sbjct) and the sequencing data confirmed that the cDNA bands represented the Homo sapiens Dectin-1R isoforms 1, 2, 3, 4 and 5.

Dectin-1 isoform 1

```
Query  1    CTATC-AGAANTAAAGAGAACCACAGTCAACCCACACAATCATCTTTAGAAGACAGTGTG  59
            ||||| |||| ||||||||||||||||||||||||||||||||||||||||||||||||
Sbjct  440  CTATCAAGAAATAAAGAGAACCACAGTCAACCCACACAATCATCTTTAGAAGACAGTGTG  499

Query  60   ACTCCTACCAAAGCTGTCAAAACCACAGGGGTTCTTTCCAGCCCTTGTCCTCCTAATTGG  119
            ||||||||||||||||||||||||||||||||||||||||||||||||||||||||||||
Sbjct  500  ACTCCTACCAAAGCTGTCAAAACCACAGGGGTTCTTTCCAGCCCTTGTCCTCCTAATTGG  559
```

A

Dectin-1 isoform 2

```
Query  1    ATGGATATACTCAATTACACTTCGACTCTCAAAGCAATACCAGGATAGCTGTTGTTTCAG  60
            ||||||||||||||||||||||||||||||||||||||||||||||||||||||||||||
Sbjct  225  ATGGATATACTCAATTACACTTCGACTCTCAAAGCAATACCAGGATAGCTGTTGTTTCAG  284

Query  61   AGAAAGGATCGTGTGCTGCATCTCCTCCTTGGCGCCTCATTGCTGTAATTTTGGGAATCC  120
            ||||||||||||||||||||||||||||||||||||||||||||||||||||||||||||
Sbjct  285  AGAAAGGATCGTGTGCTGCATCTCCTCCTTGGCGCCTCATTGCTGTAATTTTGGGAATCC  344
```

B

Dectin-1 isoform 3

```
Query  4    GGGGTTCTTTCCAGCCCTTGTCCTCCTAATTGGATTATATATGAGAAGAGCTGTTATCTA  63
            ||||||||||||||||||||||||||||||||||||||||||||||||||||||||||||
Sbjct  527  GGGGTTCTTTCCAGCCCTTGTCCTCCTAATTGGATTATATATGAGAAGAGCTGTTATCTA  586

Query  64   TTCAGCATGTCACTAAATTCCTGGGATGGAAGTAAAAGACAATGCTGGCAACTGGGCTCT  123
            ||||||||||||||||||||||||||||||||||||||||||||||||||||||||||||
Sbjct  587  TTCAGCATGTCACTAAATTCCTGGGATGGAAGTAAAAGACAATGCTGGCAACTGGGCTCT  646
```

C

Dectin-1 isoform 4

```
Query  1    ATACTCAATTACACTTCGACTCTCAAAGCAATACCAGGATAGCTGTTGTTTCAGAGAAAG  60
            ||||||||||||||||||||||||||||||||||||||||||||||||||||||||||||
Sbjct  231  ATACTCAATTACACTTCGACTCTCAAAGCAATACCAGGATAGCTGTTGTTTCAGAGAAAG  290

Query  61   GATCGTGTGCTGCATCTCCTCCTTGGCGCCTCATTGCTGTAATTTTGGGAATCCTATGCT  120
            ||||||||||||||||||||||||||||||||||||||||||||||||||||||||||||
Sbjct  291  GATCGTGTGCTGCATCTCCTCCTTGGCGCCTCATTGCTGTAATTTTGGGAATCCTATGCT  350
```

D

Dectin-1 isoform 5

```
Query  26   GAG-AGAGCTGTTATCTATTCAGCATGTCACTAAATTCCTGGGATGGAAGTAAAAGACAA  84
            ||| ||||||||||||||||||||||||||||||||||||||||||||||||||||||||
Sbjct  332  GAGAAGAGCTGTTATCTATTCAGCATGTCACTAAATTCCTGGGATGGAAGTAAAAGACAA  391

Query  85   TGCTGGCAACTGGGCTCTAATCTCCTAAAGATAGACAGCTCAAATGAATTGGGATTTATA  144
            ||||||||||||||||||||||||||||||||||||||||||||||||||||||||||||
Sbjct  392  TGCTGGCAACTGGGCTCTAATCTCCTAAAGATAGACAGCTCAAATGAATTGGGATTTATA  451
```

E

Figure 3.3 Sequence data relating to the different Dectin-1 cDNA products. The sequences (Query) were aligned with the predicted sequences of the CLEC7a (Dectin-1R) isoforms (Sbjct).

cDNA 1 corresponded to a full length *CLEC7A* isoform 1, which has a stalk region; cDNA 2 represents isoform 2, which does not have a stalk; cDNA 3 – (isoform 3) possess a stalk region but has a shorter carbohydrate binding region; cDNAs 4 and 5 (isoforms 4 and 5) do not have a stalk and have either a truncated carbohydrate region or truncated intracellular signalling region respectively. As

DNA fragment 4 showed the strongest intensity on the agarose gel this suggested it was the main isoform in RT4 cells.

These data confirmed the *CLEC7A* (Dectin-1R) gene to be expressed in RT4 bladder epithelial cells.

3.3 Protein synthesis of Dectin-1R isoforms

The next step was to use western analyses to explore and confirm Dectin-1R protein synthesis in the RT4 cells. These analyses employed the polyclonal anti-human Dectin-1 antibody (R&D Systems, AF1859). Results of the immunoblot (Figure 3.4) revealed two strong bands of 17 kDa and 27 kDa and weaker bands of 25 kDa and 21 kDa respectively. These corresponded to Dectin-1R isoforms 1, 4 and 2, 3 respectively. Interestingly in comparison the bladder biopsy western indicated only two forms, Dectin-1R isoforms 1 and 2 (Figure 3.1, B). The immunoblot data also indicated a range of bands from 50 kDa to 60 kDa suggesting Dectin-1R dimers, which had also been observed in the bladder biopsy sample.

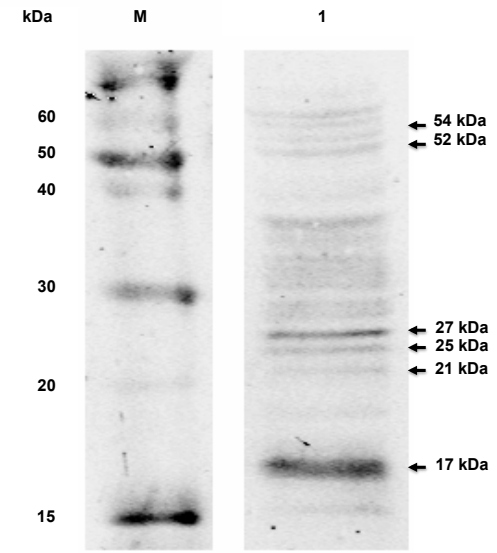

Figure 3.4 Immunoblot of Dectin-1R in RT4 cells.
M - molecular weight marker; 1- RT4 cell proteins immunoblotted with anti-Dectin-1R antibody (1:50 dilution). The gel represents two independent experiments.

These molecular and protein data validated and underpinned the use of the immortalised RT4 cell line to further investigate *CLEC7A* (Dectin-1R) gene expression, protein synthesis and function in urothelial cells.

3.4 RT4 bladder cell challenge with Dectin-1R ligands

Having identified the synthesis of two potential Dectin-1Rs the next step was to examine receptor functionality. It is well documented, albeit in myeloid derived cells, that β-glucans found in the fungal cell wall stimulate Dectin-1R and promote the expression of a number of pro-inflammatory molecules including TNF, IL1*α*, IL-8 and IL-6 [121-125]. This information was exploited to explore Dectin-1R functionality in the bladder RT4 cells. In addition a range of β-glucan ligands were tested including zymosan, scleroglucan and curdlan, which are found as part of the cell wall material of *Saccharomyces cerevisiae*, *Sclerotium rolfsii* and *Alcaligenes faecalis* respectively.

The expression and synthesis of a range of effector molecules were analysed using molecular methodologies including end-point PCR and qRT-PCR, and ELISA. Focus was on pro- and anti-inflammatory molecules including IL1α, IL1β, IL-6, IL-8 and IL-10 although genes encoding antimicrobial peptides and proteins, and including *DEFB4* and *LCN2* were also investigated. Gene expression was initially investigated using End-Point PCR following a zymosan (50 μg/ml; 6h) challenge. The resultant data (Figure 3.5), although non-quantitative, suggested that the gene expression of *DEFB4*, encoding the antimicrobial peptide hBD2 [126]; *IL1α* and *CXCL8* encoding proinflammatory cytokines IL-1α and IL-8 [121], and *LCN2* encoding the iron sequestering protein agent LCN2 [57] were increased in response to zymosan. These data were further supported by qRT-PCR analyses, which directed the use of these effectors in future investigations of bladder Dectin-1R function (Figure 3.6).

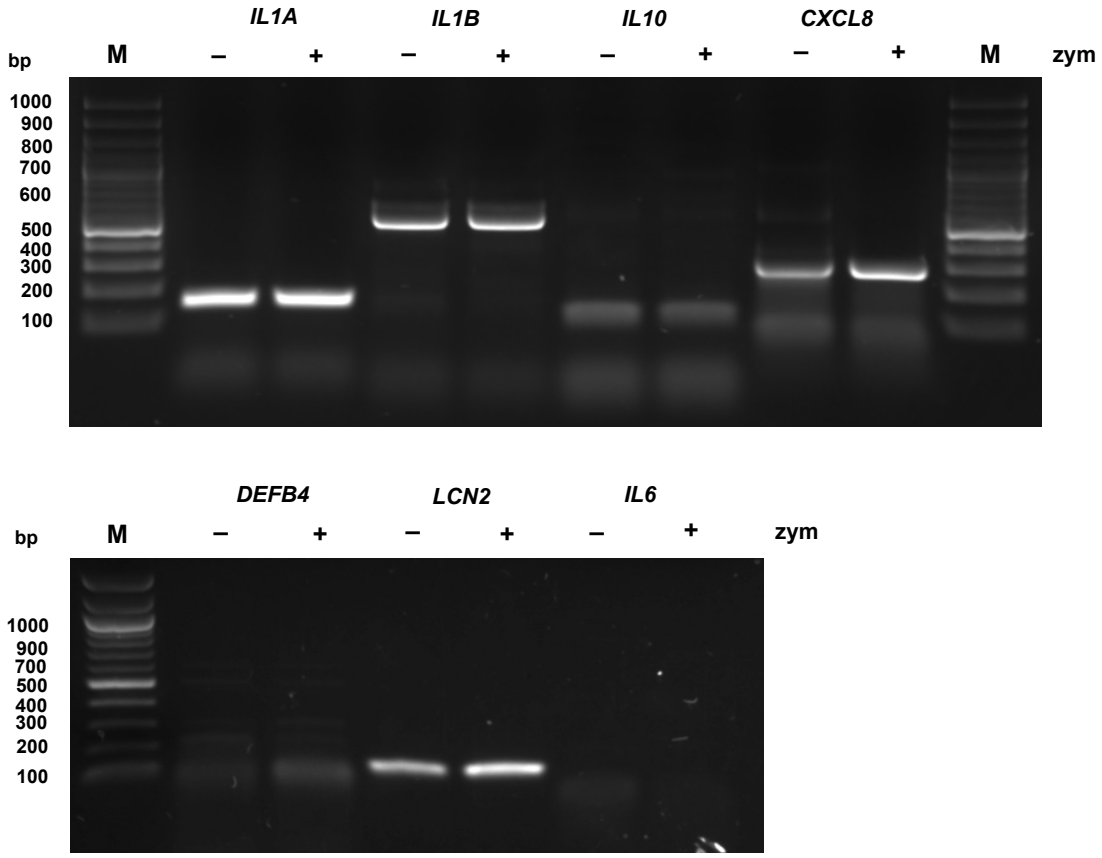

Figure 3.5 Expression of genes encoding pro-inflammatory and host defence peptides/proteins in RT4 cells following a zymosan challenge.
IL1α, IL1β, IL-10, IL-8, DEFB4, LCN2 and *IL-6* gene End-Point PCR analyses using cDNA prepared from confluent RT4 cells challenged with zymosan (50 µg/ml; 6 h) or PBS. Expected band sizes were: *IL1A* – 162 bp, *IL1B* – 553 bp, *IL10* – 110 bp, *CXCL8* – 292 bp, *DEFB4* – 83 bp, *LCN2* – 92 bp and *IL6* -79 bp. The gels represent two independent experiments.

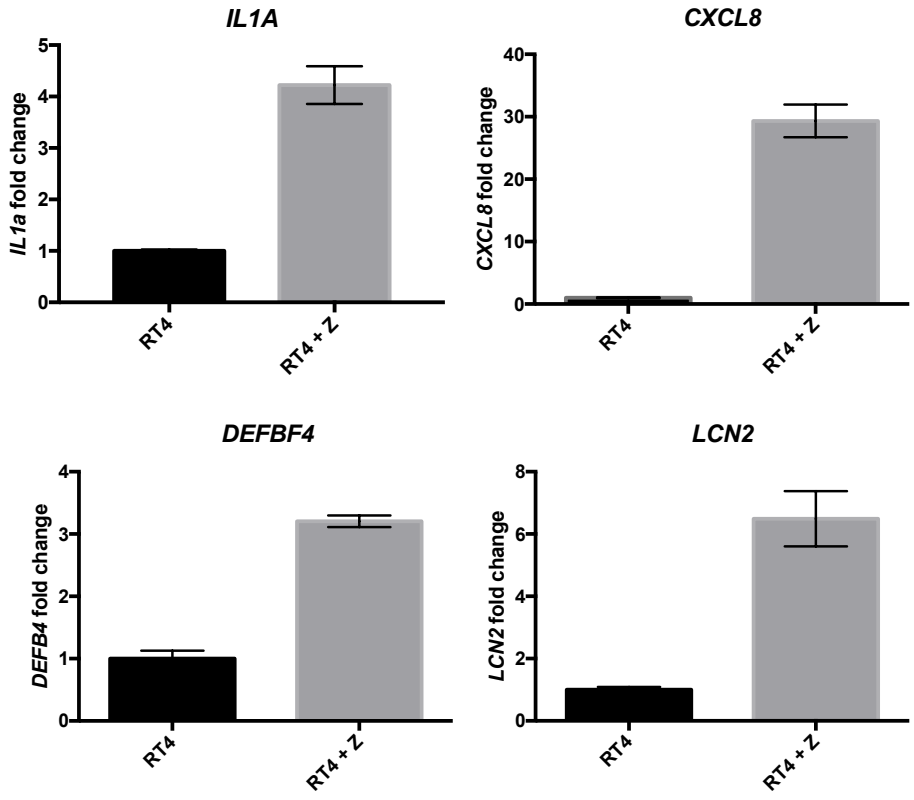

Figure 3.6 Expression of genes encoding *IL1A*, *CXCL8*, *DEFB4*, *LCN2* in RT4 cells following zymosan challenge.
cDNA material from RT4 cells challenged with zymosan (50 µg/ml; 6 h) was used to measure *IL1A*, *CXCL8*, *DEFB4*, *LCN2* gene expression using qRT-PCR. (No statistics are presented as data relate to only one experiment) ie N=1;n=3).

3.4.1 RT4 cells challenged with zymosan

To confirm these molecular data the media bathing the RT4 cells was collected following the zymosan challenges and the IL-8 and LCN2 concentrations measured by ELISA. Data shown in Figure 3.7 supported significant increases ($p<0.001$ and $p<0.01$ respectively) in these two effectors, which reflected the molecular data and suggested Dectin-1R functionality.

The initial RT4 cell challenges to explore the Dectin-1R responses followed procedures published in the literature using a zymosan concentration of 50 µg/ml and challenge times of 6, 16 and 24 hours respectively [124]. However, this dose and the challenge times were all linked to experiments performed in myeloid derived cells so to confirm this concentration was optimal for urothelial

cells the 6h time challenge was repeated, but using a range of zymosan concentrations up to 200 μg/ml. Again effector IL-8 and LCN2 concentrations were measured using ELISA and data are shown in (Figure 3.7).

IL-8 concentrations increased from a mean of 667 ± 122 pg/ml in non-challenged cells to 1364 ± 94 pg/ml, 2919 ± 460 pg/ml, 3767 ± 526 pg/ml, 4364 ± 475 and 4494 ± 492 pg/ml respectively (Figure 3.7, A). Figure 3.7, B shows data relating to the LCN2 concentrations measured. The mean LCN2 concentration was 866 ± 9 pg/ml in PBS challenged samples, which was not significantly different from the concentrations measured in the samples challenged with 5 μg/ml of zymosan (825 ± 50 pg/ml). However, mean LCN2 concentrations increased to 1322 ± 72 pg/ml, 1859 ± 159 pg/ml, 2156 ± 44 pg/ml and 2519 ± 100 pg/ml following challenges with 25, 50, 100 and 200 μg/ml of zymosan respectively.

The challenge experiments were repeated using 50 μg/ml zymosan, but using different challenge times. Figure 3.7, C shows that the IL-8 concentrations increased from a mean of 399 ± 37 pg/ml in PBS challenged cells to 4119 ± 425 pg/ml ($p<0.0001$), 4915 ± 422 pg/ml ($p<0.0001$) and 4387 ± 410 pg/ml ($p<0.0001$) in RT4 cells challenged with zymosan for 6, 16 and 24 hours respectively. Figure 3.7, D demonstrated a similar response for LCN2 with mean concentrations increasing from 2669 ± 269 pg/ml in PBS challenged cells to 4350 ± 468 pg/ml (NS compared to control), 19500 ± 1377 pg/ml ($p<0.0001$) and 22500 ± 1948 pg/ml ($p<0.0001$) at 6, 16 and 24 hours respectively.

Interestingly the LCN2 concentrations presented in panels B and D following the 50 μg/ml, 6h challenges do not concur. In panel B a statistically significant increase in LCN2 was observed while in the panel D no increase was detected compared to control. The reason(s) for this anomaly is not known, but it probably reflects the elevated LCN2 concentrations in the PBS challenged cells (panel D) compared to panel B (866 ± 9 pg/ml and 2669 ± 269 pg/ml respectively).

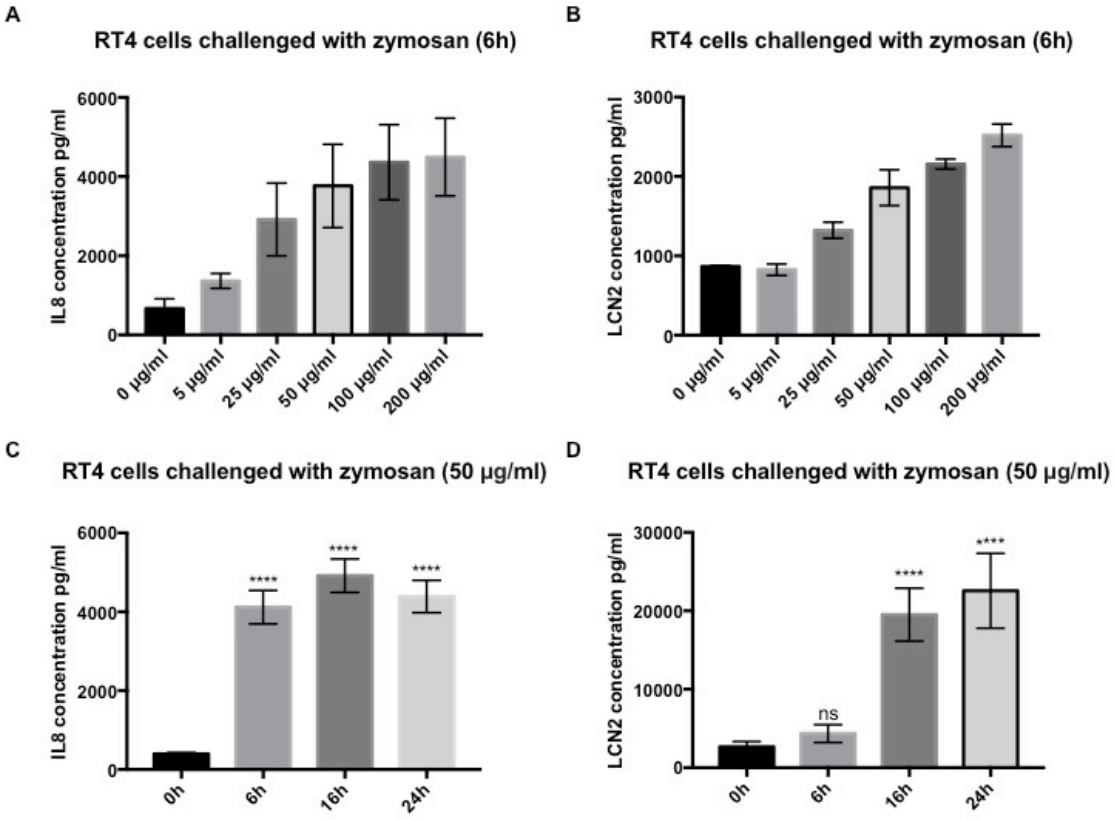

Figure 3.7 RT4 cells challenged with zymosan.
Panels A and B show IL-8 and LCN2 concentrations in RT4 cells challenged with 5, 25, 50, 100 and 200 µg/ml of zymosan for 6 hours. Panels C and D show IL-8 and LCN2 concentrations in RT4 cells challenged with 50 µg/ml of zymosan for 6, 16 or 24 hours. Data in A and B show mean ±SD and N=2, in C and D – mean ±SD and N=3. * $p<0.05$, ** $p<0.01$, *** $p<0.001$, **** $p<0.0001$.

3.4.2 RT4 cells challenged with scleroglucan and curdlan

Dectin-1R function was further investigated in RT4 bladder cells by challenging the cells with two other β-glucans – scleroglucan and curdlan. Scleroglucan is a polysaccharide, which consists of β-(1-3)-linked and β-(1-6)-linked glucose residues, while curdlan comprises β-(1-3)-linked glucose residues. It has been shown previously that these β-glucans can promote cytokine production in myeloid derived cells [124, 127].

The manufacturer recommended a challenge concentration and time of 100 µg/ml and 24 hours. However, for these experiments RT4 cells were incubated with 100, 125, 250 and 500 µg/ml of scleroglucan for 6, 12, 24 and 40 hours.

Media bathing the challenged RT4 cells were collected and analysed, using ELISA, for concentrations of the cytokine IL-8. Data are presented in Figure 3.8.

Figure 3.8, A shows the IL-8 concentrations of RT4 cells challenged with 100μg/ml scleroglucan for 6, 12 and 24 hours respectively. The IL-8 concentrations increased from 894 ± 20 pg/ml (PBS challenge) to 1097 ± 54 pg/ml, 1023 ± 12 pg/ml and 1061 ± 42 pg/ml respectively.

Increasing the challenge time to 40 hours Figure 3.8,B did not affect the data with the concentration of IL-8 increasing from 547 ± 8.8 pg/ml (PBS challenge) to 673 ± 33 pg/ml. Increasing the scleroglucan concentrations to 250 and 500 μg/ml and challenging for 40 hours, were associated with increases in IL-8 concentrations 1040 ± 97 pg/ml and 917 ± 67 pg/ml.

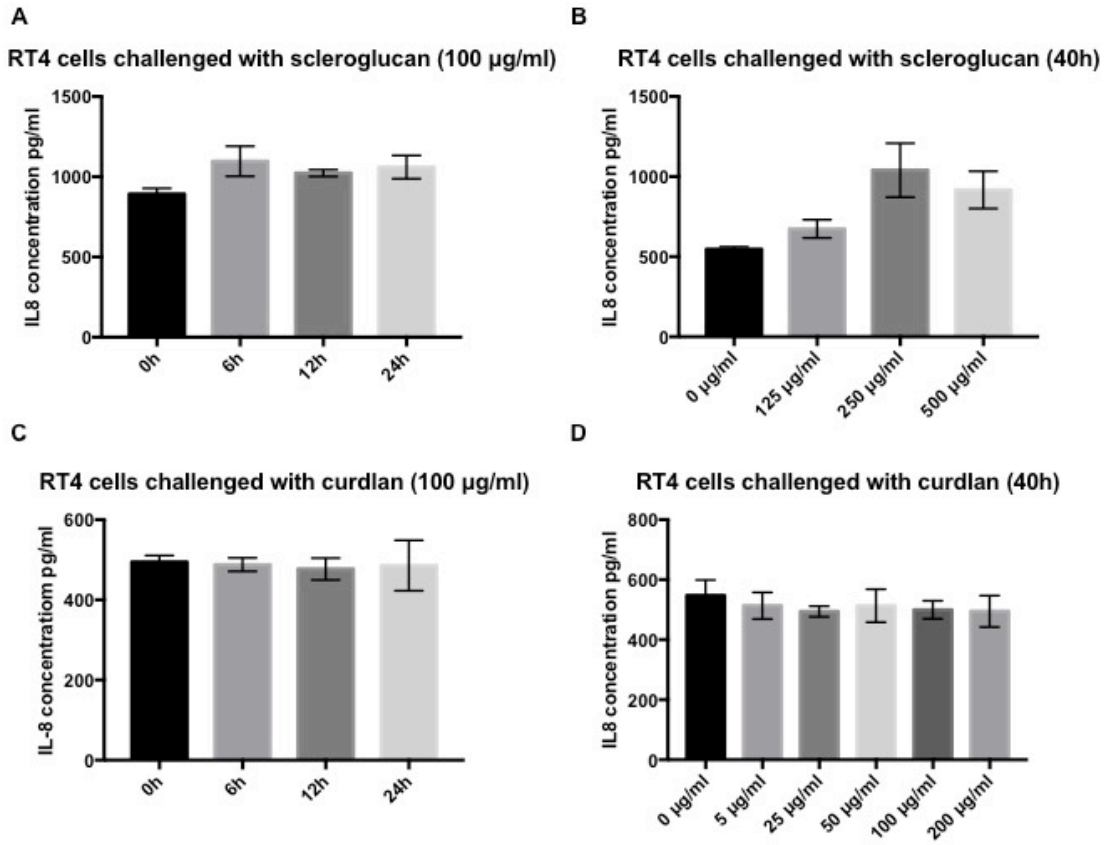

Figure 3.8 RT4 bladder cells challenged with either scleroglucan or curdlan.
A: IL-8 concentrations in RT4 cells following 100 µg/ml scleroglucan challenge at 6, 12 and 24h; B: IL-8 concentrations in RT4 cells following 40 hour scleroglucan challenge at concentrations of 125, 250 and 500 µg/ml; C: IL-8 concentrations in RT4 cells following 100 µg/ml curdlan challenge at 6, 12 and 24h; D: IL-8 concentrations in RT4 cells following 40 hour curdlan challenge at concentrations of 5 to 200 µg/ml. Data in A show mean ±SD and N=2; B – mean ±SD and N=2.

Similarly, confluent RT4 cells were challenged with 5, 25, 50, 100 and 200 µg/ml of curdlan for 6, 12, 24 and 40 hours respectively and IL-8 concentrations were measured using ELISA (Figure 3.8, C-D). Media IL-8 concentrations did not change after challenging the cells with 100 µg/ml of curdlan for 6, 12 and 24 hours compared to PBS challenged the cells (Figure 3.8, C). Similarly there were no significant changes in the IL-8 concentrations after challenging the cells with either 5, 25, 50, 100 or 200 µg/ml for 40 hours (Figure 3.8, D).

These data demonstrated that challenging the RT4 bladder cells with zymosan resulted in a rapid innate defence response (6 hours) when compared to that

seen using either scleroglucan or curdlan. The experiments using zymosan also demonstrated that a concentration of 50 μg/ml and challenge time of 6 hours were sufficient to trigger a Dectin-1R innate response in urothelial cells. These conditions were therefore used in subsequent experiments.

3.5 *CLEC7A* (Dectin-1R) knockdown in RT4 cells

The results of the challenge experiments provided novel data, which suggested that the Dectin-1R protein plays a key role in the urothelial innate defences. To explore this further and confirm these data it was necessary to knock-down *CLEC7A* (Dectin-1R) gene expression and repeat the challenge experiments. To reduce potential issues linked to variable knock-down resulting from transient gene knock-downs it was decided to engineer a RT4 cell line in which Dectin-1R gene expression was stably knocked-down. To achieve this knock-down the RT4 cells were stably transfected with a commercial siRNA, psiRNA-Dectin-1 (Invivogen), which expresses siRNA targeting *CLEC7A* (Dectin-1) gene expression (Figure 3.9).

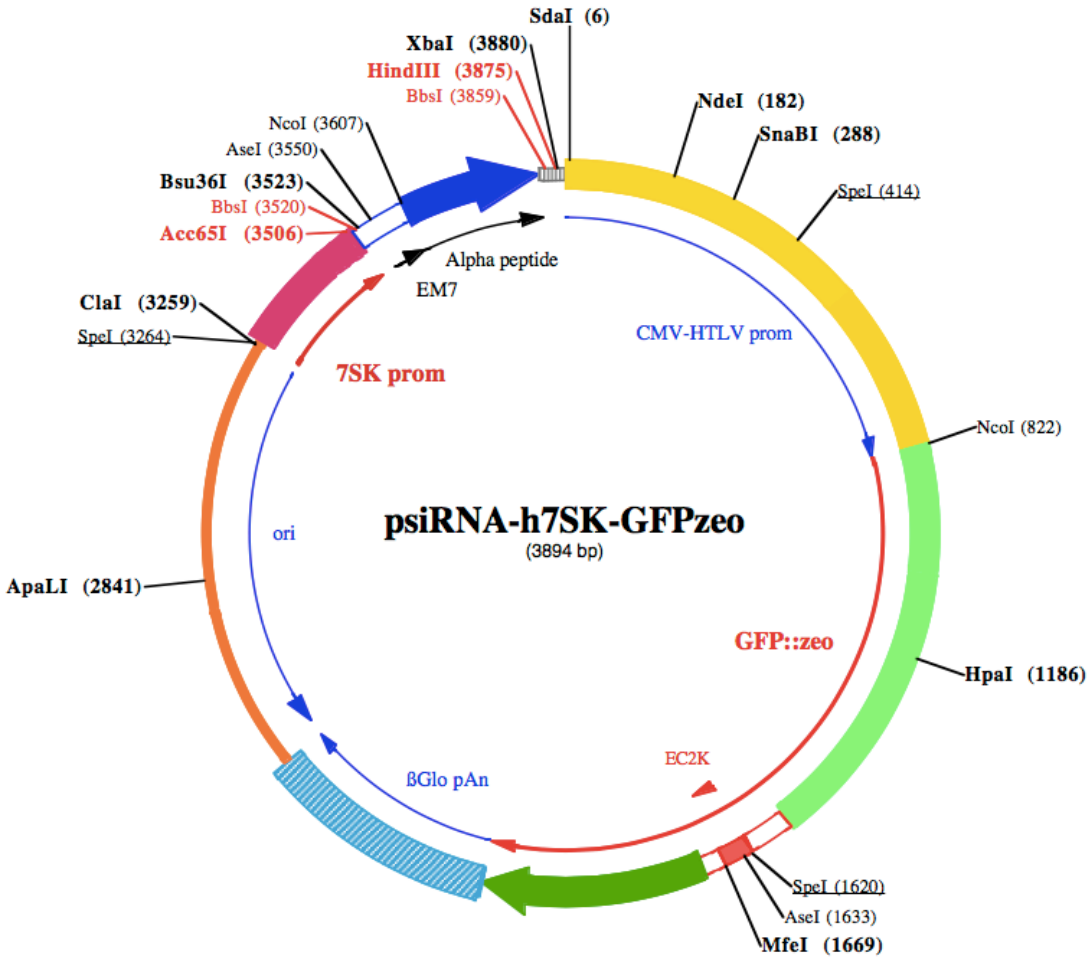

Figure 3.9 Plasmid vector psiRNA used to stably knock-down CLEC7A (Dectin-1R) gene expression in RT4 cells.
This plasmid contains the gene encoding resistance to the antibiotic zeocin (zeo) used to select stably transfected cells and the gene encoding GFP.

3.5.1 Cell transfection

Before transfection of the RT4 cells the plasmid psiRNA-Dectin-1 was amplified in *E. coli* and purified as described in Section 2.25. To validate the purified plasmid it was restricted with enzymes *Hin*dIII and *Nco*I, which as predicted produced DNA fragments of 2780 bp and 820 bp (Figure 3.10, A: lane 1) confirming the authenticity of the purified plasmid.

In addition the Dectin-1 siRNA fragment in the plasmid was amplified using End-Point PCR and analysed on an agarose gel (Figure 3.10, A: lane 2). The amplified DNA fragment of 210 bp was as predicted and this was confirmed by sequencing (Figure 3.10, B).

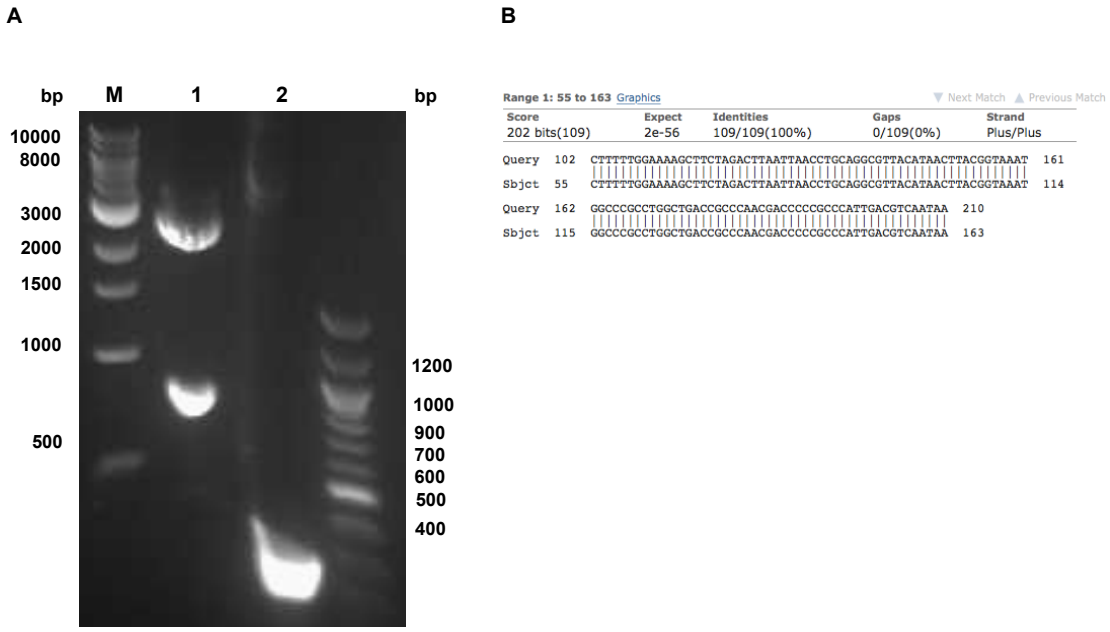

Figure 3.10 Analysis of psiRNA-Dectin-1 plasmid using restriction enzymes, End-Point PCR and sequencing.
A: M- base pair marker; Lane 1- Purified psiRNA-Dectin-1 plasmid restricted with *Hin*dIII and *Nco*I restriction enzymes; Lane 2 - Dectin-1 target sequence amplified using End-Point PCR. B: sequence data confirming Dectin-1 target sequence.

Once the plasmid was verified RT4 cells were transfected with the plasmid (Section 2.26) and cells expressing the siRNA selected using the antibiotic zeocin (100 µg/ml). Within two weeks zeocin resistant cells, which formed colonies, were identified (Figure 3.11). Surviving colonies were trypsinised, pooled, cultured, passaged, analysed and utilised in challenge experiments as a 'mixed colony' cell-line. Control RT4 cells were stably transfected with the psiRNA-Luciferase plasmid (siLuc) (Invivogen) and similarly selected using zeocin (100 µg/ml).

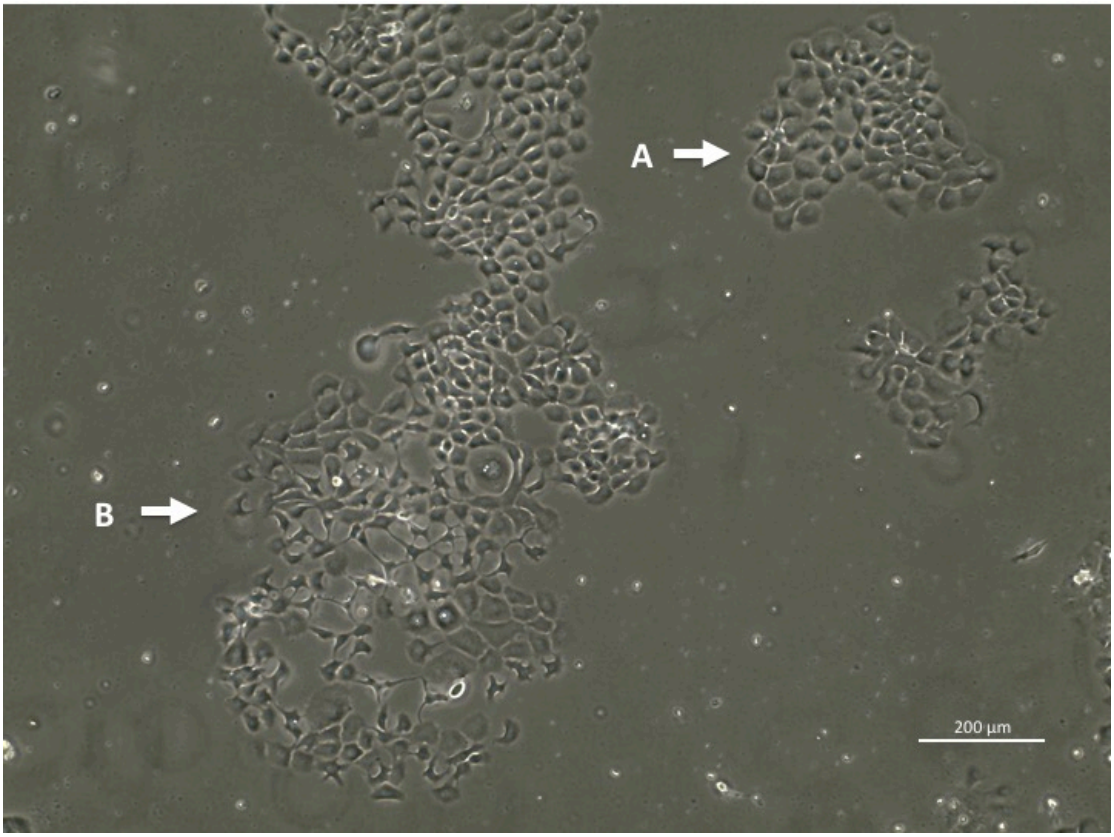

Figure 3.11 Colonies of RT4 cells expressing psiRNA-Dectin-1 and selected using zeocin containing (100 µg/ml) media.
A: a colony of surviving cells B: dying cells.

The psiRNA-Dectin-1R plasmid contains a GFP gene sequence (Figure 3.9), which is expressed in both bacteria and mammalian cells. Before any molecular or protein analyses were performed this property ie GFP expression was used to microscopically examine the pooled stably transfected RT4 cells. This approach was used as the engineered cell-line was a mix of cell clones and monitoring the cells visually for GFP variability, would provide information relating to the reproducibility of the *CLEC7A* (Dectin-1R) knock-down.

To achieve this the stably transfected cells were cultured to confluence on coverslips, fixed using 4% PFA and visualised using microscopy (Section 2.18). Typical data are shown in Figure 3.12. Panel A shows control RT4 cells stably transfected with psiRNA-Luciferase plasmid (siLuc) and panel B shows Dectin-1R knockdown RT4 cells (siDct1). While background fluorescence or auto-florescence, typified the control RT4 cells (A) the intensity of the florescence was

much stronger in the knockdown cells (B) confirming the presence and functioning of the plasmid, psiRNA-Dectin-1. Visual inspection suggested GFP expression was homogeneous which reduced the risk of variable Dectin-1R gene knock-down impacting subsequent data.

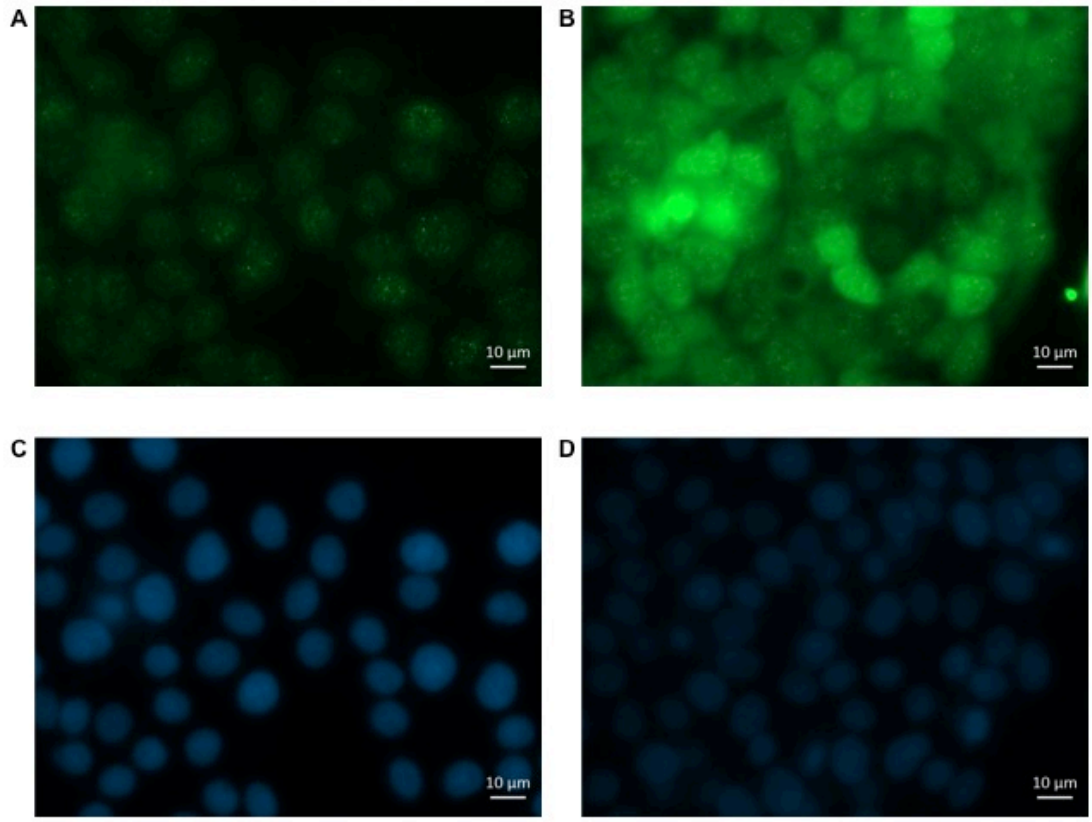

Figure 3.12 Microscopy of RT4 cells transfected with psiRNA-Luciferase and psiRNA-Dectin-1.
A: Control RT4 cells (siLuc), B: Dectin-1R knockdown RT4 cells (siDct1) examined for GFP (green colour), C: DAPI stained nuclei of siLuc RT4 cells, D: DAPI stained nuclei of siDct1 RT4 cells. Images were taken using Zeiss Axioimager II fluorescent microscope and 400x magnification.

Once the cells were verified for GFP expression using microscopy the effectiveness of the Dectin-1R knockdown in the stably transfected RT4 cells was examined using molecular (qRT-PCR) and protein (western blot) approaches.

Figure 3.13, A shows the results of the qRT-PCR analyses, in which Dectin-1R mRNA levels in RT4 cells transfected with psiRNA-Dectin-1 plasmid (siDct1) were compared to those in RT4 cells transfected with control psiRNA-Luciferase plasmid (siLuc). These data showed that the Dectin-1R mRNA level in the Dectin-

1R gene knock-down cells was 71 ± 5% (mean ± SEM; n=6) lower than that measured in the control cells. Figure 3.13, B shows the western data comparing Dectin-1R protein levels in knock down cells to those in the control cells. Using the anti-Dectin-1R antibody (AF1859), bands relating to Dectin-1R protein isoforms 1 and 4 (27 kDa and 17 kDa) were detected in the control RT4 cells (siLuc) (Figure 3.13, B). The same bands were detected in the western blots relating to the Dectin-1R knockdown cells, but the signals were significantly reduced, supporting effective receptor protein knock-down.

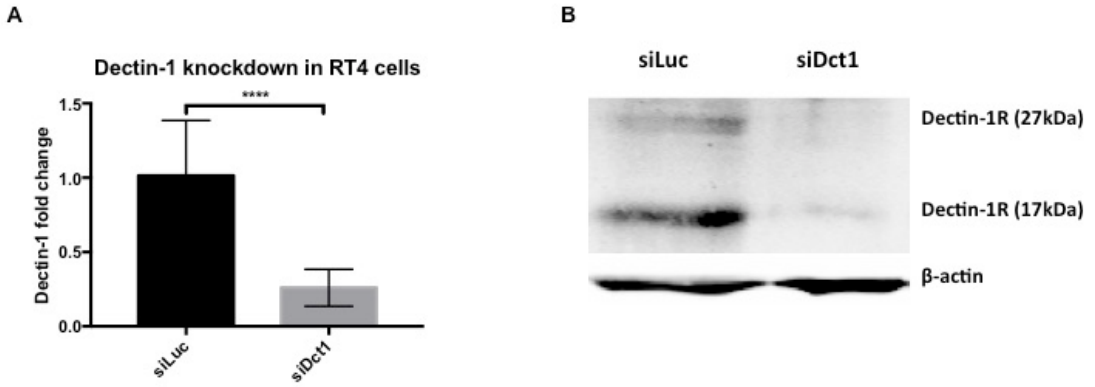

Figure 3.13 Dectin-1R mRNA expression and protein synthesis in Dectin-1 knock-down RT4 cells.
A: Fold change in Dectin-1R mRNA expression in Dectin-1R knockdown RT4 cells (siDct1) and control RT4 cells stably transfected with psiRNA-Luciferase plasmid (siLuc). B: Immunoblot of Dectin-1R proteins in Dectin-1R knockdown (siDct1) and control (siLuc) RT4 cells using anti-Dectin-1 antibody (1:50 dilution). mRNA expression data shows mean ±SD and N=4. **** $p<0.0001$. The western blot data represents two independent experiments.

These data confirmed that the RT4 cells were stably transfected with psiRNA-Dectin-1 plasmid and showed decreased expression of the *CLEC7A* (Dectin-1R) gene and synthesis of Dectin-1R. These data therefore suggested that this stably transfected cell line was a good model to further investigate Dectin-1R function in bladder epithelial cells.

3.5.2 CLEC7A (Dectin-1R) knockdown RT4 cells challenged with zymosan

The stably transfected Dectin-1R knockdown RT4 cells were used to confirm the roles of the Dectin-1R protein in sensing and responding to β-glucan in the bladder epithelia. These knockdown cells were challenged as previous with zymosan (50 µg/ml; 6h) and mRNA expression of *DEFB4*, *CXCL8* and *LCN2* measured by qRT-PCR. The resultant data demonstrated, interestingly, that the challenge was associated with the increased expression of *DEFB4* by 11.5 ± 2 and 27.7 ± 5.6 fold in the control (siLuc) and knockdown (siDct1) RT4 cells respectively (Figure 3.14, A.

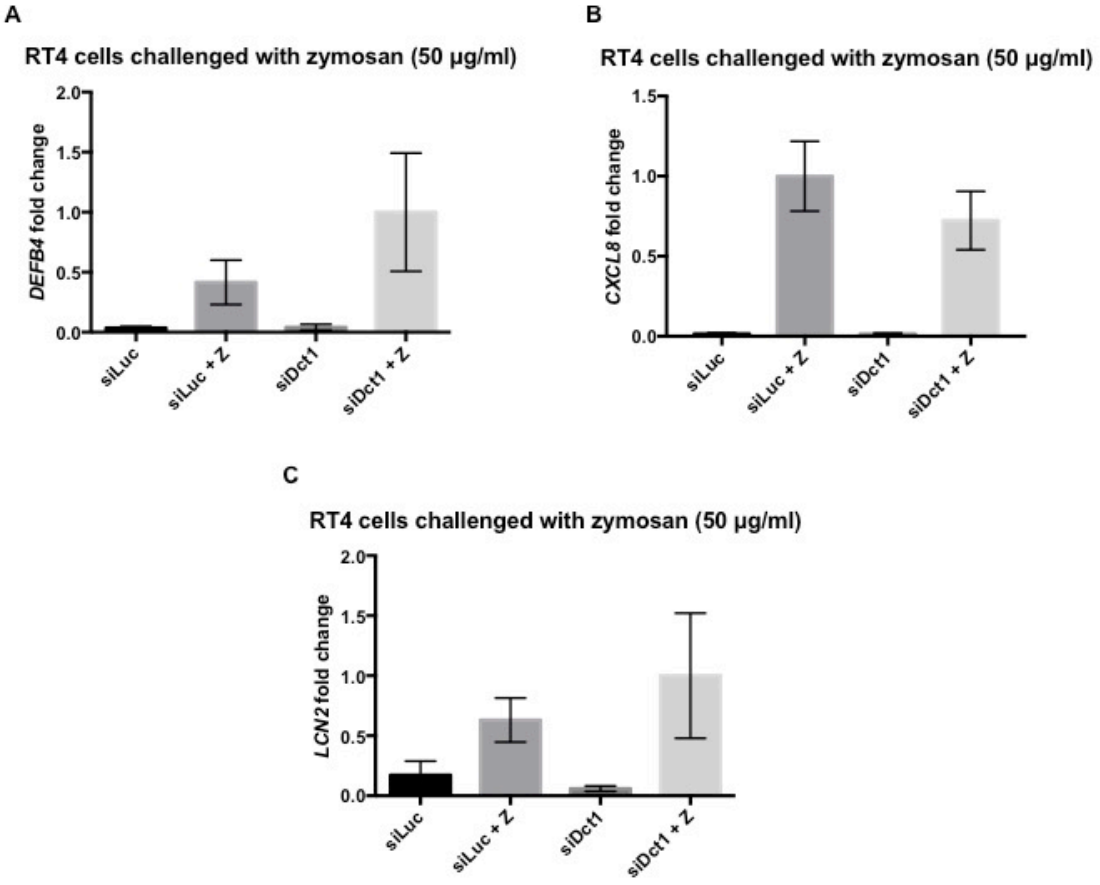

Figure 3.14 *DEFB4*, *CXCL8* and *LCN2* mRNA expression in siDct1 RT4 cells challenged with zymosan.
Panels show *DEFB4* (A), *CXCL8* (B) and *LCN2* (C) mRNA expression (fold change) in control RT4 cells (siLuc) and knock-down RT4 cells (siDct1) challenged with zymosan (50 µg/ml) for 6 hours. Data show mean ±SD and N=2.

Gene expression of *CXCL8* increased 65 ± 5.8 fold in the control cells (siLuc) and 47 ± 4.9 fold in the knock down cells (siDct1) following the zymosan challenge (Figure 3.14, B). However the knock down of *CLEC7A* (Dectin-1R) was associated with a 25% reduction in *CXCL8* expression compared to the control.

In response to the zymosan challenge *LCN2* gene expression increased 3.7 ± 0.4 fold in the control cells (siLuc) but 5.8 ± 1.2 fold in the knockdown cells (siDct1) (Figure 3.14, C). These data indicated that the challenged Dectin-1R knock-down cells expressed 60% more LCN2 compared to the control cells. However, these data were associated with large error bars.

However, these results demonstrated that challenging the Dectin-1R knockdown RT4 cells with zymosan impacted *DEFB4*, *CXCL8* and *LCN2* gene expression patterns. The knockdowns were associated with an increase in *DEFB4*, decrease in *CXCL8* but no change in *LCN2* gene expression.

Media bathing the cells was not collected from any of these experiments therefore these molecular data were not supported by effector protein measurements.

3.6 Dectin-1R blocking with antibody and challenging with zymosan

To help confirm these data a different approach was taken using the monoclonal anti-Dectin-1R antibody (MAB1859). This antibody was used to inhibit Dectin-1R functioning in RT4 cells prior to a zymosan challenge. The blocking antibody was used at two concentrations, 6 μg/ml and 3 μg/ml prior to the cells being challenged with zymosan (50 μg/ml) for 6h. Also non-specific IGG antibodies were used at 6 μg/ml in the control samples. These antibody concentrations were selected following manufacturer recommendations that indicated 100 and 50% blocking of the Dectin-1R respectively. In these experiments the media bathing the cells were analysed by ELISA for effector protein, IL-8 and LCN2, concentrations.

The IL-8 and LCN2 data are shown in Figure 3.15, which are presented as mean concentration and mean fold change.

Panel A shows that challenging the cells with zymosan resulted in increase of IL8 secretion from 590 ± 57 pg/ml to 3407 ± 325 pg/ml. When the cells were blocked with 6 or 3 μg/ml of antibody this response decreased significantly to 2384 ± 123 pg/ml and 2290 ± 251 pg/ml respectively ($p<0.01$). To address potential variability between experiments the data were also normalised to the control cells challenged with zymosan and similarly these data showed statistical significance ($p=0.001$) (Figure 3.15, C).

Data in the panel B demonstrated that challenging the cells with zymosan increased LCN2 media concentrations from 1126 ± 247 pg/ml to 3612 pg/ml ± 684 pg/ml. Blocking Dectin-1R with 6 or 3 μg/ml antibody resulted in a decrease in LCN2 concentrations to 1914 ± 495 pg/ml and 2216 ± 530 pg/ml respectively. However, this change was not statistically significant with p values of $p=0.33$ and $p=0.17$ respectively. When the data were normalised to the controls cells challenged with zymosan the decrease in LCN2 concentrations in the cells blocked with 6 μg/ml was shown to be statistically significant ($p=0.05$).

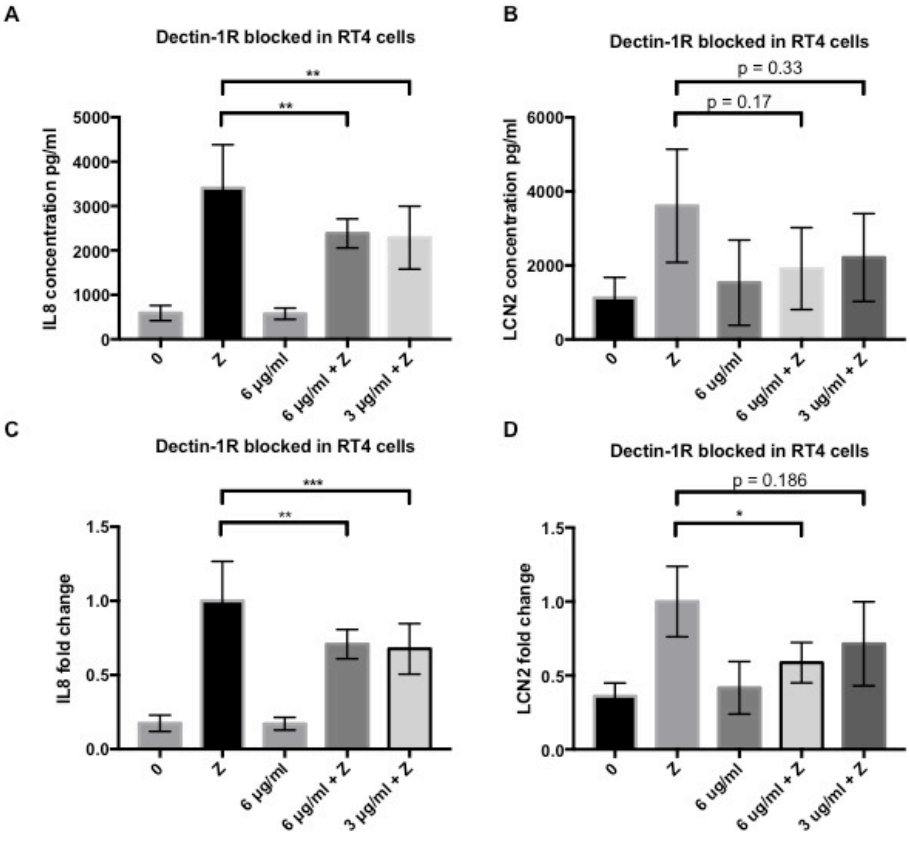

Figure 3.15 Dectin-1 blocking in RT4 cells and zymosan challenge.
A: IL-8 fold change in RT4 cells treated with Dectin-1R blocking antibody (6 µg/ml or 3 µg/ml) and challenged with zymosan (50 µg/ml) for 6 hours. B: LCN2 fold change in RT4 cells treated with Dectin-1R blocking antibody (6 µg/ml or 3 µg/ml) and challenged with zymosan (50 µg/ml) for 6 hours Data shows mean ±SD and N=3. * p=0.05.

Media hBD2 concentrations were also measured using ELISA, but in all cases the values measured were at or below the ELISA detection limit and these data have not been presented.

These data suggested that blocking of the Dectin-1 receptor protein and challenging with zymosan resulted in the decreased synthesis of IL-8 and LCN2 by the urothelial cells. These data were supportive of the molecular data reported using the Dectin-1R gene knockdown approach and validated a role for Dectin-1R in the innate response of urothelial cells to β-glucan and potentially β-glucan containing microbes.

3.7 TRL2 synthesis in RT4 cells

Previous studies demonstrated that zymosan could stimulate TLR2 in myeloid cells [74]. To investigate if TLR2 is present in RT4 cells a western blot was performed using RT4 cell lysate and anti-TLR2 antibodies. The data shown in Figure 3.16 did not suggest a TLR2 band in the RT4 sample, but a band representing TLR2 (90 kDa) was detected in the CHO cells.

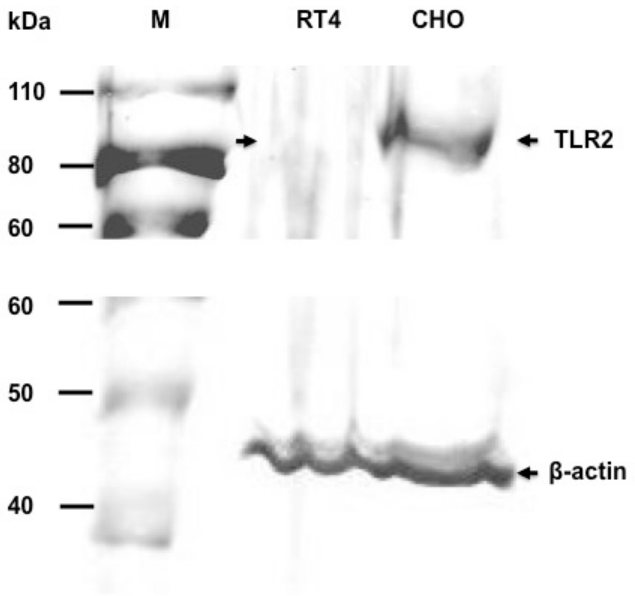

Figure 3.16 TLR2 synthesis in RT4 and CHO cells.
The immunoblot demonstrates synthesis of TLR2 (arrows) in RT4 and CHO cells. M - molecular weight marker. The blot shown is representative of two independent experiments.

3.8 Discussion

The work presented in this chapter investigated the gene (*CLEC7A)* expression and Dectin-1R protein synthesis in human bladder material and in RT4 bladder epithelial cells. It also exploited gene knock-down and antibody blocking approaches to explore the gene expression and protein synthesis of host defence peptides/proteins including hBD2, IL-8, LCN2 and IL1α in RT4 bladder cells challenged with zymosan. Zymosan is a Dectin-1R agonist, which contains β-

glucan and was used to model potential bladder pathogens containing β-glucan challenging the urinary tract tissues.

Analysis of human bladder biopsy revealed the expression of *CLEC7A* (Dectin-1R) gene transcripts with a strong cDNA band of 330 bp linking directly to the synthesis of a 25 kDa receptor protein (Figure 3.1, B). However, these data were limited in that only one bladder biopsy sample was analysed. These data would therefore be strengthened by analyses of additional bladder samples from both male and female donors. Also as there was no clinical data to either support or refute that the donor was suffering a urinary tract infection it cannot be ignored that these data actually reflected an infected state. However, this was extremely unlikely as the ethics governing biopsy procedure precluded any sampling of patients suffering an active infection.

The bladder biopsy data did however support Dectin-1R synthesis, which inferred the receptor to function directly in the bladder innate defences. Importantly however, contamination of the bladder sample with blood and therefore myeloid derived cells such as macrophages and dendritic cells, which are known to synthesise Dectin-1R [116, 128, 129] cannot be excluded. Therefore to further explore the roles of the Dectin-1R in the bladder epithelium an in vitro approach was adopted and the RT4 urothelial cell-line which closely models the bladder was selected for all further studies [119].

Molecular analyses of the RT4 cell RNA revealed five Dectin-1 cDNA bands reflecting five different transcripts including those encoding Dectin-R isoforms 1 and 2 identified in the bladder biopsy (Figure 3.2, A). The most intense band related to cDNA band 4 although the corresponding encoded protein isoform was not detected in the bladder biopsy. Interestingly it has been reported previously that this isoform cannot bind zymosan and regulatory roles, comparable to other cell receptors including CD40 and scavenger receptor type A, have been attributed to its function [102].

Interestingly immunoblotting of RT4 material detected the non-functional isoform 4 (17 kDa) protein band, but also isoforms 1 and 2 (27 kDa and 25 kDa respectively) that link to functional Dectin-1Rs. The major difference between

Dectin-1R isoform 4 and isoforms 1 and 2 is that isoform 4 has a shorter carbohydrate binding domain and four cysteine amino acids compared to six, which prevents it, structurally, from binding zymosan. None-the-less, since human bladder and RT4 cells both synthesised the functional Dectin-1R isoforms 1 and 2, RT4 cells were chosen as an appropriate *in vitro* model to investigate Dectin-1R functioning in the innate protection of the bladder epithelium.

To date there has been little research relating to Dectin-1R synthesis and functionality in epithelia. Dectin-1Rs have been identified in the gut, lung and cornea [91, 130, 131], which like the bladder are directly exposed to potential fungal infections from organisms including the yeast *Candida*. However, most of the Dectin-1R research has focussed on the innate protection mechanisms operating in myeloid derived cells including monocytes, macrophages and dendritic cells [116, 120, 128, 129, 132].

Eight Dectin-1R isoforms have been shown to be produced in human macrophages [102], with two major isoforms known as A and B, corresponding to isoforms 1 and 2 in this study. These data suggest that regardless of tissue isoforms 1 and 2 are key receptors functioning to help protect against infection from β-glucan containing microbes. Isoform 1 is characterised by a carbohydrate binding domain bound to a stalk region, while isoform 2 lacks the stalk. In relation to functionality it has been shown in murine fibroblasts that the full-length Dectin-1R (isoform A/isoform 1) binds β-glucans with higher affinity at temperatures lower than 37°C than the truncated isoform (isoform B/isoform 2) [101] although the functional significance of this observation remains to be determined.

Challenging RT4 bladder cells with zymosan, which is a natural ligand of the Dectin1R, resulted in the upregulation of genes encoding innate host defence effector molecules including hBD2, IL-8 and LCN2 within a six hour period. Gene knockdown and antibody blocking studies confirmed the role of the Dectin-1R and supported the receptor functioning as a key player in the innate protection of the bladder tissue. This probably extends to the uro-genital tract as previous work in the laboratory showed, using the vaginal epithelial cell line VK2 E6/E7

that hBD2 synthesis is increased in response to zymosan [83]. Similarly, hBD2 and IL1α up-regulation were reported in PK E6/E7 cells [123].

HBD2 is a potent microbial killing agent and activator of antigen presenting cells [47, 133, 134] and it has also been shown to be synthesised in response to zymosan challenge in epithelial cells [40, 131]. Similarly secretion of the pro-inflammatory molecule, IL-8, has been widely reported in various cells and in response to various β-glucans [122, 135, 136]. The data reported in this study in relation to LCN2 is novel although upregulation of *LCN2* gene expression has been shown in primary hepatic cells challenged with zymosan [137]. The scarcity of LCN2 data probably relates to fact that most Dectin-1R research relates to myeloid derived cells, which do not synthesise LCN2.

In fact data from studies focussed on human DCs, monocytes and macrophages have reported that zymosan can stimulate the secretion of a number of pro-inflammatory cytokines including IL1β, IL-6, IL-12, TNF-α and anti-inflammatory cytokines namely IL-10 [121, 135, 138]. In contrast data from this study, focussed on bladder RT4 cells, suggested no change in the expression of genes encoding either IL1β, IL-6 or IL-10. These data suggest that the response of epithelial cells to β-glucan containing microbes may differ slightly when compared to that of myeloid derived cells and that this response may reflect the defence mechanisms operating. For example, while macrophages and dendritic cells can switch on phagocytosis to clear potential pathogens from an infection site, epithelial cells do not have this option. Epithelial cells need to kill pathogens directly e.g. through the synthesis of direct killing agents such as the defensins and LCN2; their back-up is the synthesis of pro-inflammatory molecules that attract other immune cells to the infection site and which function as reinforcements.

Increasing the zymosan challenge concentration from 50 μg/ml to 200 μg/ml did not significantly affect the IL-8 concentrations measured at 6 hours in the media bathing the RT4 cells (Figure 3.7, A). This observation contrasted to the increased IL-8 concentrations observed in whole blood cells challenged with increasing doses of zymosan [124]. These RT4 bladder cell data therefore

suggest that either the Dectin-1 receptors on the RT4 cells were saturated at 50 μg/ml zymosan or that IL-8 expression was regulated by a negative feedback loop mechanism functioning presumably to control inflammation and prevent cell damage. The fact that the IL-8 data at 6 hours post challenge was also comparable to the 16 and 24 hour data (Figure 3.7), supported a negative feedback loop mechanism. Interestingly, it has been shown in monocytes that the IL-8 concentration increased, but then stabilised after 8 hours of stimulation with zymosan [136], again suggesting that there are factors operating to control IL-8 production and the inflammatory response.

This pattern was not observed with LCN2 as increasing concentrations of zymosan were associated with significantly increased LCN2 concentrations (Figure 3.7, B). These data probably reflect the killing mechanism of the effector. Essentially LCN2 is a potent microbial killing agent that directly targets microbes. Therefore its synthesis is in direct response to β-glucan concentrations which *in vivo* reflect pathogen numbers. It would have been optimal for these LCN2 data to be supported by hBD2 data. However, issues with the hBD2 ELISA relating different batches of antibody meant these data were not available.

Interestingly knock-down of the *CLEC7A* (Dectin1- R) gene was associated with increased *DEFB4* and *LCN2* gene expression (Figure 3.14, A & C). These observations were difficult to explain and thought initially to reflect technical issues. However, focussing on LCN2 the effect was also observed in experiments described in chapter Chapter 4 and these data are discussed further in the discussion accompanying chapter Chapter 4.

The ability of RT4 cells to respond to other Dectin-1R ligands was investigated by challenging RT4 cells with the polysaccharides scleroglucan and curdlan. Scleroglucan consists of β-(1-3)-linked and β-(1-6)-linked glucose residues, while curdlan contains β-(1-3)-linked glucose residues. These β-glucans have been reported to bind to Dectin-1 receptors and stimulate the production of pro-inflammatory cytokines in blood cells including monocytes, macrophages and dendritic cells [124, 127, 139, 140]. Scleroglucan, but not curdlan, induced IL-8 synthesis in the RT4 bladder cells. This was surprising as curdlan comprises β1-3

linked glucose residues and has been shown in other studies using macrophages, dendritic cells and lymphocytes to induce pro-inflammatory molecules including TNFa, IL6, IL2, IL8 and IL12 [124, 125, 141]. These data therefore indicated that either the size and/or structure of curdlan did not facilitate Dectin-1R binding/signalling in RT4 cells.

The curdlan used was sourced commercially and is purified from the soil bacterium, *Alcaligenes faecalis*. Unlike antigen presenting cells circulating in the blood the bladder tissues are less likely to be exposed to a soil organism. Therefore it is feasible that the RT4 bladder Dectin-1R proteins bound the β-glucan material relating to *A.faecalis,* but that binding did not result in a signalling cascade and an effector response. However, as *Sclerotium rolfsii* used to purify scleroglucan is also a soil organism this seems unlikely. It is also feasible that the *A.faecalis* preparation was not pure and contained molecules that inhibited curdlan binding to the RT4 bladder Dectin-1R proteins although this needs further investigation for example by using different sources and batches of curdlan.

It is acknowledged that the zymosan preparation used in these challenges was also not pure and was probably contaminated with LPS, which stimulates Toll-like receptors 2 and 4 [142]. The argument could be made therefore that it was the LPS and not the β-glucan that triggered the effector response in the bladder RT4 cells. However, it has been shown previously that challenging RT4 cells with LPS for 6 hours does not stimulate a significant host effector response [40] suggesting that LPS was not directly responsible for the effects observed following the zymosan challenges. Additionally incubating RT4 cells with antibody to TLR2 before challenging with zymosan (50 μg/ml for eight hours) did not affect the NF-κB signalling response [83], which supports a direct zymosan-Dectin-1R effect.

In summary these data demonstrated that RT4 bladder cells expressed transcripts encoding five potential Dectin-1R isoforms and the synthesis of two isoforms – a full-length Dectin-1R (isoform 1) and a truncated Dectin-1R (isoform 4) was detected. The Dectin-1R ligands zymosan and scleroglucan

stimulated the expression of genes encoding the host defence effector molecules hBD2, IL1α, IL-8 and LCN2. Gene (*CLEC7A*) knockdown and antibody blocking of Dectin-1R confirmed that zymosan stimulated the Dectin-1 receptor to activate the synthesis of pro-inflammatory molecules eg IL-8 and host antimicrobial agents eg LCN2. However, it is not known from the knock-down and antibody blocking data, which Dectin-1R receptor, isoform 1 or 2 or both, were responsible for the host effector response. To explore this further isoform specific knock-down experiments will be necessary.

Chapter 4. Co-operation of Dectin-1R and TLR5 in RT4 cells

Data reported in previous chapter supported the presence of functional Dectin-1Rs on urothelial cells. The fact that these receptors responded to β-glucan (zymosan) through the increased synthesis of host defence peptides/proteins suggested important roles for the receptors in the innate defence of the urothelial tissues. Additionally these data predict that the receptors respond to and help defend against β-glucan containing microbes, specifically yeasts which can contaminate the urinary tract through the gut-faecal route.

The urinary tract as discussed in Section 1.2 (page 5) is susceptible to infection by uropathogenic bacteria, which are characterised by the presence of flagella and their motility. Uropathogenic bacteria such as uropathogenic *Escherichia coli* (UPEC) are detected via TLR5 receptors located on host bladder cells, which respond to flagellin proteins by activating the innate host antimicrobial defences [40]. Interestingly previous data from the laboratory exploring TLR5 NFκB signalling responses showed that blocking TLR5 functionality in RT4 bladder epithelial cells and challenging with zymosan reduced NF-κB signalling (Figure 4.1; [83]), which hinted at potential cooperation between Dectin-1R and TLR5 receptors in the bladder epithelial cells. These data were surprising as the literature, albeit focussed on antigen presenting cells, suggests that Dectin-1R cooperates with TLR2 and TLR4, but not TLR5 [103, 104, 129, 143] and that TLR5 unlike other TLRs only functions as a homodimer [78, 118, 144].

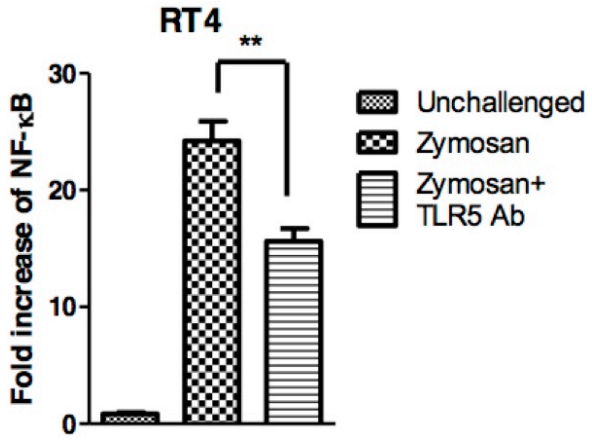

Figure 4.1 NF-κB activity in RT4 cells in which TLR5 was blocked with antibody and challenged with zymosan. (Lanz, 2013) [83].

Using the RT4 bladder cell line this Chapter aimed to further explore the potential TLR5/Dectin-1R relationship in urothelia.

4.1 Immunostaining of Dectin-1 and TLR5 proteins in RT4 cells

Immunocytochemistry, using antibodies raised to the Dectin-1R (monoclonal, R&D systems, MAB1859) and TLR5 (polyclonal, Abcam, ab37071) receptors was initially utilised to confirm Dectin-1R and TLR5 synthesis in the bladder RT4 cells and to explore potential co-localisation of the two receptors (Section 2.16).

Data presented in Figure 4.2 show TLR5 (blue), Dectin-1R (green) immunostaining in RT4 cells challenged with zymosan (50 μg/ml, 6h). Panel A demonstrates RT4 cell nuclei stained with propidium iodide (red), panel B shows immuno-staining with TLR5 and panel C staining with Dectin-1R antibodies respectively. Panels E and F show results of staining with IgG control antibodies and secondary Alexa Fluor 488 or 350 antibodies. Interestingly the Dectin-1R immuno-staining was characterised by regions of punctate staining. In panel D the channels detecting Alexa 488 and Alexa 350 were merged with the resultant cyan colour indicating co-localisation of TLR5 and Dectin-1R.

These data suggested co-localisation of the TLR5 and Dectin-1 receptors following a zymosan challenge of RT4 bladder cells.

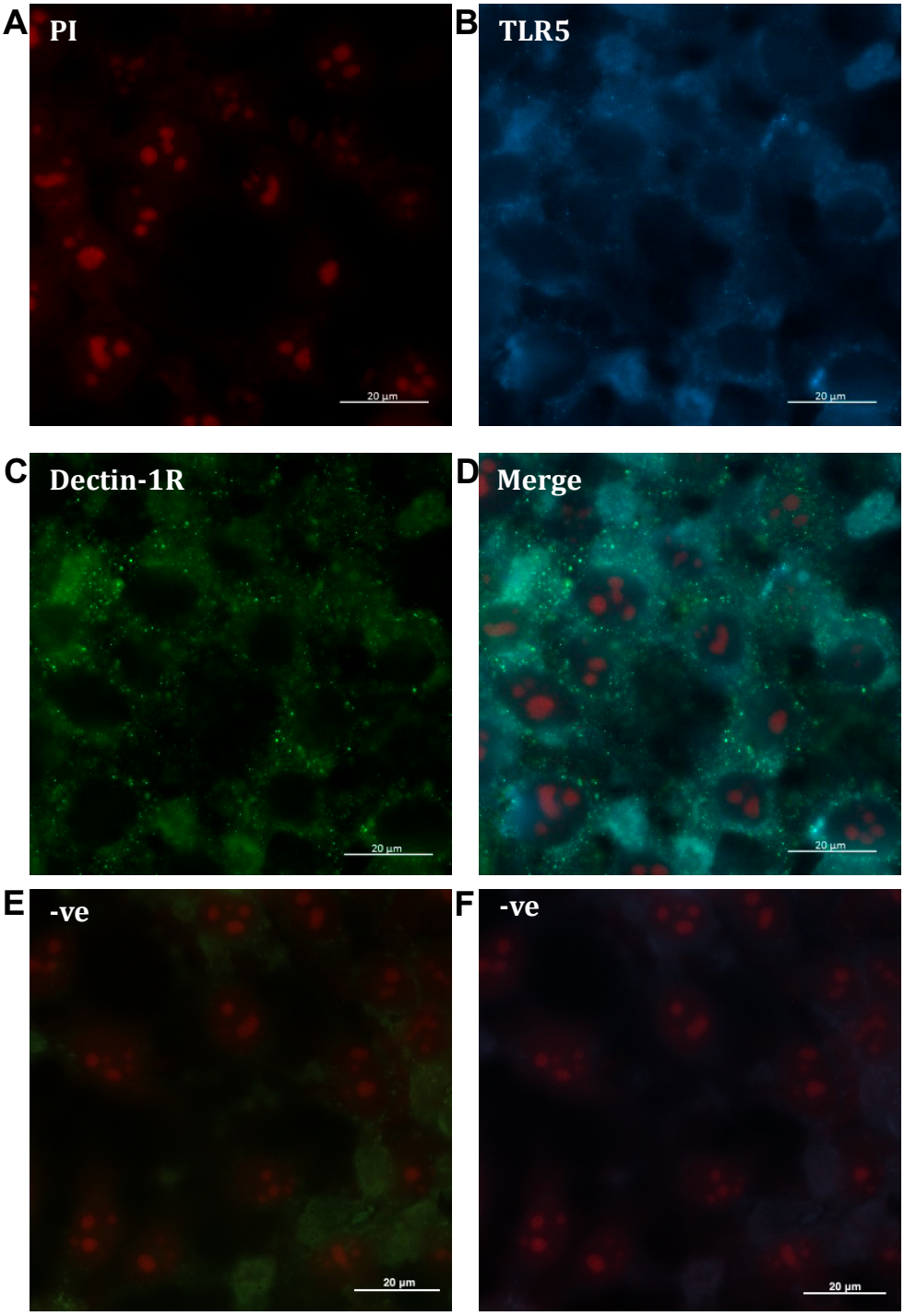

Figure 4.2 Immunostaining of Dectin-1R and TLR5 in RT4 zymosan challenged cells.
RT4 cells were challenged with zymosan (50 µg/ml, 6h) then fixed with 4% formaldehyde and incubated overnight with anti-Dectin-1 and anti-TLR5 antibodies (dilutions 1:50). A: nuclei stained with propidium iodide; B: RT4 cells stained with anti-TLR5 antibody; C: RT4 cells stained with anti-Dectin-1R antibody; D: merged red, blue and green channels; E and F: RT4 cells stained with IgG control antibodies and secondary Alexa Fluor 488 or 350 antibodies.

4.2 Expression and synthesis of host defence peptides/proteins in siTLR5 RT4 cells challenged with zymosan

To further investigate co-operation between the Dectin-1R and TLR5 receptors and/or signalling response siRNA knock-down methodology was used. This focussed initially on repeating the Lanz experiment, but using a *TLR5* knock-down approach. Using siRNA primers designed to *TLR5* (Section 2.28), *TLR5* expression was transiently reduced by 73% ($p < 0.0001$) in the RT4 cells (Figure 4.3).

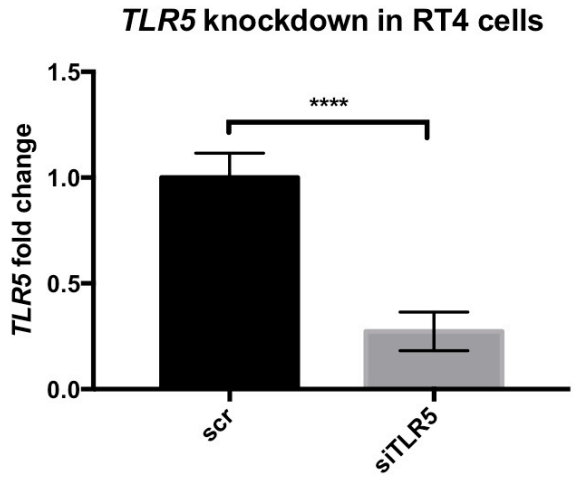

Figure 4.3 Efficiency of *TLR5* knockdown in RT4 cells.
TLR5 was knocked down in RT4 cells using siRNA technology and *TLR5* gene expression measured using qRT-PCR. N=3, **** $p<0.0001$.

4.2.1 Expression of *DEFB4*, *CXCL8*, *IL1A* and *LCN2* genes in siTLR5 RT4 cells challenged with zymosan

Following *TLR5* gene knockdown the RT4 cells were challenged with zymosan (50 μg/ml) for 6 hours and analysed using qRT-PCR for the gene expression of an array of effectors, specifically *DEFB4* (encodes hBD2), *CXCL8* (encodes IL8), *IL1A* (encodes IL1α) and *LCN2* (encodes LCN2). To address variability between experiments the expression data were normalised to the control cells (transfected with scrambled siRNA) similarly challenged with zymosan (scr + Z). Data presented in Figure 4.4, A shows that reduced *TLR5* gene expression was

associated with a significantly reduced *DEFB4* expression ($p<0.001$). Similarly the expression of *CXCL8* ($p<0.0001$), *IL1A* ($p<0.0001$) and *LCN2* ($p<0.01$) were significantly reduced.

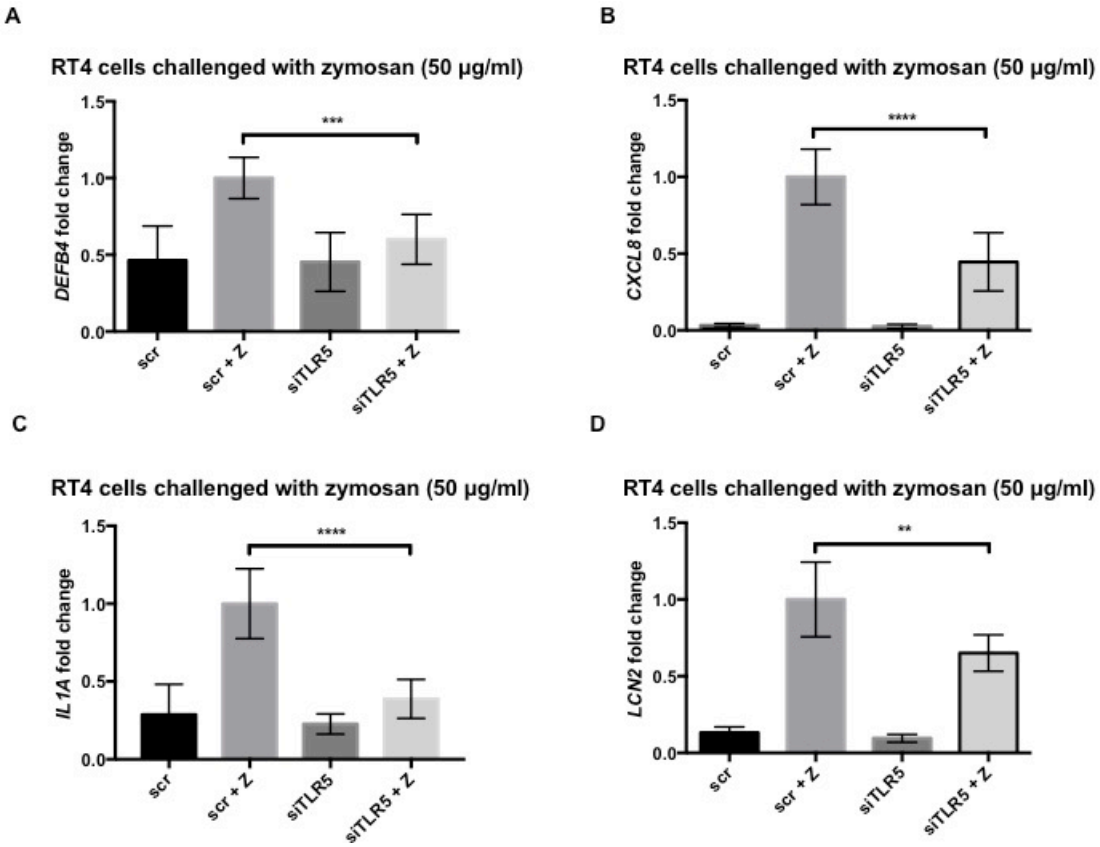

Figure 4.4 *DEFB4*, *CXCL8*, *IL1A* and *DEFB4* mRNA expression in siTLR5 RT4 cells challenged with zymosan.
Panels A, B, C and D show *DEFB4*, *CXCL8*, *IL1A* and *LCN2* mRNA expression synthesis in control RT4 cells (scr) and RT4 cells in which *TLR5* was reduced (siTLR5) before and after zymosan (50 µg/ml) challenge. Data shows mean ±SD and N=2. ** $p<0.01$, *** $p<0.001$, **** $p<0.0001$.

These data showing reduced *DEFB4*, *CXCL8*, *IL1A* and *LCN2* gene expression in *TLR5* knockdown RT4 cells challenged with zymosan added further support to the NF-κB data of Lanz (2013) [83]. As zymosan is acknowledged as containing β-glucan, a ligand that specifically activates the Dectin-1R receptor, these data again suggested cooperation between the Dectin-1 and TLR5 receptors in RT4 cells.

4.2.2 IL-8 and LCN2 protein synthesis in siTLR5 RT4 cells challenged with zymosan

To further investigate cooperation between Dectin-1R and TLR5 the synthesis of the host defence peptides/proteins IL8 and LCN2 were investigated. In these analyses the media from the control cells (transfected with scrambled siRNA) and *TLR5* knockdown RT4 cells were collected and ELISA used to measure IL8 and LCN2 concentrations.

Data presented in Figure 4.5 panel A shows that the concentration of IL8 increased from 1438 ± 304 pg/ml in unchallenged cells to 4044 ± 849 pg/ml in the zymosan challenged cells. However, in the *TLR5* knock-down cells challenged with zymosan the IL8 concentration increased to only 2158 ± 458 pg/ml. Essentially the challenged *TLR5* knockdown cells secreted 50% less IL8 compared to the challenged control cells. However, to account for experimental variability, these data were normalised to that of the control cells challenged with zymosan (scr + Z) (Figure 4.5, B.

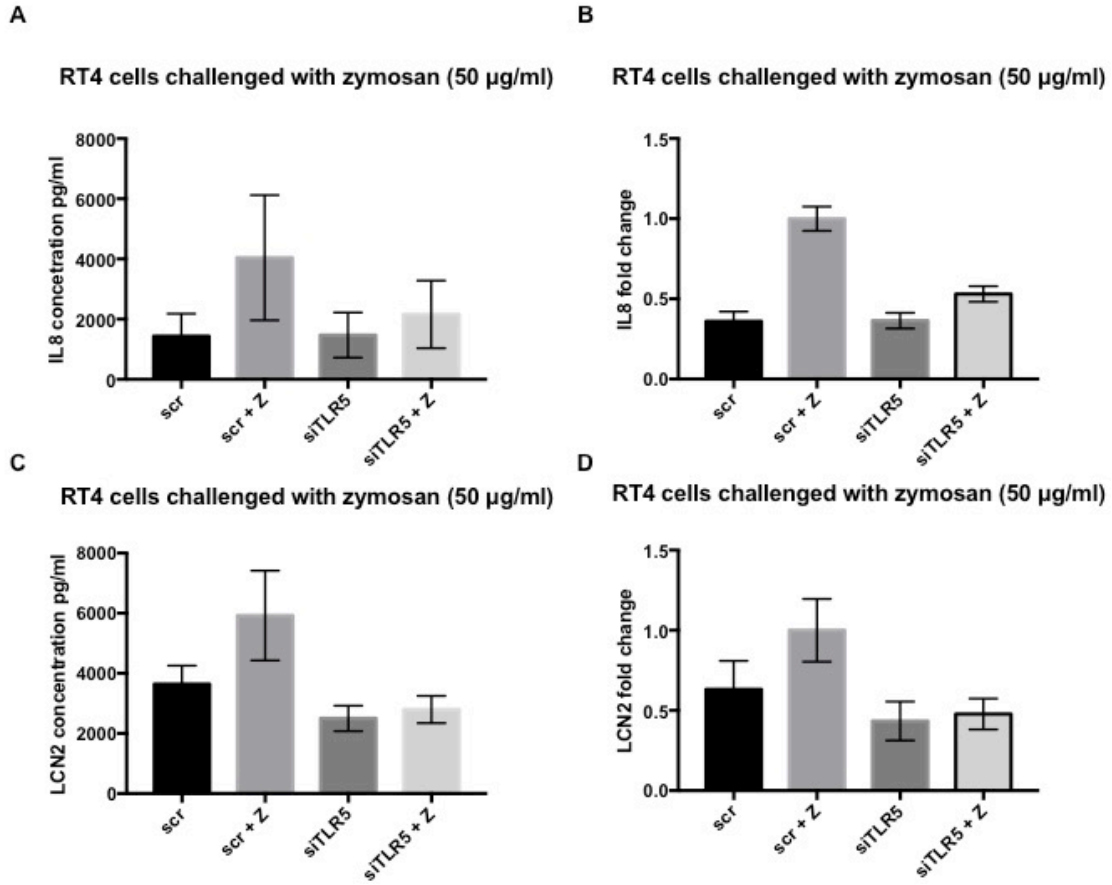

Figure 4.5 IL8 and LCN2 protein synthesis in siTLR5 RT4 cells challenged with zymosan (50µg/ml; 6h).
Panels A and C show IL8 and LCN2 concentrations in control RT4 cells (scr) and *TLR5* knock-down RT4 cells (siTLR5). In the panels B and D the data were normalised to the challenged control cells (scr + Z). The cells were challenged with zymosan (Z) (50 µg/ml) and ELISA was used to measure concentration IL8 and LCN2 in growing medium. Data shows mean ±SD and N=2.

Similarly the results in Figure 4.5 panel C indicated that LCN2 synthesis was affected in the TLR5 knockdown RT4 cells challenged with zymosan. The concentration of LCN2 was 3640 ± 252 pg/ml in siRNA control cells which increased to 5923 ± 609 pg/ml in the zymosan challenged cells. In the TLR5 knockdown cells LCN2 synthesis increased from 2502 ± 173 pg/ml to 2800 ± 185 pg/ml following incubation with zymosan. Interestingly LCN2 secretion by knockdown cells (siTLR5) was lower by 31% compared to the control cells (scr) however this difference was not statistically significant.

These data indicated that IL-8 and LCN2 synthesis were reduced in the challenged TLR5 knockdown cells, again supporting cooperation between Dectin-1 and TLR5 receptors in RT4 bladder cells.

4.3 *CLEC7A* knockdown cells challenged with flagellin

To explore co-operation further the reciprocal experiment was performed in which the *CLEC7A* gene (encodes Dectin-1R) was knocked down in RT4 cells (siDct1 – stable knock-down; siLuc – control Section 2.28) and the cells challenged with flagellin, the TLR5 ligand (100 ng/ml; 6h). In these analyses only gene expression was measured and using qPCR targets were *CXCL8*, *IL1A* and *LCN2* respectively. *DEFB4* gene expression was measured but the resulting values were below the qRT-PCR detection limits and these data are not reported.

Flagellin challenge of the Dectin-1R knock-down cells resulted in the increased expression of *CXCL8* in siLuc (control) and siDct1 cells, with these data (Figure 4.6, A) revealing 14 ± 0.5 fold and 11.4 ± 0.7 fold increases respectively. However the mean increase in *CXCL8* was 20 % reduced in the challenged Dectin-1 knock-down cells (siDct1 + F) compared to the challenged control cells (siLuc + F) and this difference was statistically significant ($p < 0.001$).

Expression of *IL1A* in the challenged control (siLuc) and knockdown (siDct1) cells increased by 2.5 ± 0.15 fold and 1.6 ± 0.13 fold respectively (Figure 4.6, B). The mean increase of *IL1A* was 40% lower in Dectin-1 knock down cells (siDct1 + F) compared to the control cells (siLuc + F) and this difference was statistically significant with $p < 0.0001$.

Flagellin challenge increased *LCN2* in the control cells (siLuc) and knockdown cells (siDct1) by 4.3 ± 0.52 fold and 8 ± 1.65 fold respectively (Figure 4.6, C). The mean increase of *LCN2* in the knockdown cells (siDct1 + F) increased by 82% compared to the control cells (siLuc + F). The mean increase of *LCN2* was 75% lower in the knockdown cells (siDct1) compared to the control cells (siLuc), but this difference was not statistically significant ($p=0.86$).

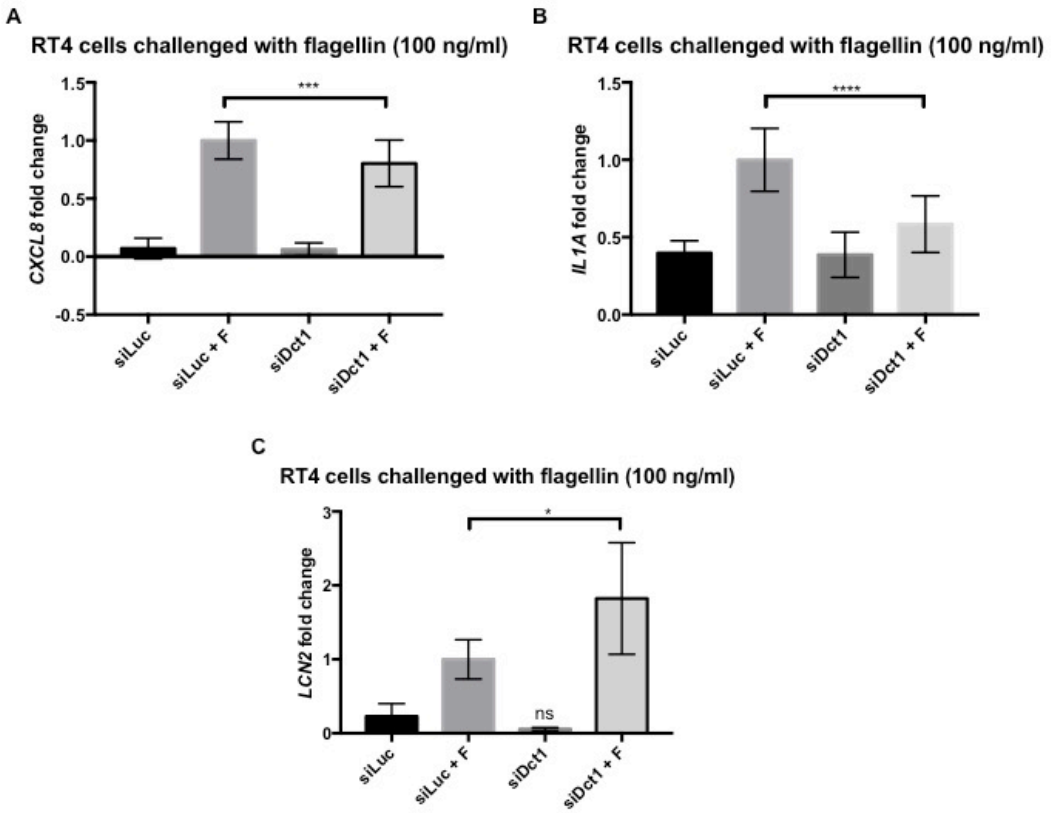

Figure 4.6 *CXCL8*, *IL1A* and *LCN2* mRNA expression in siDct1 RT4 cells challenged with flagellin.
Panels A, B and C demonstrate *CXCL8*, *IL1A* and *LCN2* mRNA expression by control RT4 cells (siLuc) and *CLEC7A* knock-down RT4 cells (siDct1) challenged with flagellin (100 ng/ml) for 6 hours. Data show mean ±SD and N=4. * $p<0.05$, *** $p<0.001$, **** $p<0.0001$.

Overall, these data reported in Figure 4.6 showed that in *CLEC7A* knockdown RT4 cells challenged with flagellin significantly less *CXCL8* and *IL1A* expression were observed when compared to the wild type cells. However expression of *LCN2* was significantly higher. Again these data suggested cooperation between Dectin-1R and TLR5 receptors.

It is acknowledged that these data relate to gene expression only and as such still need to be supported by protein data by measuring IL8, IL1α and LCN2 protein concentrations in the challenged siLuc and siDct1 cells.

4.4 Proximity ligation assay (PLA)

Immunostaining data presented in Section 4.1 supported co-localisation of the Dectin-1R and TLR5 receptors, while effector data shown in sections 4.2 and 4.3 suggested receptor co-operation/collaboration. To investigate potential physical interactions between the Dectin-1R and TLR5 receptors in RT4 cells the proximity ligation assay approach was used (Figure 4.7). This assay detects interactions between two proteins when the distance between them is less than 40 nm [145]. The technique utilises primary antibodies to Dectin-1R and TLR5, and unique secondary antibodies, which if close enough to each other ligate resulting in a fluorescent signal.

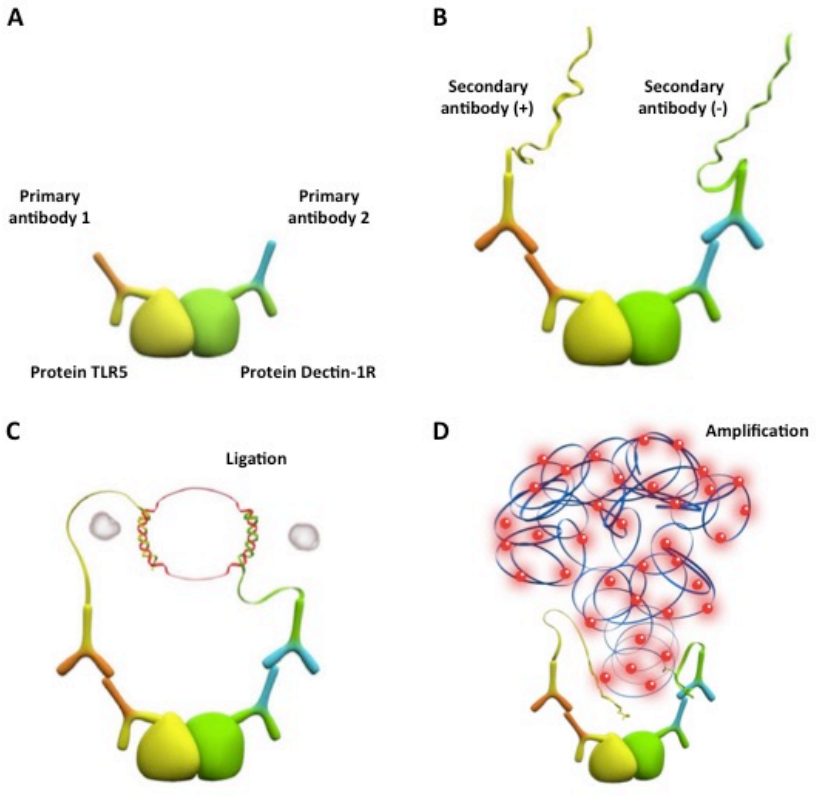

Figure 4.7 Proximity ligation assay.
(A) Primary antibodies bind to proteins TLR5 and Dectin-1R; (B) secondary antibodies bind to the primary antibodies; (C) ligation of the secondary antibodies; (D) amplification of fluorescent signal.

The procedure of cell fixation and incubation with primary antibodies was the same as for immunocytochemistry (Section 2.16). Further steps are listed in the Section 2.17.

4.4.1 Dectin-1 and TLR5 Receptors form heterodimers in RT4 cells

A typical set of results relating to the proximity ligation assay experiments are shown in Figure 4.8. Panel A demonstrates proximity ligation assay data showing Dectin-1R and TLR5 co-localisation in non-challenged RT4 cells while Figure 4.8, panel B shows the negative control data i.e. cells incubated with secondary antibodies only. The blue colouration in the panels A and B represent RT4 cell nuclei stained with DAPI while the red dots reflect receptor co-localisation. In panel A the red dots suggested random dimerisation events between the Dectin-1R and TLR5 receptors indicating that the two receptors interact physically.

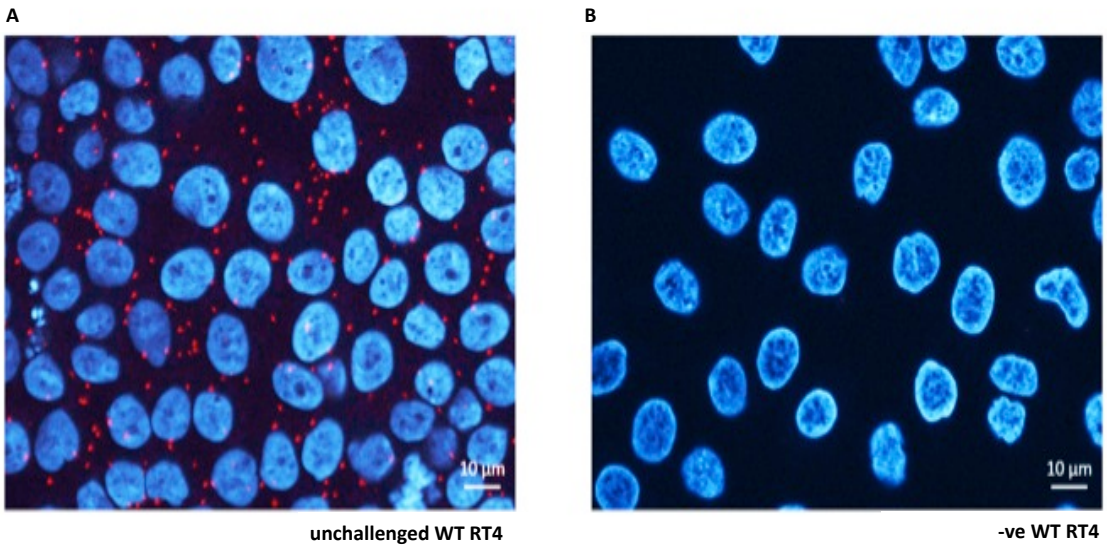

Figure 4.8 Dectin-1R and TLR5 form heterodimers in RT4 cells.
Panel A shows proximity ligation assay with anti-Dectin-1R and anti-TLR5 antibodies and secondary antibodies from proximity ligation assay kit. Red coloured dots suggest dimerisation between two receptors. Panel B demonstrates RT4 cells incubated with proximity ligation assay secondary antibodies and no primary antibodies.

4.4.2 Zymosan promotes clustering of Dectin-1 and TLR5 heterodimers

To investigate if zymosan impacted Dectin-1R and TLR5 dimerisation in RT4 cells, the cells were challenged with zymosan (200 μg/ml) for 20 and 30 minutes respectively and again analysed using the proximity ligation assay methodology. In these experiments a higher concentration of zymosan was used (x4) to maximise Dectin-1R stimulation. The challenge times were guided by previous publications that showed Dectin-1R interactions with the TLR2 receptor at 5 and 10 minutes respectively [143]. A typical set of results is shown in Figure 4.9.

Panel A shows unchallenged RT4 cells; blue colour represents DAPI stained cell nuclei and red dots reflect random dimerisation between Dectin-1R and TLR5 receptors. When the cells were challenged with zymosan for 20 and 30 minutes (panels B and C respectively) significant numbers of Dectin-1R and TLR5 dimer clusters were observed (white arrows). Panel D shows data related to assay using no primary antibody but incubation with secondary antibodies.

As a further control the zymosan challenge experiment was repeated (200 μg/ml; 30 minutes) and the RT4 cells analysed using primary antibodies to TLR5 and TLR6. Panel E shows small numbers of red dots indicating that dimerisation was occurring, but importantly no clustering was observed. Importantly similar experiment with antibodies for Dectin-1R and TLR6 was not done because primary antibodies for these receptors were of same species.

Panel F demonstrates RT4 cells challenged with flagellin (100 ng/ml) for 30 minutes. The red dots represent dimerisation of Dectin-1R and TLR5 proteins. However no clustering of these dimers was observed.

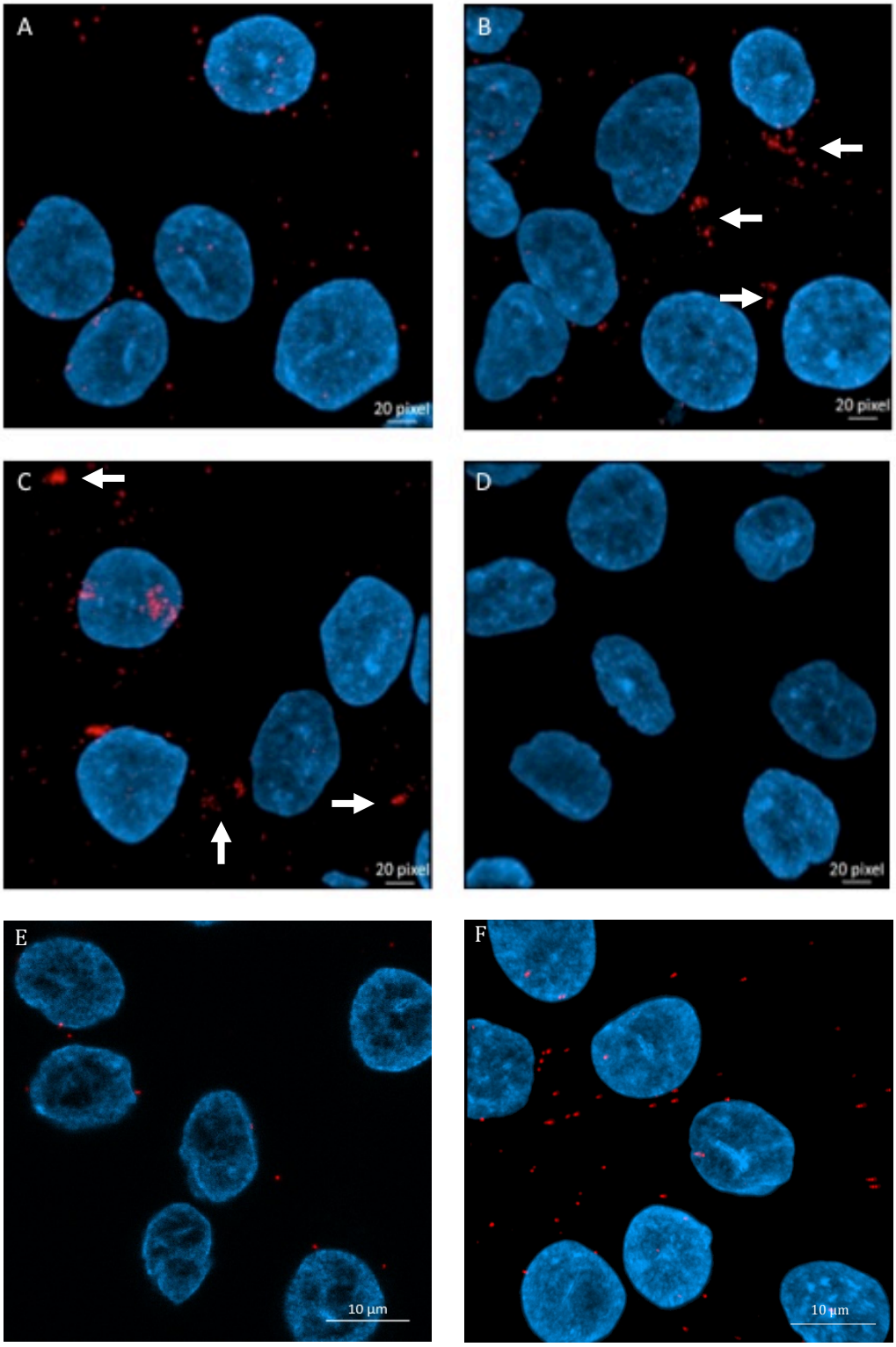

Figure 4.9 Zymosan stimulates clustering of Dectin-1R and TLR5 heterodimers in RT4 cells.
A: non-challenged RT4 cells; B and C: – challenged RT4 cells with zymosan (200 µg/ml) for 20 and 30 minutes respectively; D: negative control where the cells were incubated with IgG_{2b} control antibody; E: proximity ligation of TLR5 and TLR6 in RT4 cells challenged with zymosan for 30 minutes; F: RT4 cells challenged with flagellin for 30 minutes.

These proximity ligation data demonstrated that the Dectin-1R and TLR5 receptors interacted physically in RT4 bladder cells forming heterodimers. Moreover significant clustering of these heterodimers was evident following challenge of the cells with zymosan.

4.5 Discussion

This chapter, focussing on RT4 bladder cells, investigated the physical and functional cooperation of two receptors, Dectin-1R and TLR5, in protecting the bladder from infection by potential pathogens namely fungi and flagellated bacteria. It is well established that the Dectin-1R binds and is activated by zymosan – a component of the fungal cell wall [138], while flagellin, a key component of flagellum, is found in bacteria and activates TLR5 signalling [146]. These studies exploring potential co-operation of the two receptors were prompted by NF-kB signalling data using RT4 cells that showed NF-kB signalling to be significantly reduced in such cells following TLR5 blocking and challenging with zymosan [83].

Results of the experiments reported in this chapter and involving immunocytochemical staining, proximity ligation assays and gene knock-down all strengthened the NF-kB signalling story and further supported the physical and functional co-operation between the Dectin-1 and TLR5 receptors in RT4 bladder epithelial cells. Additionally this co-operation functioned seemingly to protect the bladder cells from infection.

It is known that in myeloid derived cells the Dectin-1R co-operates with other Toll-like receptors including TLR2 and TLR4 in the fight against infection. For example, in macrophages and dendritic cells, Dectin-1R and TLR2 co-operate resulting in the production of cytokines including IL-12 and TNFα [103]. Knock-out mice have also been used to highlight co-operation, with the Dectin-1 and TLR2 receptors functioning to activate a macrophage pro-inflammatory response following a mycobacterium infection [113]. Similarly physical and functional collaboration of Dectin-1 and TLR2 receptors was reported in mouse

macrophages following challenge with *Mycobacterium abscessus* (Mab) a quick growing non-tuberculous mycobacterium [143]. Additionally it has also been shown that the Dectin-1R and TLR4, together with the mannose receptor collaborate in the activation and expansion of Th17 and Tc17 cells following *Paracoccidioides brasiliensis* stimulation of murine dendritic cells [129]. All of these effects function, presumably, to enhance the innate response and potentiate the host defence mechanisms through activation, recruitment and expansion of effective immune cells. However, to date there is no published data that directly shows co-operation between the Dectin-1 and TLR5 receptors.

TLR5 is unique amongst the TLRs in that it only recognises flagellin and functions in host defence through homodimer formation [118, 144, 146-148]. There are no reports of it forming heterodimers with other TLRs. However, data reported in this chapter indicates that in the bladder epithelium TLR5 co-operates physically and functionally with the Dectin-1R in defending the bladder against infection. Potentially there are hints in the literature of this TLR5/Dectin-1R relationship. For example in the corneal epithelium, flagella induced expression of CXCL-10 was shown to be associated with fungal killing and Natural Killer [NK] cell recruitment in response to a *Candida albicans* infection [149].

TLR5 receptors have been reported in ocular cells [150, 151]. Dectin-1 receptors have also been reported in corneal epithelial cells with activation by *Aspergillus fumigatus* associated with the production of cytokines and chemokines including IL-1β, IL-6 and IL-8 [152]. Therefore the data reported by Liu et al (2014) [152] , linked to a *Candida* infection suggests a potential Dectin-1R/TLR5 collaboration although this was neither recognised nor discussed by the authors. Additionally, Rodland et al, (2011), observed in vitro that conidia from *Aspergillus fumigatus* up-regulated TLR5 gene expression in human monocytes [153]. From this work the authors proposed a role for TLR5 in *A.fumigatus* monocyte infections, but a literature search has provided no further publications either supporting or developing these 2011 findings.

The immunocytochemical and proximity ligation assay data demonstrated co-localisation and clustering of the two receptors following zymosan challenge of

RT4 bladder cells (Figure 4.2 and Figure 4.9). From these observations it was not possible to identify whether receptor co-localisation was associated with the membrane or also included intracellular receptors. Such analyses would necessitate further staining for example using an array of antibodies directed specifically to membrane localised proteins.

Receptor clustering was an interesting observation; it has been suggested that clustering functions, potentially, to stabilise cell membrane transporters and/or receptors as well as to facilitate signal amplification [154, 155]. Signal amplification is mediated through either better retention of the receptor ligands or increased ligand rebinding. While in this study the factors underpinning receptor clustering remain unclear, cooperation between the Dectin-1 and TLR5 receptors resulting in the activation of shared intracellular signalling molecules to maximise the effector response is very plausible. Interestingly it was reported in human dendritic cells stimulated with curdlan and LPS that the Dectin-1R is required for potentiation of TLR2 signalling and cytokine IL-10 and IL-12 production [111] although receptor clustering was not mentioned. Clustering may therefore be unique to Dectin-1/TLR5 receptor interactions or specifically bladder epithelial cell Dectin-1/TLR5 receptor interactions.

The proximity assay ligation data indicated dimerisation of Dectin-1 and TLR5 receptors in response to flagellin, but clustering similar to that seen with zymosan was not observed. This suggested that the zymosan or β-glucan challenge was essential and driving the receptor clustering effect. Again, the reasons for this are not known. It is known however, that bladder cells, within hours, respond to flagellin, synthesised by UPEC as a major component of their flagella and linked to motility, to produce a strong innate response, which involve the synthesis of pro-inflammatory molecules and antimicrobial agents to clear the bacterial infection. In contrast yeast infections are more challenging to detect. During growth or colonisation yeasts such as *C. albicans* hide their β-glucan by covering it in a coat of mannan, which masks their detection by Dectin-1 receptors. During infection, which involves hyphal growth the β-glucan is unmasked, but the concentrations are low [156]. This means that once β-glucan is detected the bladder cells need to maximise their innate response to quickly

clear the infection. Clustering of the Dectin-1 and TLR5 receptors, which in bladder are the major TLR and present in higher concentrations than either TLR2 and TLR4 [157], would facilitate this. It is therefore feasible that the Dectin-1R/TLR5 clustering mechanism observed in response to zymosan has specifically evolved in bladder epithelial cells as a mechanism to defend against yeast infections.

In myeloid derived cells Dectin-1receptors have been shown to co-operate with TLR2 and TLR6 receptors. Previous work in RT4 cells in which TLR2 receptors were blocked using antibody did not support a Dectin-1/TLR2 receptor collaboration. It is acknowledged that this relationship should have been further investigated by repeating the proximity ligation assay using Dectin-1R antibody and antibodies to TLR2 and TLR6. However as all the available Dectin-1R, TLR2 and TLR6 antibodies were raised in the same species, it meant the assay would not work and therefore these analyses were not performed. For completeness these experiments need to be completed.

LCN2 is a host defence protein involved in the innate protection of the bladder epithelium from fungal and bacterial infections as observed by the increase in gene expression and protein synthesis in response to zymosan (Figure 3.5-Figure 3.6) and flagellin challenges [40]. As expected *TLR5* gene knockdown was linked to a significant decrease in *LCN2* gene expression and protein synthesis. However, the *LCN2* expression data associated with the siDct1 treated ie *CLEC7A* knockdown cells was surprising, with expression actually significantly increased ($p<0.05$). The reasons for this increase are not known and these data were compromised by the lack of LCN2 protein measurements to help confirm and/or explain the result. The increased gene expression may however, have reflected the *CLEC7A* gene knockdown cells compensating the loss of Dectin-1R by producing more LCN-2 to fight infection. Yet, this appears unlikely as genes encoding the cytokines *CXCL8* and *IL1A,* which also encode proteins involved in the innate response were suppressed. However, this theory cannot be totally excluded. Essentially IL-8 and IL-1α are pro-inflammatory cytokines while LCN2 is an antimicrobial agent with a microbial killing function. Therefore a direct consequence of Dectin-1R loss may be the increased production of host

antimicrobials ie killing agents, such as LCN2 and the defensin peptides. Further in vitro analyses, for example *DEFB4* gene expression and hBD2 and LCN2 protein measurements need to be done in *CLEC7A* gene knock-down RT4 cells to investigate this further.

Clinical data indicates that patients who are Dectin-1R deficient suffer persistent *Candida* infections [158, 159] with monocytes and macrophages recovered from such patients defective in producing IL-6, TNFα and IL-Iβ. Mice deficient in Dectin-1 also show an increased susceptibility to *C. albicans,* but it is argued that *Candida* killing itself is not impacted [160, 161] with neutrophils being responsible for killing fungi and clearing fungal infections. However, as none of the Dectin-1R deficient patient and transgenic mice model material published has examined the mucosal concentrations of host defence agents such as LCN2 and the defensins, their increased synthesis and killing roles in Dectin-1R defective patients cannot be ignored.

In summary, data presented in this chapter showed that Dectin-1 and TLR5 receptors co-operated physically and functionally when RT4 bladder epithelial cells were challenged with zymosan resulting in an innate immune response involving the synthesis of host cytokines and antimicrobial agents.

Chapter 5. Engineering overexpression of Dectin-1 and TLR5 receptors in RT4 bladder cells

Data from experiments performed thus far indicated that:

(i) the RT4 bladder epithelial cells expressed the *CLEC7A* gene encoding the Dectin-1R and that transcripts encoding receptor isoforms 1 (stalk), 2, 3, 4 and 5 (no stalk) were synthesised,
(ii) western data supported the synthesis of isoforms 1, 2 and 4, and
(iii) the Dectin-1 receptor co-operates with TLR5 in RT4 bladder cells which results in an innate response to zymosan.

In humans TLR5 is a key pathogen receptor protein of the lower urogenital tract tissues recognising flagellated bacteria, mainly UPEC from gut-faeces, and orchestrating an innate response to prevent bacterial ascent of the urinary tract [40]. It is known however, that approximately 10% of population carry a truncated TLR5 receptor due to the SNP 1174C> T which encodes a STOP codon and that this correlates with susceptibility to recurrent UTIs [86]. Interestingly, however, a study has also shown a significant association between the presence of the TLR5 SNP and the risk of developing invasive aspergillosis following an allogenic stem cell transplant [162], which again provides support to investigate potential Dectin1R/TLR5 interactions further.

Therefore, the aim of this part of the project was to attempt to model these Dectin-1R isoform/TLR5 wild-type and truncated receptor interactions *in vitro* to help further understand the innate defences of the urinary tract.

The approach was to amplify DNA sequences encoding the Dectin-1 and TLR5 receptor isoforms, clone these DNA isoforms into pVitro2-neo-mcs (Figure 5.1), which is able to co-express two DNA sequences simultaneously, (Figure 5.2), stably transfect the resultant plasmids into CHO cells and study interactions of encoded receptor isoforms in response to zymosan, flagellin and zymosan/flagellin challenges.

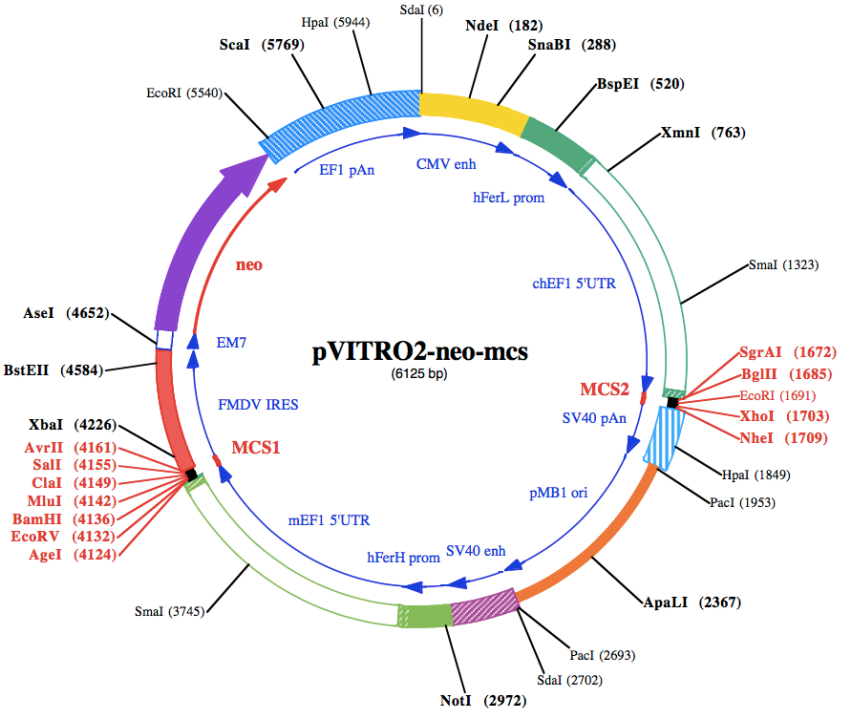

Figure 5.1 pVitro2-neo-mcs plasmid.
pVitro2 plasmid was used to overexpress *CLEC7A* and *TLR5* genes simultaneously.

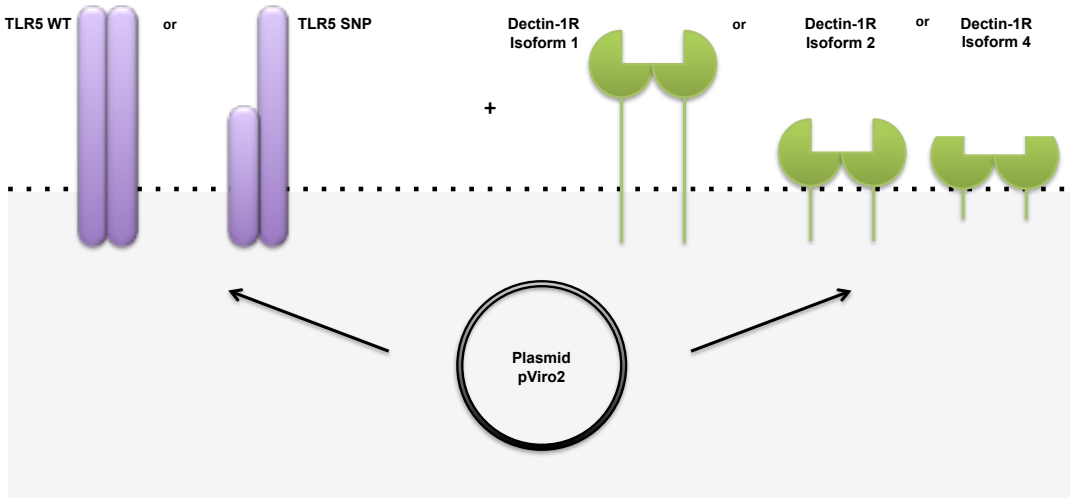

Figure 5.2 Co-expression of wild type or SNP TLR5 with Dectin-1R isoforms 1, 2 or 4.
TLR5 wild type or SNP cDNAs were inserted into plasmid pVitro2 together with *CLEC7A* (encoding Dectin-1R) isoform 1, 2 or 4. Six combinations of the genes in the plasmids were envisaged.

5.1 Construction of plasmids expressing *CLEC7A* and *TLR5*

The process of plasmid construction included gene amplification, separation of cDNA products on an agarose gel, purification of the cDNA fragments, restriction of cDNA fragments and vector plasmid pVitro2, and ligation of the cDNA fragments into the plasmid vector. Step 1 (Figure 5.3) involved ligating the *CLEC7A* and *TLR5* cDNA fragments into separate plasmid vectors and then in step 2 the second cDNA was ligated in.

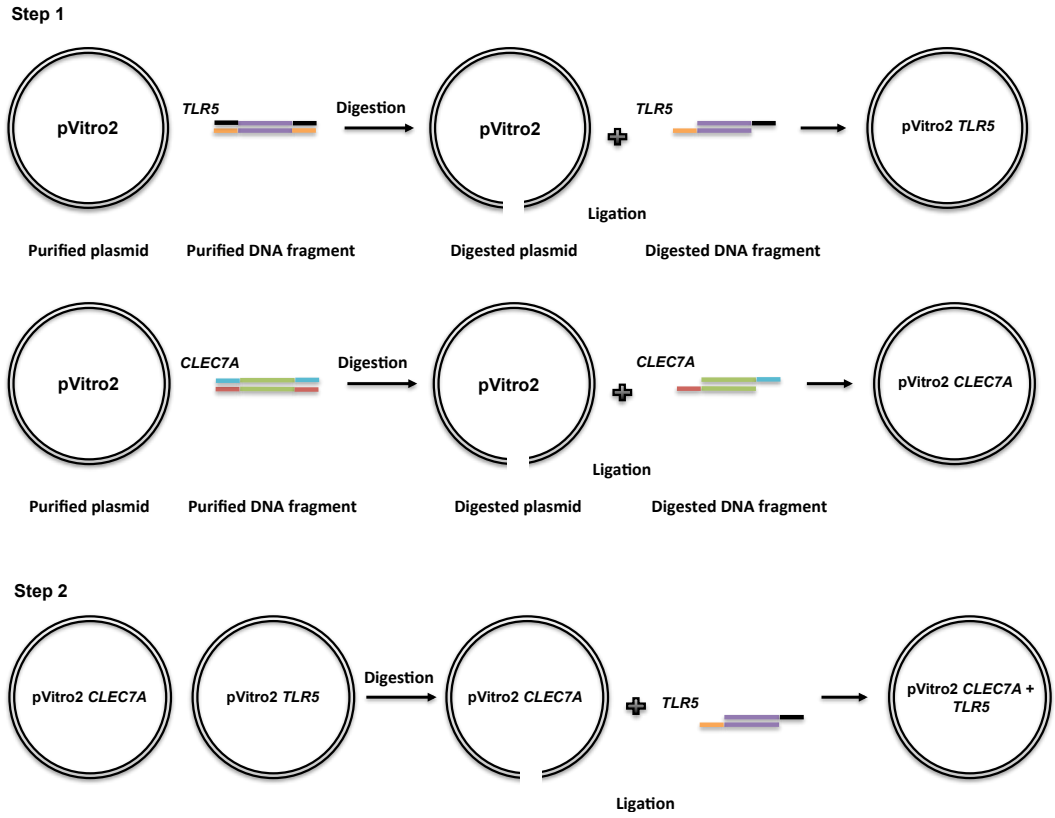

Figure 5.3 Schematic representation of *CLEC7A* and *TLR5* cloning into pVitro2 plasmid.
pVitro2 plasmid and amplified *CLEC7A* and *TLR5* DNA sequences were restricted with appropriate enzymes and ligated to engineer final plasmid construct.

Complementary DNA sequences of *CLEC7A* isoforms 1, 2 and 4, wild type *TLR5* and truncated *TLR5* were amplified from RT4 cDNA material. Primers were designed to contain 3' and 5' restriction sites (BglII and XhoI for *CLEC7A*) and (BamHI and SalI for *TLR5*) to facilitate cloning of the resultant cDNAs into the plasmid vector pVitro2 plasmid (Figure 5.4).

Figure 5.4 Primers designed for insertion of *CLEC7A* and *TLR5* into plasmid pVitro2.

A: Primers to amplify all isoforms of *CLEC7A* with sequences for *Bgl*II and *Xho*I restriction sites. B: Primers to amplify full length or truncated *TLR5* with sequences for *Bam*HI and *Sal*I restriction sites.

End-point PCR resulted in cDNA bands of 2750 bp and 1250 bp representing *TLR5* wild type and *TLR5* truncated sequences and 750, 620 and 500 bp representing *CLEC7A* isoform 1, 2 and 4 (Figure 5.5). These cDNA bands were excised and purified for cloning into pVitro2.

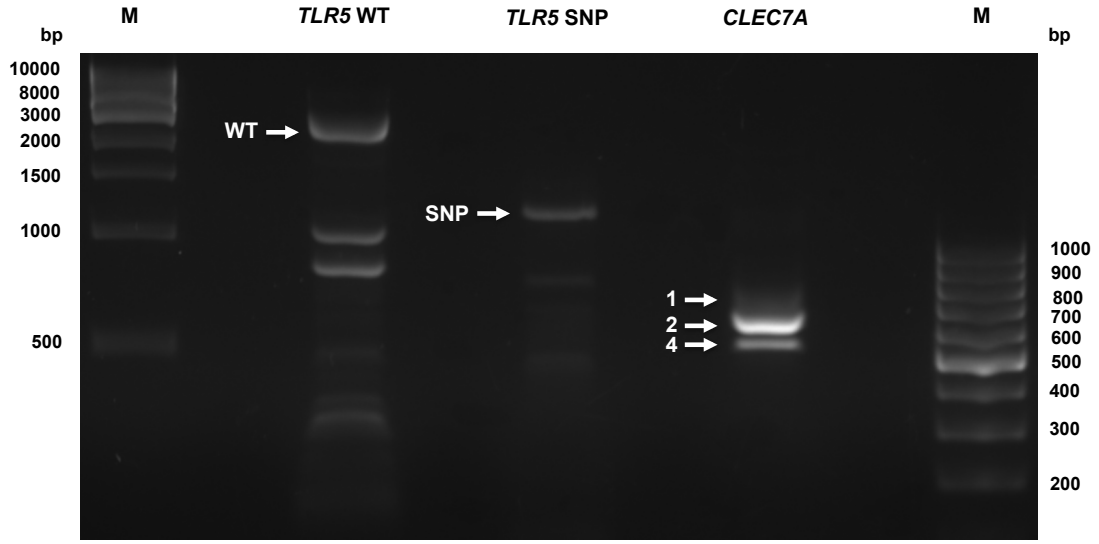

Figure 5.5 Amplification of *TLR5* and *CLEC7A* DNA sequences for cloning into plasmid pVitro2.
TLR5 wild type, *TLR5* SNP and *CLEC7A* sequences were amplified for cloning into pVitro2. End-point PCR produced cDNA bands of 2750 bp and 1250 bp representing *TLR5* wild type and *TLR5* truncated sequences and 750, 620 and 500 bp representing *CLEC7A* isoform 1, 2 and 4 (white arrows). M: base pair marker.

The purified cDNA sequences and pVitro2 vector plasmid were restricted with appropriate restriction enzymes *Bgl*II and *Xho*I (for *CLEC7A* sequences) or *Sal*I and *BamH*I (for *TLR5* sequences) and the DNA sequences ligated into the vector plasmid (Figure 5.6).

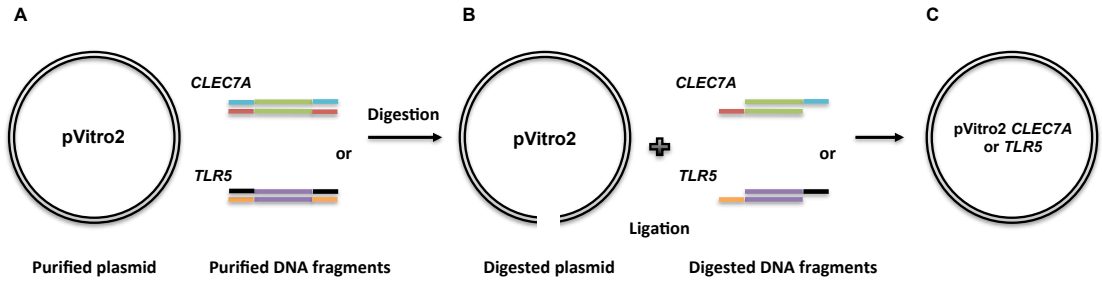

Figure 5.6 Restriction and ligation of pVitro2 vector plasmid, *CLEC7A* and *TLR5* DNA sequences. Vector/DNA combinations.

The engineered plasmids (Figure 5.6, C) were transformed into bacteria, transformants selected and the plasmids purified. Each plasmid was checked by restriction analyses ie *Bgl*II and *Xho*I for CLEC7A sequences, and *Sal*I and *BamH*I for TLR5 sequences to confirm that the cDNAs were inserted successfully and correctly. These data are shown in Figure 5.7. Panel A lane 1 shows a band of 750 bp representing *CLEC7A* isoform 1. Panel B, lanes 2 and 3 reveal bands of 620 and 500 bp representing isoforms 2 and 4 respectively. Restricted plasmids containing wild type *TLR5* and truncated *TLR5* cDNA sequences are shown in Figure 5.7 panel C (lanes 4 and 5) at 2700 bp and 1200 bp respectively.

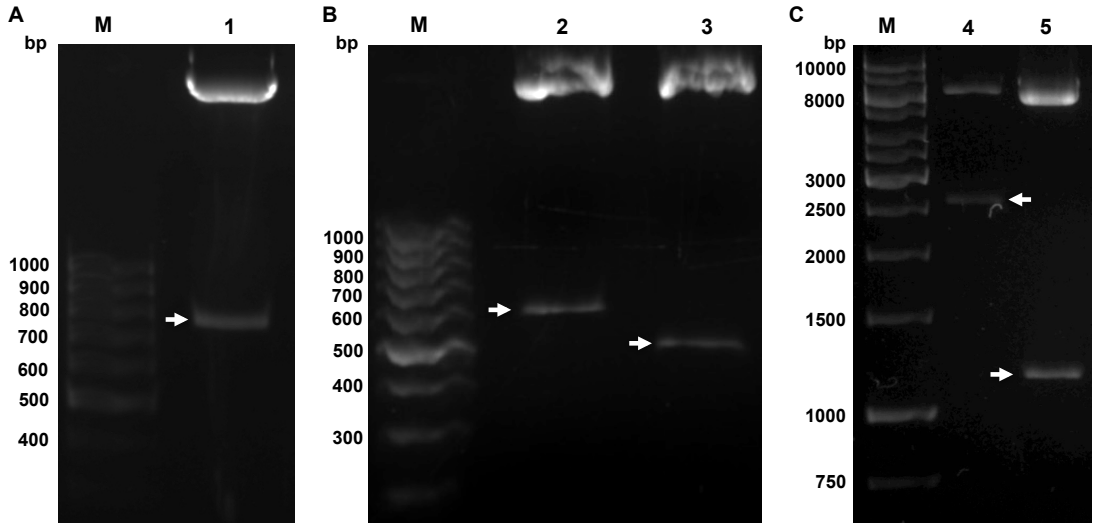

Figure 5.7 Analyses of pVitro2 plasmids with *CLEC7A* and *TLR5* cDNA insertions.
cDNAs of interest indicated with an arrow. Panel A shows *CLEC7A* isoform 1 (lane 1) at 750 bp; panel B – isoforms 2 and 4 (lanes 2 and 3) at 650 bp and 500 bp respectively; panel C – *TLR5* wild type gene and truncated form (lanes 4 and 5) at 2700 bp and 1200 bp respectively. M: base pair marker.

The next step was to clone the *TLR5* cDNAs into the relevant vector plasmids containing *CLEC7A* cDNAs. For example the pVitro2 containing an *CLEC7A* insertion was restricted with *Sal*I and *Bam*HI and the wild type cDNA sequence ligated into it (Figure 5.8).

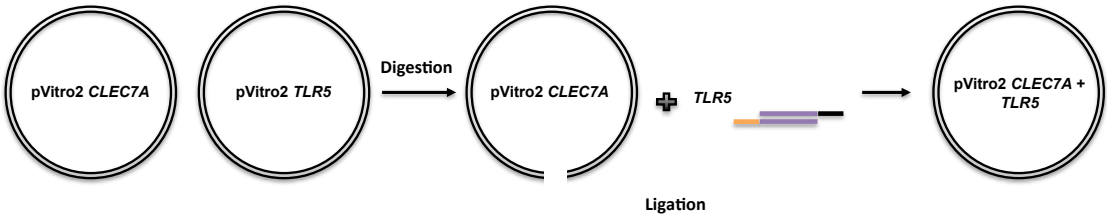

Figure 5.8 Scheme of cloning TLR5 into pVitro2 Dectin-1 plasmid.

Initially two plasmids were successfully engineered – pVitro2-(*CLEC7A* isoform 1 + *TLR5* WT) and pVitro2-(*CLEC7A* isoform 1 + *TLR5* SNP). Data presented in Figure 5.9 show pVitro2 plasmids containing *CLEC7A* isoform 1 and *TLR5* wild type (lanes 1 and 2) or truncated *TLR5* sequences (lane 3 and 4). Plasmid vector acted as the control (lane 5). The 2.7 Kbp bands in the lanes 1 and 2 corresponded to the *TLR5* wild type cDNAs. The 3.2 Kbp bands in the lanes 1 - 4 corresponded to vector DNA plus *CLEC7A* isoform 1 sequences. This band in the control lane 5 was 2.5 Kbp reflecting lack of *CLEC7A* cDNA. The 3.7 Kbp bands in lanes 1 - 4 represent a vector DNA and are of comparable size in lane 5.

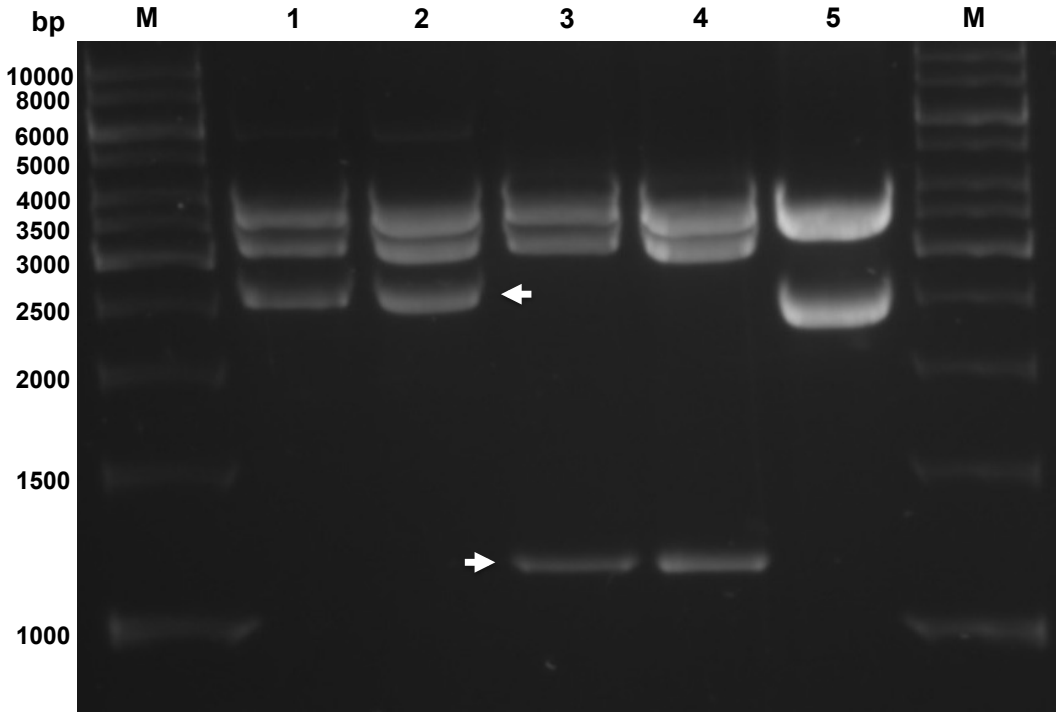

Figure 5.9 pVitro2 engineered to contain *CLEC7A* and *TLR5* cDNAs.
TLR5 wild type or SNP cDNA sequences were inserted into pVitro2 containing *CLEC7A* isoform 1 cDNA. The plasmids were digested with restriction enzymes *Bam*HI, *Bgl*II and *Sal*I. Lanes 1 and 2 – enzyme restricted pVitro2 with inserted *CLEC7A* isoform 1 and a wild type *TLR5*; Lanes 3 and 4 – enzyme restricted pVitro2 with inserted *CLEC7A* isoform 1 and a truncated *TLR5*. Lane 5 – enzyme restricted pVitro2. M: base pair marker.

Before the transfection procedures were initiated the *CLEC7A* and *TLR5* insertions were all sequenced and aligned to predicted sequences of both receptors using the BLAST alignment tool. These alignments (Figure 5.10) confirmed that the *CLEC7A* and *TLR5* sequences in the plasmids were correct.

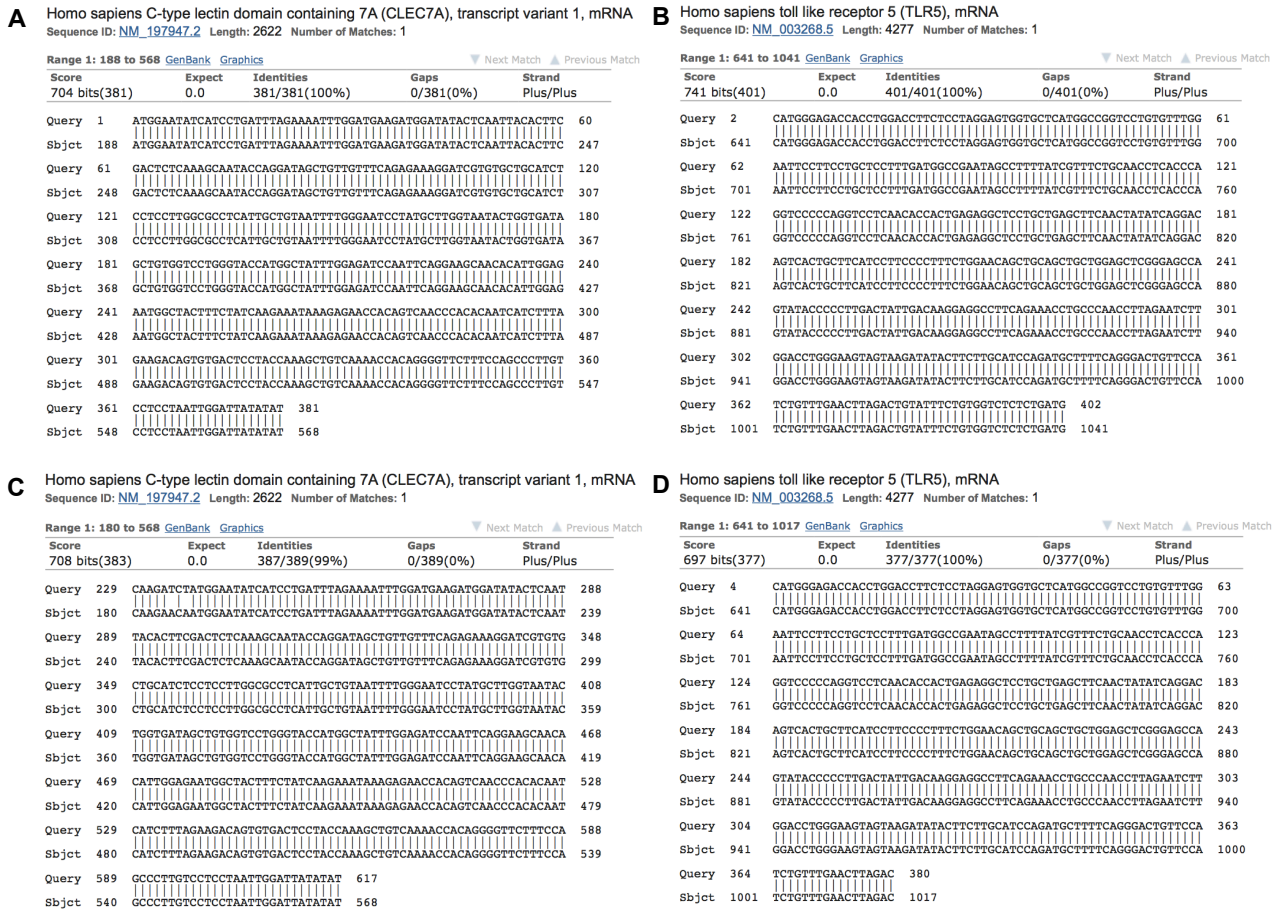

Figure 5.10 Confirmation of *CLEC7A* isoform 1 and *TLR5* insertions by sequencing and alignment.
CLEC7A and *TLR5* insertions were sequenced in two different pVitro2 recombinant plasmids and aligned to predicted sequences using the BLAST alignment tool. A and B: alignment to a predicted sequence (Sbjct) of sequenced *CLEC7A* and *TLR5* fragments (Query) from plasmid pVitro2-(*CLEC7A* isoform 1 + *TLR5* WT). C and D demonstrated alignment to a predicted sequence (Sbjct) of sequenced *CLEC7A* and *TLR5* fragments (Query) from plasmid pVitro2-(*CLEC7A* isoform 1 + *TLR5* SNP).

These data indicated the successful construction of a recombinant plasmid containing *CLEC7A* and a wild type or truncated *TLR5* gene.

The next stage was to repeat these manipulations but insert a wild type or truncated *TLR5* cDNA into the pVitro2 construct containing *CLEC7A* isoform 4. Again two different plasmids were created – pVitro2-(*CLEC7A* isoform 4 + *TLR5* WT) and pVitro2-(*CLEC7A* isoform 4 + *TLR5* SNP). Plasmids were prepared and purified as previously described and subjected to analyses with the restriction enzymes *Bam*HI and *Sal*I. Data in Figure 5.11, lanes 1 and 2 revealed bands of 1.2 Kbp and 2.7 Kbp bands that corresponded to the *TLR5* SNP and *TLR5* WT cDNAs. These data confirmed the successful insertion of the *TLR5* cDNA sequences. cDNA bands of 8 Kbp in lanes 1 and 2 represented pVitro2 plasmid plus *CLEC7A* isoform 4 cDNA.

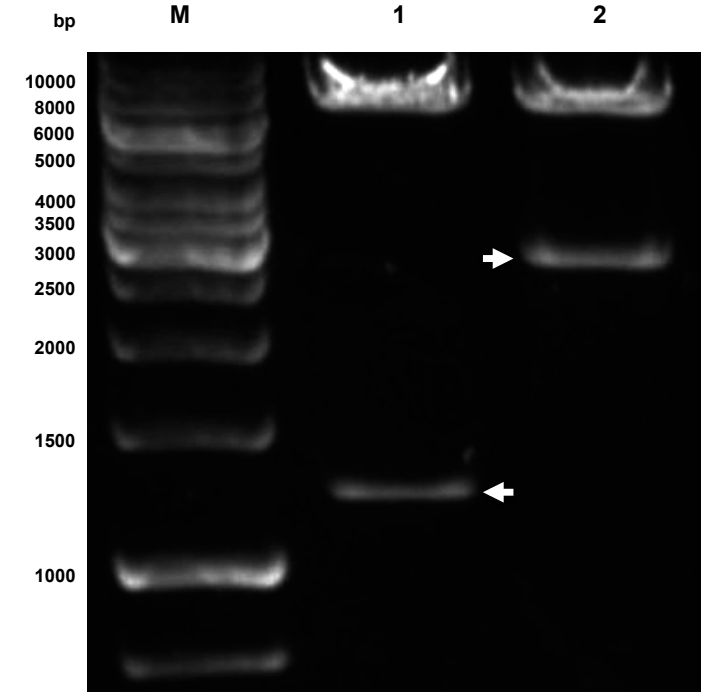

Figure 5.11 pVitro2 engineered to contain *CLEC7A* and *TLR5* cDNAs.
TLR5 wild type or *TLR5* SNP sequences were inserted into pVitro2 plasmid containing *CLEC7A* isoform 4 gene. The plasmids were digested with restriction enzymes *BamH*I and *Sal*I. Lane 1 – enzyme restricted pVitro2 with inserted *CLEC7A* isoform 1 and a truncated *TLR5*. Lane 2 – enzyme restricted pVitro2 with inserted *CLEC7A* isoform 4 gene and a wild type *TLR5*.

The purified plasmids pVitro2-(*CLEC7A* isoform 4 + *TLR5* WT) and pVitro2-(*CLEC7A* isoform 4 + *TLR5* SNP) were verified by sequencing and these data are presented in Figure 5.12.

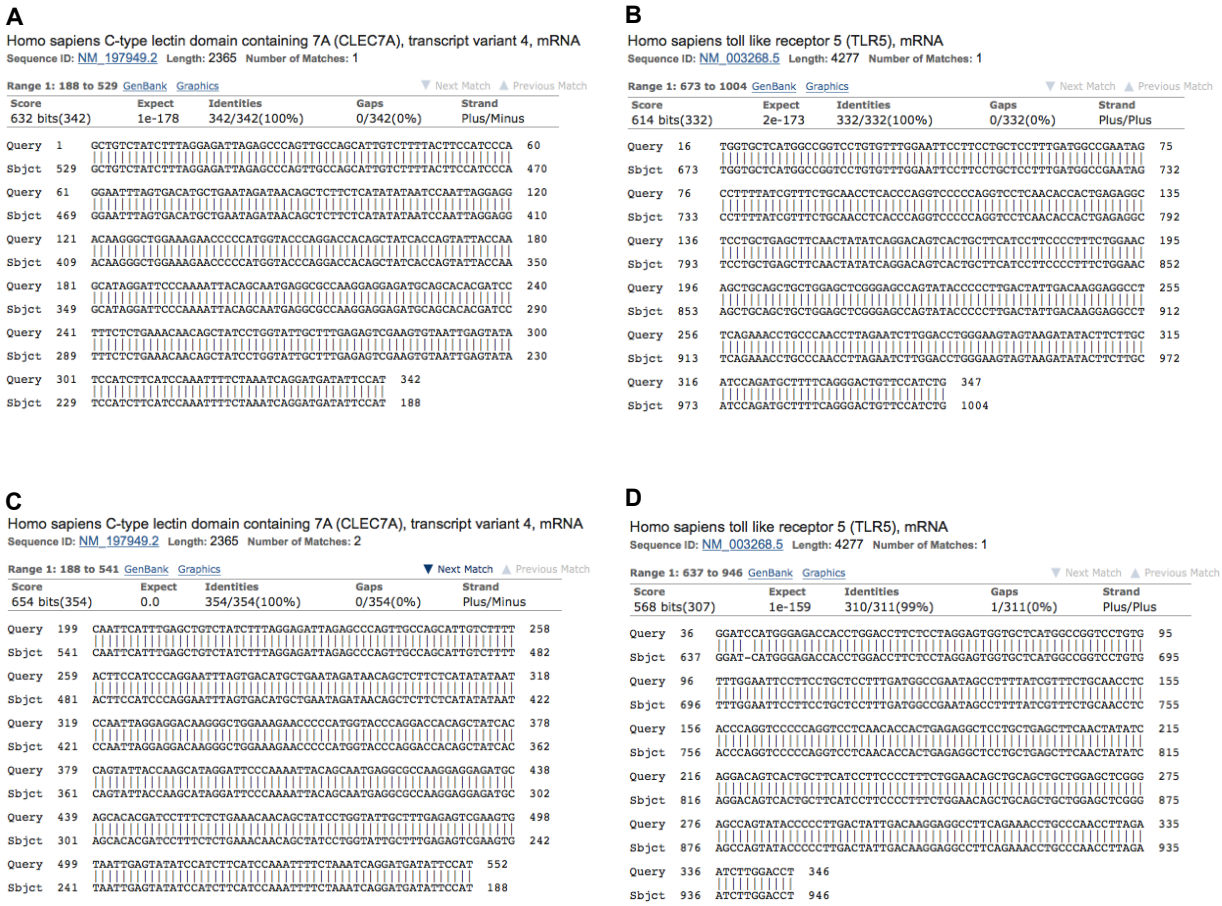

Figure 5.12 Confirmation of *CLEC7A* isoform 4 (A & C) and TLR5 cDNA insertions by sequencing and alignment (B & D).
A and B: alignment to a predicted sequence (Sbjct) of sequenced *CLEC7A* and *TLR5* fragments (Query) from plasmid pVitro2-(*CLEC7A* isoform 4 + *TLR5* WT). C and D demonstrated alignment to a predicted sequence (Sbjct) of sequenced *CLEC7A* and *TLR5* fragments (Query) from plasmid pVitro2-(*CLEC7A* isoform 4 + *TLR5* SNP).

At this point a decision was taken to transfect the *CLEC7A* isoform 1 and 4/TLR5 plasmids and depending on the subsequent data then decide whether or not to engineer the *CLEC7A* isoform 2 constructs.

5.2 Transfection of the pVitro2 plasmids into CHO cells

CHO cells were selected to overexpress and examine interactions between the Dectin-1R and TLR5 proteins in eukaryote cells. The selection marker was geneticin (G418) (Figure 5.1) so before any transfections were initiated the cells were incubated with increasing concentrations, 50, 100, 200, 300, 400, 500 μg/ml of the antibiotic G418. Fresh antibiotic was added every two days. However the CHO cells selected for use were not affected by the antibiotic and did not die. These data suggested that the CHO stocks held were mislabelled as wild-type cells and had previously been transfected with a plasmid carrying resistance to G418.

5.3 RT4 cells stably transfected with pVitro2 constructs containing Dectin-1 and TLR5 cDNAs

Since the CHO cells available were resistant to G418 it was decided to use the bladder RT4 cells to overexpress the Dectin-1R and TLR5 proteins. These cells unlike CHO cells were known to support the two different receptors naturally and contain all the signalling apparatus relating to the Dectin1/TLR5 receptor collaboration. These cells were incubated with 70 μg/ml of the antibiotic G418 to select transfected cells. An optimal concentration of the antibiotic was determined previously in our laboratory [157].

In reporting subsequent experiments and data the plasmid constructs containing the cDNAs were named as follows: pVitro2-(*CLEC7A* isoform 1 + *TLR5* WT) – "D1T1"; pVitro2-(*CLEC7A* isoform 1 + *TLR5* SNP) – "D1T2"; pVitro2-(*CLEC7A* isoform 4 + *TLR5* WT) – "D4T1" and pVitro2-(*CLEC7A* isoform 4 + *TLR5* SNP) – "D4T2".

The plasmids were stably transfected into RT4 cells using attractene as described in Section 42. Non-transfected RT4 cells died, while transfected cells survived (Figure 5.13). A mixture of individual colonies was used for further analysis.

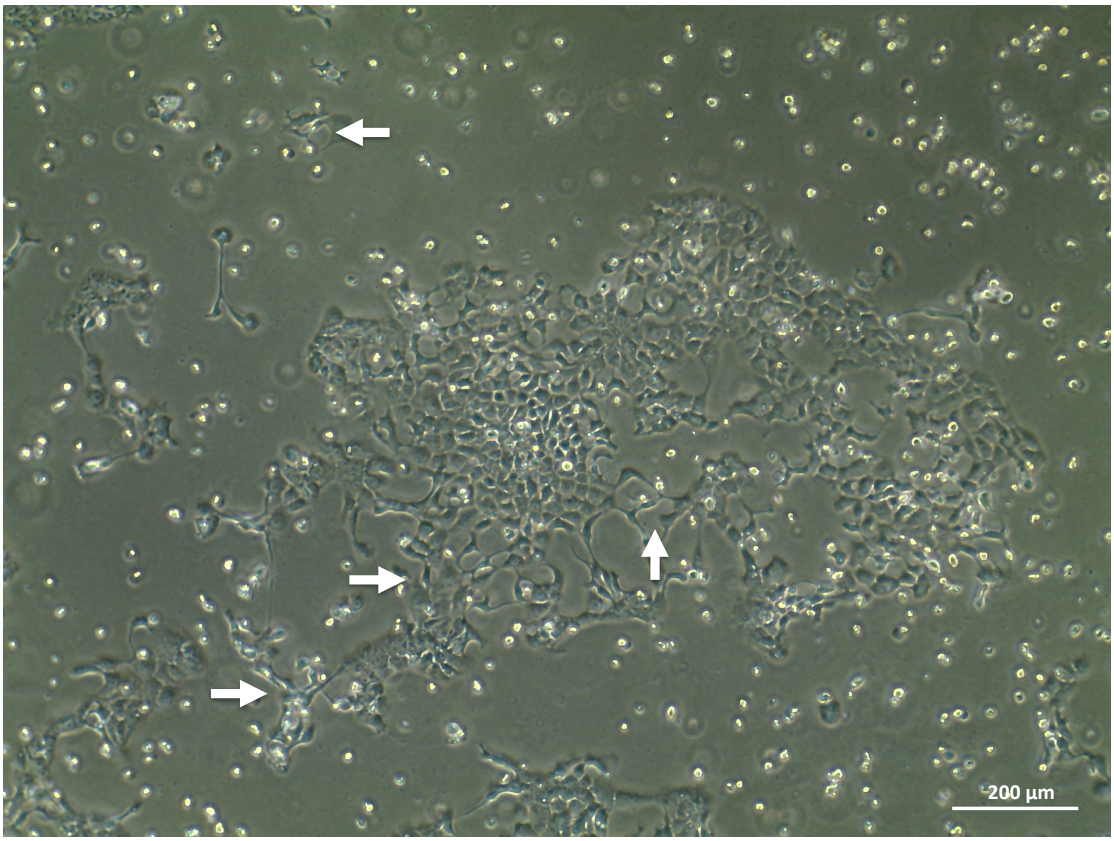

Figure 5.13 Selection of stably transfected RT4 cells with G418 antibiotic. RT4 cells were transfected with pVitro2 plasmid constructs and after three days G418 antibiotic (70 µg/ml) was added. Transfected RT4 cells survived, while non-transfected – died (white arrows).

Once stocks of the pooled transfected RT4 cells had been banked genomic DNA was isolated (Section 2.7) to verify that the plasmid DNA had been successfully incorporated into the eukaryote DNA. To facilitate this primers, which amplified DNA fragments at the junctions between pVitro2 and the receptor cDNA sequences were used (Figure 5.14 & Table 5). These primers were used to amplify plasmid/insertion sequences from the genomic DNA using end-Point PCR and the DNA products were analysed on an agarose gel.

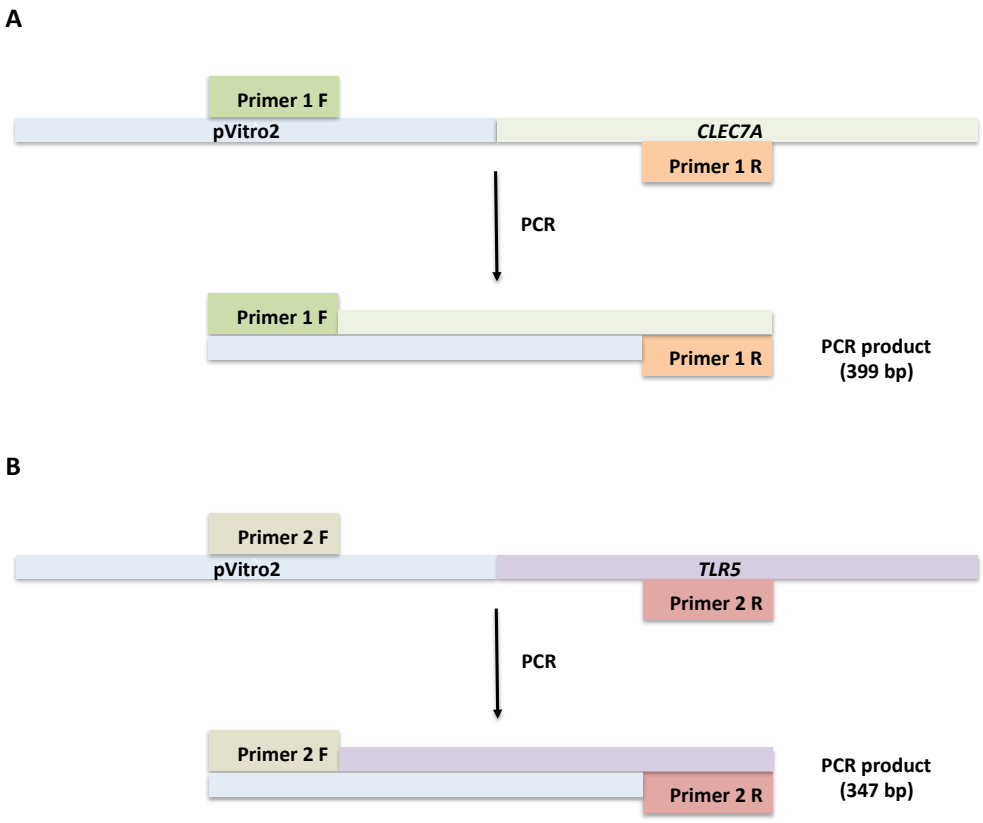

Figure 5.14 Schematic representation of End-Point PCR approach to confirm plasmid insertion into RT4 cell DNA.
A: Primers 1 R and F were used to amplify DNA at pVitro2/*CLEC7A* junction. B: Primers 2 R and F were used to amplify DNA at pVitro2/*TLR5* junction.

The end-point PCR data presented in Figure 5.15 lanes 1 – 4 shows fragments (400 bp) amplified using Primers 1 F and R (Figure 5.14, A). The expected size of the fragments was 399 bp. DNA templates in lanes 1 and 2 were genomic DNA from the cells transfected with D1T1 and D1T2 respectively, while in the lanes 3 and 4 the DNA templates were the purified plasmids D1T1 and D1T2.

Lanes 6 - 9 show DNA bands (380 bp) amplified using Primers 2 F and R (Figure 5.14, B). The expected size of the bands was 347 bp. DNA templates in lanes 6 and 7 were genomic DNA from the cells transfected with D1T1 and D1T2 respectively, while in lanes 8 – 9 the templates were plasmids D1T1 and D1T2 respectively.

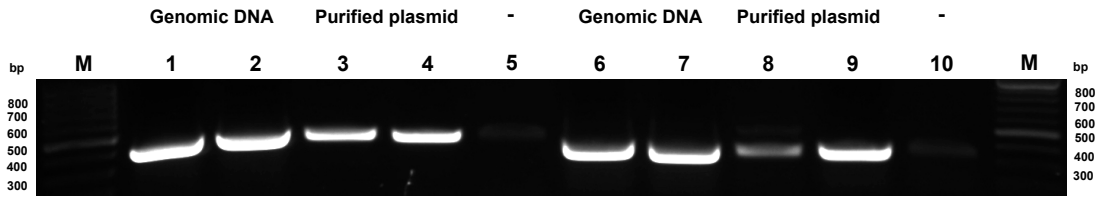

Figure 5.15 pVitro2 plasmids containing *CLEC7A* and *TLR5* genes in genomic DNA of RT4 cells.
Lanes 1 – 4 shows fragments (400 bp) amplified using Primers 1 F and R and lanes 6 - 9 show fragments (380 bp) amplified using Primers 2 F and R. DNA templates in lanes 1, 2, 6 & 7 were genomic DNA from the cells transfected with D1T1 and D1T2 respectively, while in the lanes 3, 4, 8 & 9 the DNA templates were plasmids D1T1 and D1T2. Lanes 5 and 10 no template DNA. M: base pair marker.

These PCR data confirmed that the engineered pVitro2/*CLEC7A/TLR5* constructs were incorporated into the genomic DNA of the bladder RT4 cells.

5.4 Immunocytochemical staining of transfected RT4 cells

To confirm the gene expression data and explore protein 'overexpression' of the Dectin-1 and TLR5 receptors in the transfected RT4 bladder cells, the cells were cultured to confluence and immunostained with anti-Dectin-1R (R&D Systems, MAB1859) and anti-TLR5 (Abcam, ab3701) primary antibody Section 2.16 (Table 3).

Dectin-1R immunostaining data are presented in Figure 5.16. Panel A shows RT4 cells transfected with empty pVitro2 plasmid; panels B and C show RT4 cells transfected with plasmid D1T1 (B) or D1T2 (C) respectively and panel D demonstrates RT4 cells transfected with control plasmid and stained with secondary antibody only.

Strong Dectin-1R staining was observed in panel B compared to panel A (control) suggesting that the D1T1 transfected cells were overexpressing the Dectin-1R. However, Dectin-1R signal intensity in the panel C cells, which were transfected

with D1T2 was similar to that of panel A suggesting that these cells did not overexpress the Dectin-1R.

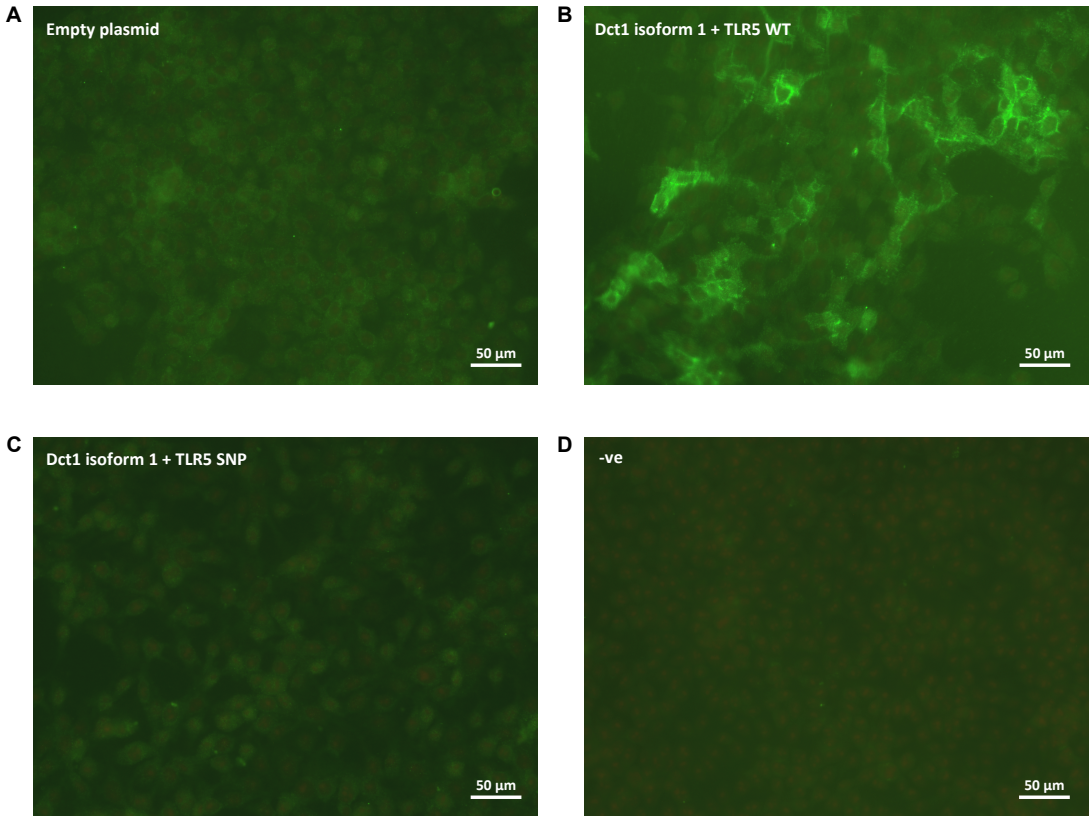

Figure 5.16 Dectin-1R immunostaining of transfected RT4 cells.
RT4 cells transfected with pVitro2 plasmids overexpressing Dectin-1R and TLR5 were fixed with 4% paraformaldehyde and incubated with anti-Dectin-1R antibody (1:50) and Alexa Fluor 488 secondary antibody (green colour). A: RT4 cells transfected with pVitro2 plasmid; B: RT4 cells transfected with D1T1 plasmid; C: RT4 cells transfected with D1T2 plasmid; D: RT4 cells transfected with empty plasmid but stained with secondary antibody only.

The comparable transfected cells immunostained with anti-TLR5 antibody are presented in the Figure 5.17. The cells in panel A stained green indicating TLR5 receptor protein. Staining of panels B and C was similar to A suggesting that there was no TLR5 overexpression in the RT4 cells transfected with the D1T1 and D1T2 plasmids.

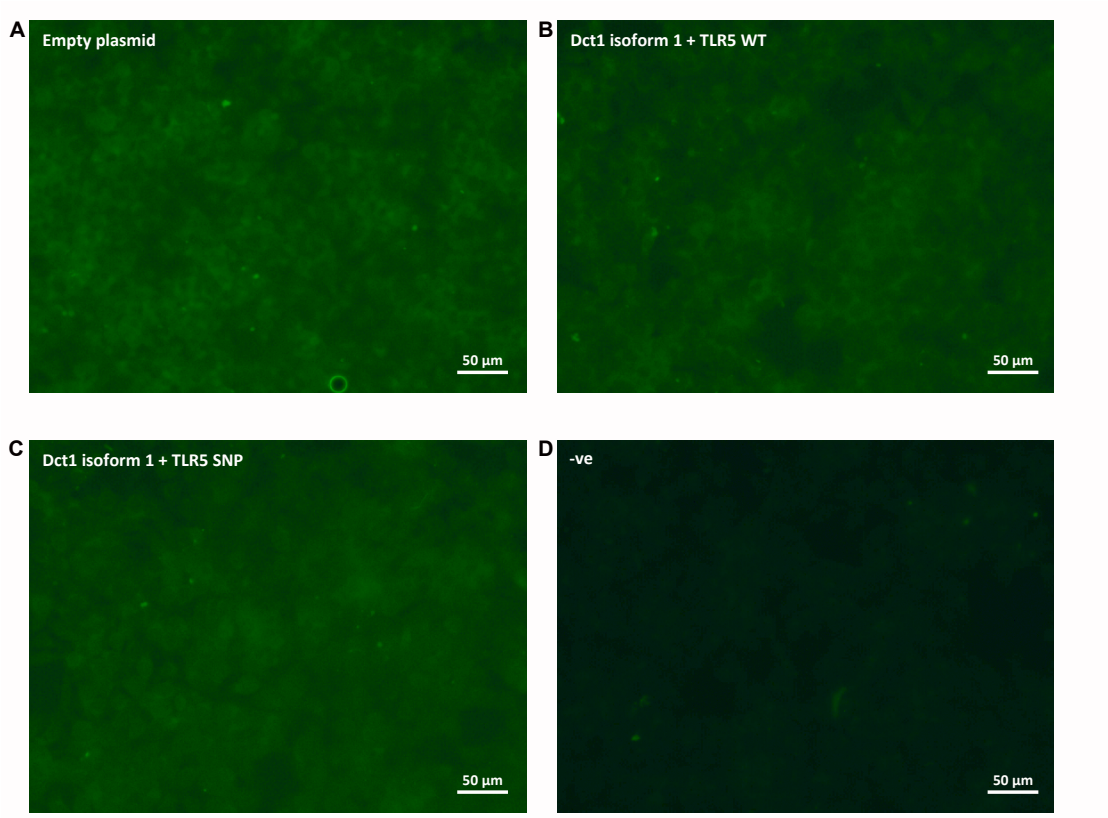

Figure 5.17 TLR5 immunostaining of transfected RT4 cells.
RT4 cells transfected with pVitro2 plasmids overexpressing Dectin-1R and TLR5 were fixed with 4% paraformaldehyde and incubated with anti-TLR5 antibody (1:50) and Alexa Fluor 488 secondary antibody (green colour). A: RT4 cells transfected with pVitro2 plasmid; B: RT4 cells transfected with D1T1 plasmid; C: RT4 cells transfected with D1T2 plasmid; D: RT4 cells transfected with empty plasmid but stained with secondary antibody only.

Overexpression of *CLEC7A* gene in the transfected cells was analysed using qRT-PCR. Data in Figure 5.18 shows that in D1T1 cells *CLEC7A* expression increased by 3% ± 20% compared to the control cells but decreased by 40% ± 20% in the D1T2 cells. However the difference was not statistically significant (p=0.5).

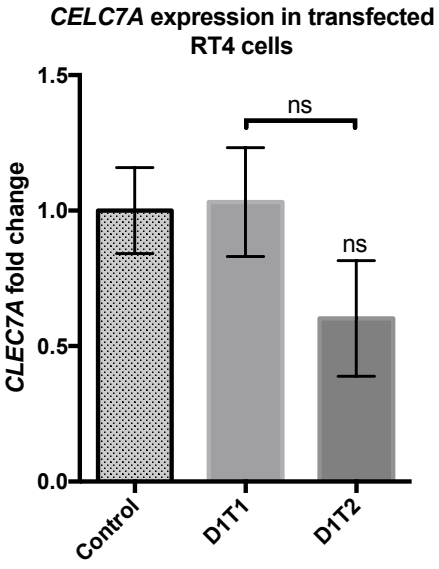

Figure 5.18 *CLEC7A* expression in transfected RT4 cells D1T1 and D1T2. qRT-PCR was used to analyse *CLEC7A* expression in the transfected RT4 cells.Data show mean ±SEM and N=2, n=6.

These results were disappointing. The constructs had been checked carefully before their transfection into the RT4 cells therefore these data suggested that the approach of using the pVitro2 plasmid to overexpress the Dectin-1 and TLR5 receptors to examine Dectin-1R and TLR5 physical and functional co-operation was flawed. It was therefore decided not to transfect the RT4 cells with the D4T1 and D4T2 constructs. Additionally as the immunostaining was comparable to wild-type RT4 cells it was decided to focus on using the non-transfected RT4 cell model to examine the Dectin1R signalling pathways.

5.5 Discussion

Previous data supported human bladder RT4 cells to express the *CLEC7A* gene and synthesise Dectin-1R proteins (Figure 3.2 and Figure 3.4) particularly isoforms 1, 2 and 4. Isoform 1 represents the full length Dectin-1R; isoform 2 does not have an extracellular stalk domain while isoform 4 lacks a stalk and has a shorter carbohydrate binding domain (Figure 1.10). In contrast human bladder epithelial cells express one TLR5 isoform although approximately 10% of population carry a SNP 1174C> T which encodes a STOP codon and results in the synthesis of a truncated TLR5. Data presented in Chapter 4 demonstrated

physical and functional co-operation between the Dectin-1 and TLR5 receptors and showed that zymosan promoted formation of Dectin-1R/TLR5 clusters in RT4 epithelial cells. Key questions arising therefore related to which Dectin-1R isoforms, either 1, 2, 4 or all three isoforms participated in this cooperation and clustering, and whether carrying a truncated TLR5 receptor impacts significantly on this co-operation. To further explore this, stably transfected RT4 cell lines overexpressing the Dectin-1R isoform 1 and either the wild-type or truncated TLR5 were engineered.

The expression vector chosen for this work was pVitro2, which facilitates the universal and constitutive co-expression of two genes or cDNAs of interest. The plasmid contains two human ferritin promoters, FerH (heavy chain) and FerL (light chain) with the endogenous 5'UTRs replaced by the 5'UTR of the mouse and chimpanzee EF-1α genes. This adjustment prevents any interference or regulation of expression due to iron. Driving the choice of this promoter was the need to express two different genes at same time and initially at the same concentrations. The advantage of this system was that the resultant transfected cell model would carry comparable numbers of Dectin-1 and TLR5 receptors facilitating the interpretation of subsequent data. The disadvantage was that the model may not reflect the in vivo situation although there is no *in vivo* data to either support or disprove equal numbers of receptors in bladder cells.

It was decided to focus on creating a stable cell model to provide reproducible and robust data. The original choice of cells was CHO cells as these are easy to transfect and culture. However as these proved resistant to the selection antibiotic G418 it was decided to utilise the original RT4 cells for the transfection studies. The advantages of using these cells were that they transfected easily. In fact stable transfectant lines had been engineered in the laboratory previously [83]. Additionally using bladder derived cells meant the cells contained all the required endogenous signalling apparatus to examine potential Dectin-1R/TLR5 interactions. The disadvantage was these cells synthesised endogenous Dectin-1 and TLR5 receptors and therefore forcing over-expression of these receptors could stress and kill the cells, which was a significant risk. Previous work used mouse fibroblasts to successfully overexpress eight different Dectin-1R isoforms

[102]. It could be argued therefore that human fibroblasts should have been used to overexpress the human Dectin-1 and TLR5 receptors although as with CHO cells it was not possible to predict whether these cells also contained the appropriate signalling systems to examine potential Dectin-1R/TLR5 interactions.

Although a series of Dectin1/TLR5 DNA constructs were engineered the transfection experiments were limited to using the Dectin-1R isoform 1/TLR5 and TLR5SNP constructs. These transfections were successful although it was noted that many of the original transfectant cell clones grew poorly, did not expand in cell numbers and died out.

Molecular analyses and immunostaning of the stably transfected cell lines supported increased Dectin-1R expression in the Dectin1/TLR5 cells but not in the Dectin1/TLR5SNP cells. In fact Dectin-1R signal intensity in the latter cell line was comparable to wild type cells. These data suggested that co-expression of truncated *TLR5* gene impacted on *CLEC7A* expression and Dectin-1R synthesis, meaning that the surviving cells selected and used to expand the cell line were flawed experimentally as they had actually down-regulated *CLEC7A* expression. If this was the case then it probably explained the early cell death of a number of transfectant clones.

Interestingly immunostaining did not support elevated levels of TLR5 protein in either cell line. There were no measurements of *TLR5* gene expression performed, which was an experimental flaw, and it is recognised that this lack of molecular data has impacted the ability to fully interpret and explain the results. However the immunostaining data as presented suggested no overexpression of TLR5 receptors. However it should be noted that the cells when stained with antibody were not permeabilised therefore increased intracellular localisation of receptors may have been missed.

Overall, these data were disappointing and indicated that engineering eukaryote cell models to explore the Dectin1/TLR5 receptor interactions was more challenging than originally anticipated. Simultaneous over expression of two plasma membrane receptors while defendable experimentally probably needed

additional finer control mechanisms. For example, the pVitro2 promoters were constitutive meaning the expression of both genes was switched on continuously, therefore using regulated promoters e.g. T-REx may have provided a better experimental option.

The *TLR5* gene has been successfully expressed in eukaryote cells. Early experiments investigating TLR5/Flagellin interactions involved COS-1 cells transfected, albeit transiently, with the *TLR5* gene [163]. Later work has also shown functionally active TLR5 receptors in HEK293 [164]. In addition stably transfected TLR5 HEK cells are available commercially (Invivogen). This suggests that potential issues linked to receptor protein synthesis and trafficking were probably not a problem in this study although the use of different cells lines and DNA constructs means this concern cannot be ignored totally.

In summary the construction of DNA plasmids engineered to allow co-expression of genes encoding Dectin-1 isoform 1 or 4 and wild type or truncated TLR5 receptor proteins in eukaryote epithelial cells was successful. However, following stable transfection of RT4 bladder cells only overexpression of the Dectin-1 receptor ie Dectin-1R isoform1 was detected. Therefore new approaches are needed to create a eukaryotic cell model that allows dissection and further study of Dectin1/TLR5 receptor interactions.

Chapter 6. Dectin-1R signalling in RT4 cells

Results from the gene knockdown and proximity ligation assay experiments presented in Chapter 4 supported the physical interaction and cooperation of Dectin-1R and TLR5 in the innate defence of the urothelium. To attempt to investigate this cooperation further, particularly intra-cellular signalling events following stimulation of the cells with zymosan, *in vitro* cell models overexpressing the wild type and/or Dectin-1R isoforms and wild type and/or truncated TLR5 receptors were engineered. However, as the resultant RT4 bladder cell models were only partially successful it was decided to use the original RT4 cells to explore downstream signalling events focussing initially on the response to a zymosan challenge.

It is known from work using myeloid derived cells including monocytes, macrophages and dendritic cells, that Dectin-1R stimulation results in a number of different effects, including phagocytosis, ROS production and/or the secretion of pro-inflammatory cytokines that play key roles in innate defence [165]. As discussed in Section 1.10 (page 17) studies have shown that Dectin-1R intracellular signalling underpinning such effects involves a number of different intracellular pathways (Figure 1.11), with the canonical signalling pathway, in these antigen presenting cells, being Syk dependant [166]. In this pathway stimulation of Dectin-1R results in phosphorylation of tyrosine protein kinase Syk leading to the activation of either the CARD9 complex or NF-κB-inducing kinase (NIK), both of which are associated with activation of the IKK complex. Phosphorylation and degradation of IκBα releases NF-κB, which translocates into the nucleus and activates the transcription of genes associated with the Dectin-1R response.

Signalling can, however, also occur via a non-canonical pathway, or Syk independent pathway, which involves activation of the protein kinase Raf-1 (Figure 1.11). Although less common it has been shown that activation of the Dectin-1R/Raf-1 signalling pathway in dendritic cells promotes secretion of IL-12 leading to the differentiation of T-helper cells [111].

Previous work in our laboratory showed that zymosan challenges of vaginal VK2 E6/E7 and bladder RT4 cells stimulated NF-κB activity [83]. Additionally using zymosan challenged vaginal VK2 E6/E7 cells and western blotting of the isolated proteins using an anti-phospho-Syk antibody, activation of the canonical Syk phosphorylation intracellular signalling pathway was proposed [83]. The aim of this chapter was to confirm these signalling data in RT4 bladder epithelial cells and further investigate the signalling cascade in relation to Dectin-1R/TLR5 cooperation.

6.1 Syk-P and Dectin-1R signalling cascade

At the onset it was predicted that the Dectin-1R signalling mechanism in the VK2 E6/E7 cells, in which Syk phosphorylation was identified following a zymosan challenge, would also function in the RT4 bladder epithelial cells. To confirm this the VK2 E6/E7 zymosan challenge experiment was repeated [83], but using RT4 bladder cells. Essentially RT4 bladder cells were challenged with zymosan (50 µg/ml) for 0, 15, 30, 45, 90 and 150 minutes. The protein samples were extracted and blotted onto nitrocellulose (Section 2.13) and the membranes probed with antibody to Syk and two anti-phospho-Syk antibodies each directed against two different phosphorylation sites Tyr525/526 and Tyr323 (Table 2).

Data shown in Figure 6.1 A & B indicated that no phospho-Syk protein bands were detected (72 kDa) following the zymosan challenge. However, following probing with antibody to Syk a 72kDa band was detected in all the samples (72 kDa).

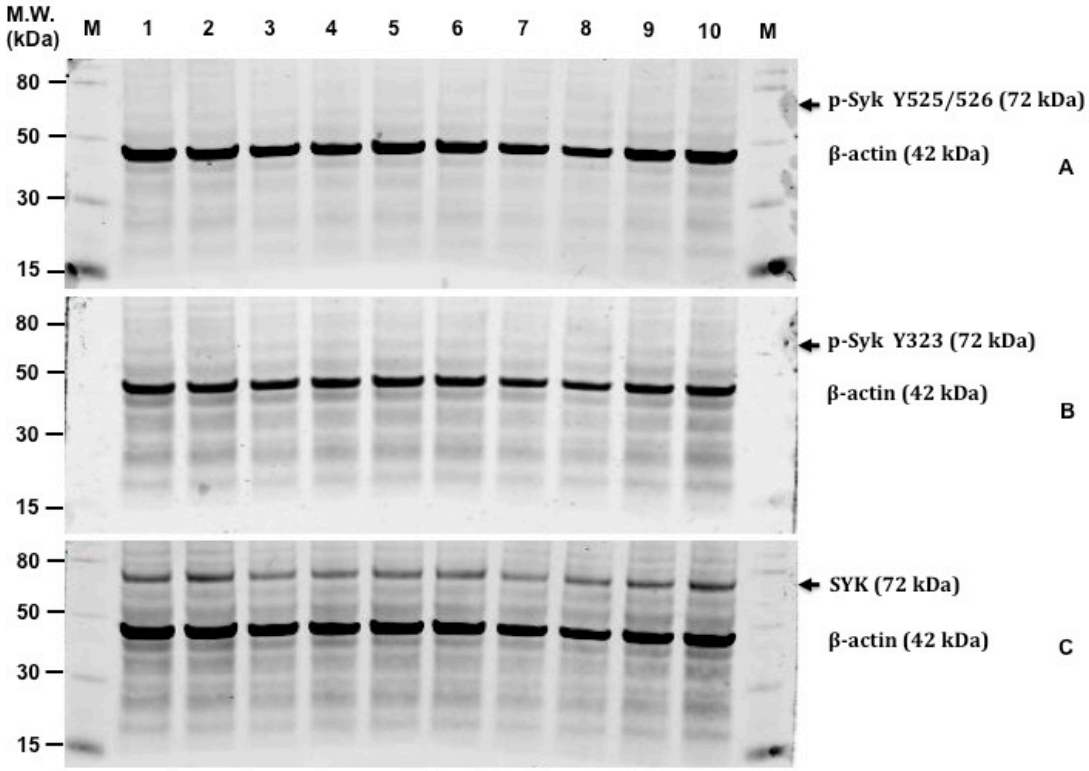

Figure 6.1 Immunoblot of phosphorylated Syk in RT4 cells challenged with zymosan (50 μg/ml**).**
M – molecular weight marker. Lanes were each loaded with 30 ug/ml protein. Lanes 1 and 2 – non-challenged RT4 cells; lanes 3 and 4 – RT4 cells challenged with zymosan (50 μg/ml) for 15 mins; lanes 5 and 6 –30 min challenge, lanes 7 and 8 –45 min challenge; lanes 9 and 10 – 90 min challenge; lanes 5 and 6 –150 min challenge. A: phospho-Syk Tyr525/526; B: phospho-Syk Tyr323; C: total Syk.

6.1.1 *SYK* gene knockdown with siRNA

These data were unexpected but the immunoblots were reproducible. These data therefore suggested that Syk was not involved in the Dectin-1R intra-cellular signalling pathway in RT4 cells. To explore this further a knockdown approach was taken. In these experiments *SYK* gene expression was reduced via siRNA knockdown and the zymosan (50 μg/ml) challenge experiments repeated. ELISA was used to measure the concentration of an effector, in this case IL-8, in the bathing media. Figure 6.2A demonstrated that expression of *SYK* mRNA was decreased by 95 % ± 2 % ($p<0.001$) following *SYK* gene knock-down (siSYK) when compared to RT4 cells transfected with a scrambled siRNA (scr).

Following the zymosan challenge the concentration of IL-8 (effector) in the bathing media of the wild type RT4 cells treated with scr siRNA was increased significantly from 1119 ± 141 pg/ml to 2247 ± 95 pg/ml ($p<0.0001$) (Figure 6.2, B). Similarly the concentration of IL-8 in the media bathing the *SYK* gene knockdown cells increased significantly from 898 ± 64 pg/ml to 2474 ± 124 pg/ml ($p<0.0001$). These data suggested, therefore, that *SYK* gene knockdown did not impact the synthesis of IL-8 following Dectin-1R activation and did not support the hypothesis that Syk was involved in Dectin-1R signalling in RT4 bladder epithelial cells. These gene knock-down data supported the western blot results reported in Figure 6.1.

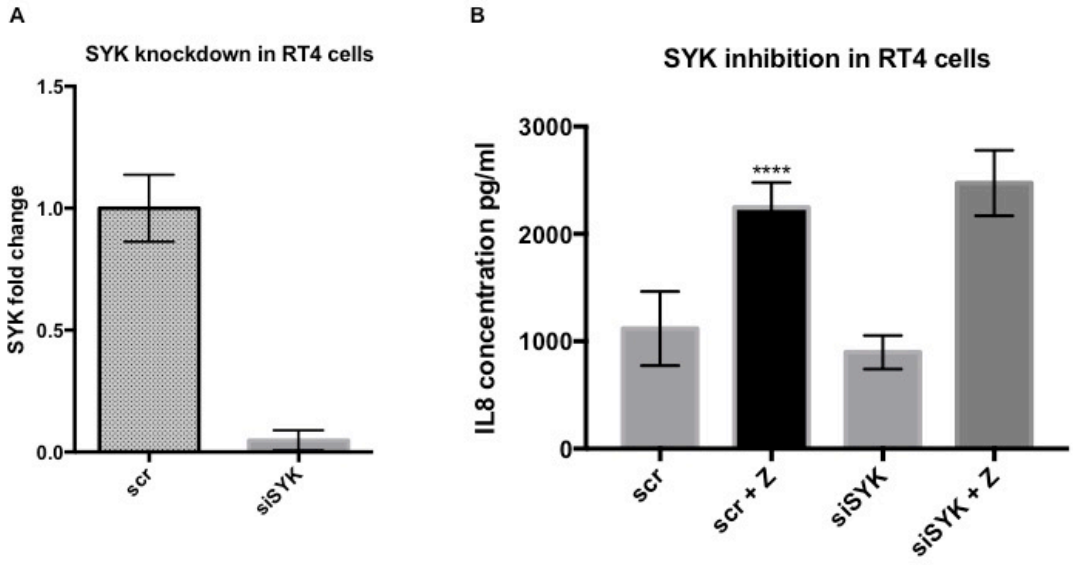

Figure 6.2 *SYK* gene knockdown in RT4 cells.
(A) The *SYK* gene was knocked down using an siRNA approach in RT4 cells and *SYK* expression measured using qRT-PCR. (B) siRNA treated RT4 cells were challenged with zymosan (50 µg/ml) for 6 hours and ELISA was used to measure IL-8 concentrations in the bathing media Data shows mean ±SD and N=2. *** $p<0.001$; **** $p<0.0001$

6.1.2 Inhibition of Syk with piceatannol

To further verify these results a third approach was taken involving use of the Syk inhibitor piceatannol [167-170]. In these experiments RT4 bladder cells were pre-treated with the inhibitor at concentrations of 0 µg/ml, 10 µg/ml, 20 µg/ml, 30 µg/ml and 100 µg/ml for 30 minutes and then challenged with zymosan (50 µg/ml) for 6 hours. These inhibitor concentrations were chosen as they had been shown previously to inhibit Syk activity in bronchi, endothelial and breast cancer cells [167-170].

Media bathing the cells was collected and the IL-8 concentrations measured using ELISA (Figure 6.3). Zymosan challenge of the wild-type cells resulted in an increase in IL-8 from 911 ± 66 pg/ml in unchallenged cells to 2742 ± 394 pg/ml in challenged cells. IL-8 bathing media concentrations in RT4 cells pre-treated with piceatannol concentrations of 100, 30, 20 and 10 µg/ml were 2380 ± 577, 3008 ± 484, 2952 ± 324 and 2778 ± 419 pg/ml respectively.

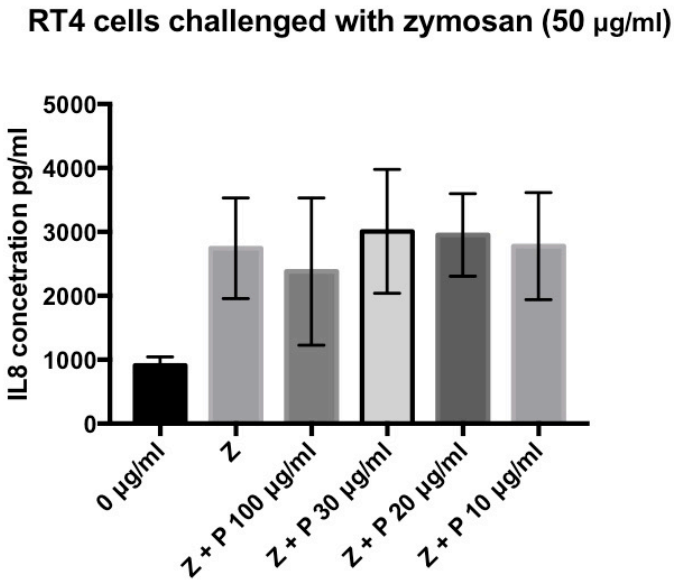

Figure 6.3 RT4 cells challenged with Zymosan following Syk inhibition with Piceatannol.
RT4 cells were pre-treated with Piceatannol (P) concentrations of 10, 20, 30 and 100 µg/ml for 30 minutes. The cells were challenged with zymosan (50 µg/ml) for 6 hours and media IL-8 concentrations measured using ELISA. Data shows mean ±SD and N=2.

These three sets of data using western blot, *SYK* gene knockdown and Syk inhibitor approaches all suggested that Syk was not involved in the Dectin-1R signalling cascade in RT4 bladder cells challenged with zymosan. These results contradicted the Lanz data [83].

6.1.3 Further analyses of Syk phosphorylation in RT4 cells

It was deduced that the signalling data was cell specific and that the VK2 E6/E7 data was unique to the vaginal cell line. To investigate this conundrum further the zymosan challenge experiment of Lanz (2013), was repeated exactly as described [83], but also using a higher concentration (200 ug/ml) of zymosan. The higher concentration of zymosan was used in an attempt to trigger a stronger signal for easier detection of phosphorylated Syk. The cells were also lysed in RIPA lysis buffer as used by Lanz, the lysed samples separated using SDS-PAGE, transferred to a nitrocellulose membrane, incubated overnight with anti-phospho-Syk antibodies (Table 3), 1 hour with secondary antibody and the membrane visualised using the Licor Odyssey imaging system. Data presented in Figure 6.4A (lanes 1, 2 and 3) demonstrated, conclusively, that no phospho-Syk was detected either in non-challenged or zymosan challenged RT4 cells.

Furthermore, additional experiments, using pervanadate treated RT4 cells, 2 mM and 5 mM for 15 minutes, showed the detection of protein bands relating to phospho-Syk Y323 (72 kDa) (Figure 6.4, A lanes 4 & 5). Pervanadate, is an accepted stimulant of Syk phosphorylation [171]. Bands relating to Syk protein (72 kDa) and β-actin (42 kDa) were also detected in all samples (Figure 6.4, B & C).

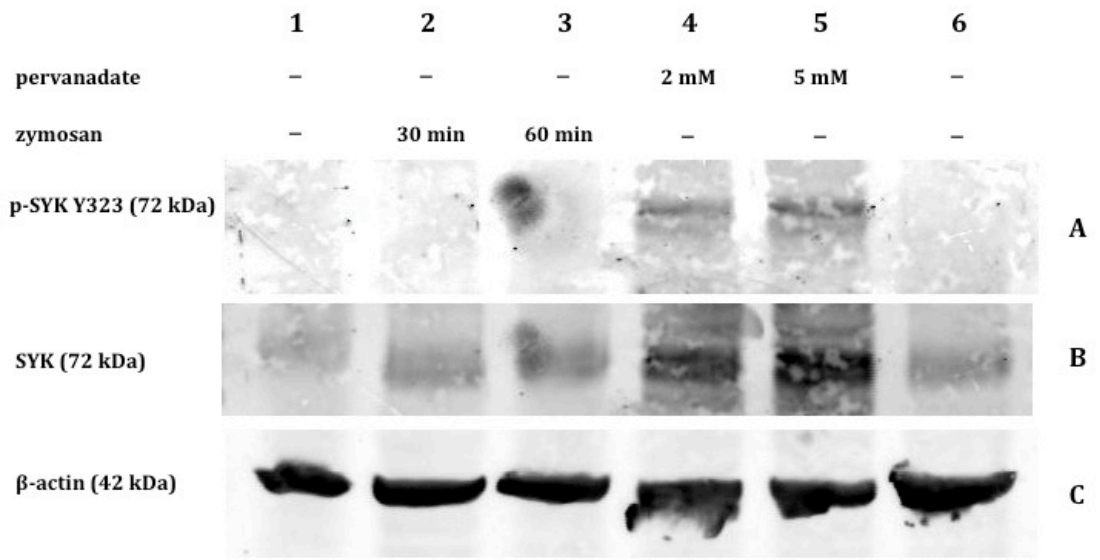

Figure 6.4 Immunoblot of Syk in RT4 cells challenged with zymosan.
RT4 cells were challenged with 200 µg/ml of zymosan for 0, 30 or 60 minutes (lanes 1-3) and pervanadate (2 mM or 5 mM) (lanes 4 and 5) for 15 minutes. Western analyses used anti-phospho-Syk Y323 antibody. The immunoblot represents two independent experiments (N=2).

In summary these data did not support the results of Lanz (2013). Moreover these data indicated that Dectin-1R signalling in RT4 bladder cells was probably functioning via a Syk independent pathway, which suggested a non-canonical signalling pathway.

6.2 Involvement of Raf-1 kinase in Dectin-1 signalling

The non-canonical pathway is a Syk independent Dectin-1R signalling pathway. This involves phosphorylation of Raf-1, NF-κB activation and effector gene expression. To investigate this pathway in zymosan challenged RT4 cells a siRNA knock-down approach was taken in which *RAF-1* gene expression was targeted.

In these experiments *RAF1* gene expression was reduced via siRNA knockdown and the zymosan challenge experiments repeated (50 µg/ml for 6 hours). ELISAs were used to measure the concentration of two effectors, IL-8 and LCN2 in the bathing media.

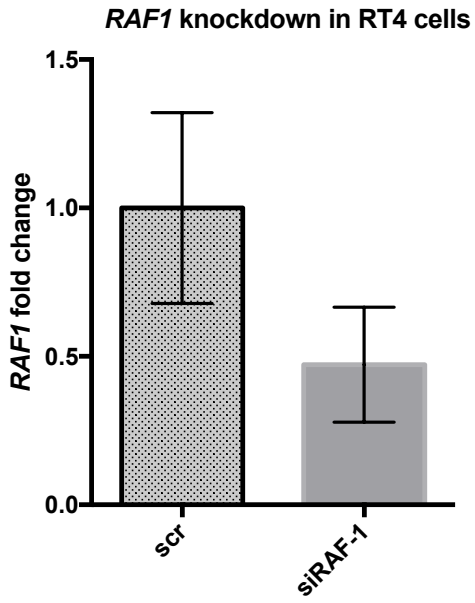

Figure 6.5 Raf-1 knockdown using siRNA.
The *RAF1* gene was knocked down using an siRNA in RT4 cells and *SYK* expression measured using qRT-PCR. Data shows mean ±SD and N=1.

Knock-down data are shown in Figure 6.5 and revealed reduction in *RAF-1* gene expression by 53 % ± 11%. Data resulting from the challenges of the knock-down cells are shown in Figure 6.6. Panel A shows the IL-8 concentrations following *RAF-1* gene knockdown and a 6h zymosan challenge. The mean IL-8 concentration of the RT4 cells treated with scr-siRNA was 937 ± 402 pg/ml and this increased 4 fold to 4148 ± 1445 pg/ml when challenged with zymosan. The mean IL-8 concentration of the *RAF-1* knockdown RT4 cells (siRAF-1) cells was 858 ± 384 pg/ml and following zymosan challenge this increased 3 fold to 3047 ± 848 pg/ml. When the data were normalised to eliminate variability between experiments, the error bars were decreased (Figure 6.6 B).

Data presented in Figure 6.6C shows the LCN2 data. The mean LCN2 concentration in the non-challenged wild type RT4 cell media (scr-siRNA) was 1365 ± 103 pg/ml and this increased to 2120 ± 506 pg/ml when the cells were zymosan challenged. Non-challenged *RAF-1* knockdown RT4 cells (siRAF-1) produced 806 ± 129 pg/ml of LCN2, which increased to 1370 ± 211 pg/ml in the challenged cells (si*RAF-1* + Z). The mean LCN2 concentration in the zymosan challenged control cells (scr + Z) was significantly increased ($p < 0.01$) compared

to the challenged knockdown cells (si*RAF-1* + Z). To eliminate variability between experiments the data were normalised (Figure 6.6 D).

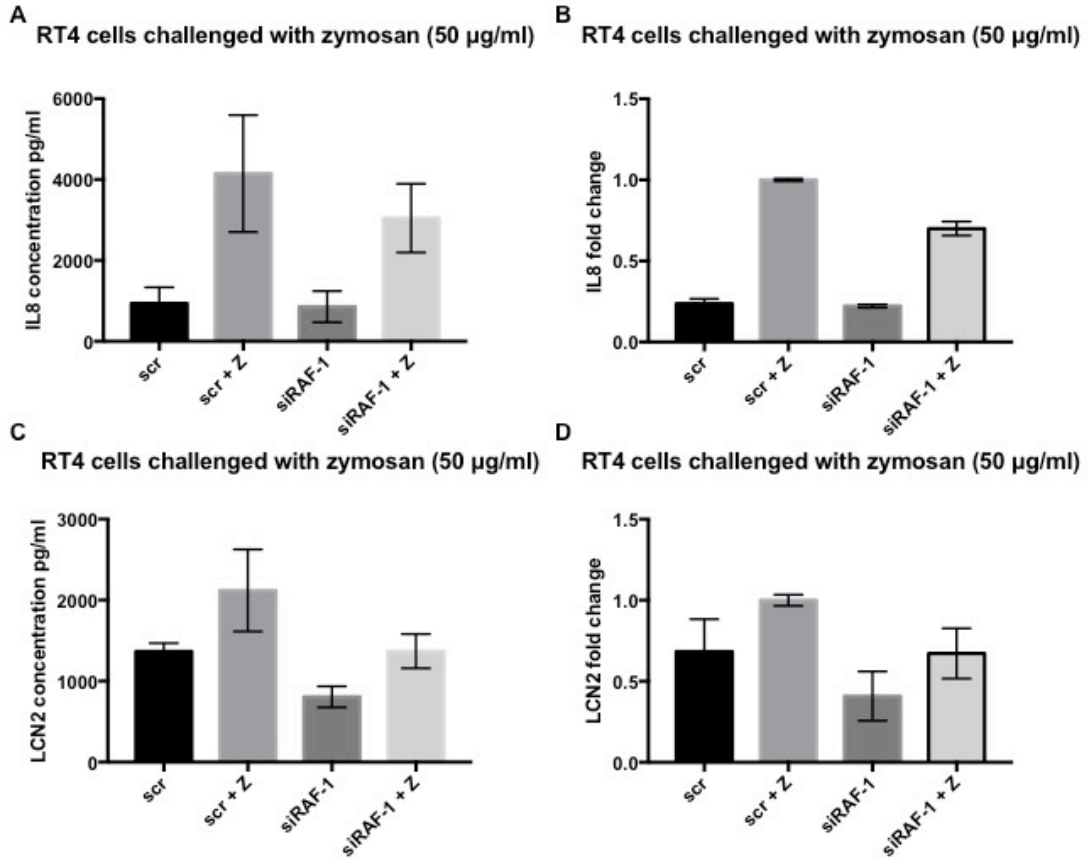

Figure 6.6 *RAF1* knockdown in RT4 cells and zymosan challenge.
RAF1 was knocked down with siRNA (siRAF-1) and the cells challenged with zymosan (50 µg/ml) for 6 hours. IL-8 and LCN2 media concentrations were measured using ELISA. Data show mean ±SD and N=2.

Interestingly the mean LCN2 concentration in the non-challenged knockdown cells (siRAF-1) was lower (40%) compared to the non-challenged control cells (scr) (Figure 6.6, C-D). These data suggested that *RAF-1* knockdown decreased the constitutive synthesis of LCN2.

These data analysing IL-8 and LCN2 effector concentrations in *RAF1* knockdown RT4 bladder epithelial cells supported a Syk independent Dectin-1R signalling pathway functioning in RT4 bladder cells in response to a zymosan challenge.

6.3 IkBa and Dectin-1R signalling

Previous data from our laboratory using a RT4 bladder NF-κB reporter cell line indicated that zymosan challenge of RT4 cells stimulated NF-κB signalling activity (Figure 4.1) [83]. In the absence of a stimulus NF-κB is bound to IκBα which inhibits or blocks any NF-κB activity (Figure 6.9, page 129) [172, 173]. However, following a stimulus phosphorylation of IκBα leads to its degradation [174, 175] allowing NF-κB to translocate into the nucleus and activate gene transcription [172, 173]. To further investigate this pathway operating in bladder epithelia in response to zymosan/Dectin-1R activation confluent RT4 cells were challenged with zymosan (200 μg/ml) for 30 and 60 minutes, the cell lysates collected, electrophoresed via SDS-PAGE and western blots used to analyse IκBα and phospho-IκBα proteins. The antibodies used in these analyses are shown in Table 3.

The resultant data are shown in Figure 6.7. Phospho-IκBα data is shown in A. No phospho-IκBα bands were detected in the PBS challenged RT4 cells (lane 1). However, strong bands of 39 kDa were detected in the cells challenged with zymosan for 30 or 60 minutes (lanes 2 & 3). Phospho-IκBα bands were also detected in RT4 cells challenged with flagellin, a classic activator of the NF-κB pathway (lanes 5 & 6) [147, 148, 176].

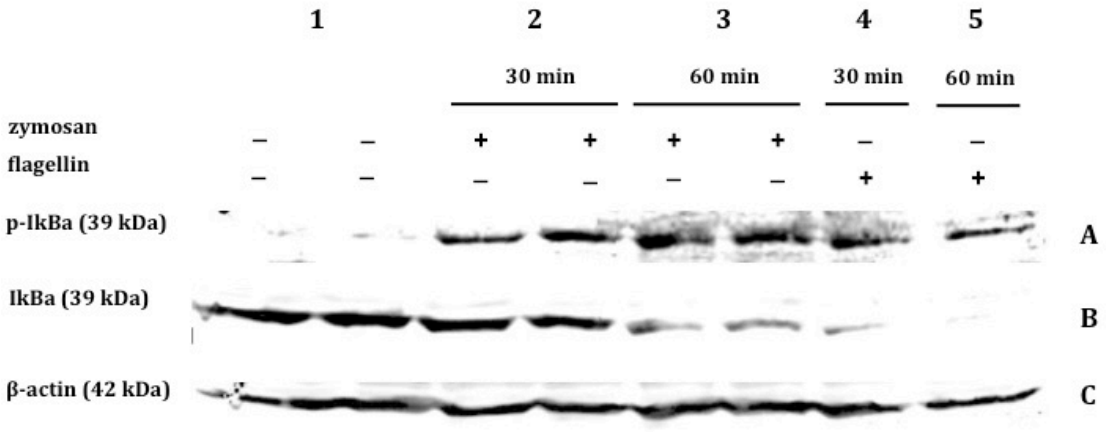

Figure 6.7 Immunoblot of IκBα and phosphorylated IκBα in RT4 cells challenged with zymosan.
RT4 cells were challenged with PBS (lane 1), 200 μg/ml of zymosan for 30 or 60 minutes (lane 2 and 3) or with 50 ng/ml of flagellin for 30 and 60 minutes (lane 4 and 5). SDS-PAGE was used to separate proteins and immunoblotting was used to detect phospho-IκBα (A), IκBα (B) and β-actin (C) proteins. Data shown are representative of two independent and reproducible experiments.

These western blots were re-probed using anti-IκBα antibody (Figure 6.7B). These data showed that IκBα bands were detectable in PBS challenged cells (lane 1) and cells challenged with zymosan (50 ng/ml) for 30 minutes (lane 2). However, when the cells were incubated with zymosan for 60 minutes the IκBα bands were weaker suggesting protein degradation (lane 3). Similarly the intensity of the IκBα bands was also reduced in the RT4 cells challenged with flagellin compared to PBS challenged cells (lanes 4 & 5).

These western analyses revealed that zymosan challenge of RT4 bladder cells stimulated phosphorylation and consequently degradation of IκBα, which supports this protein being part of the Dectin-1R activated intracellular signalling cascade.

These data provided further evidence that in zymosan challenged RT4 bladder cells Dectin-1R signalling involves a Raf-1 - IκBα - NF-κB pathway, which supports a non-canonical signalling mechanism.

6.4 Discussion

This chapter investigated Dectin-1R signalling pathways in immortalised RT4 bladder epithelial cells. It has been shown in myeloid derived cells that activation of the Dectin-1R promotes Syk phosphorylation, which promotes a signalling cascade involving NF-κB translocation into the nucleus and transcription of effector genes involved in innate defence [107]. Defence mechanisms include cytokine synthesis, ROS production and phagocytosis [165]. This is known as the canonical signalling pathway. However, a second pathway, known as the Syk independent or non-canonical signalling pathway has also been reported in dendritic cells. For this pathway it has been shown that Dectin-1R stimulation by in response to curdlan and/or *Candida albicans* phosphorylates the serine-threonine protein kinase Raf-1, which activates NF-κB to promote the synthesis and secretion of cytokines including IL-12 that facilitates T helper cell differentiation [111]. This suggests the pathway functions to bridge the innate and adaptive immune systems in protecting the body against fungal infections.

Previous data from our laboratory, but using vaginal VK2 E6/E7 cells suggested that the Dectin-1R ligand, zymosan, activated the tyrosine kinase Syk phosphorylation pathway [83]. Interestingly data exploring antifungal immunity in human corneal cells [152] and intestinal cells [91] likewise indicated Syk activation to play a key role in regulating inflammatory responses to fungal β-glucans in epithelia. Therefore the aim of this work was to confirm comparable Syk signalling in the RT4 bladder epithelial cells and explore the signalling responses relating to TLR5/Dectin-1R co-operation.

However, despite significant efforts involving three different approaches - western analyses, *SYK* siRNA knockdown and the Syk inhibitor piceatannol, used at the same concentrations that inhibited the secretion of pro-inflammatory proteins in epithelial cells [167, 168] - the resultant data strongly suggested that Syk phosphorylation was not involved in Dectin-1R signalling in RT4 bladder cells.

Lanz, in his work, reported phospho-Syk bands on immunoblots containing protein samples prepared from VK2 E6/E7 cells challenged with zymosan for 15

minutes or longer and probed with antibody to phospho-Syk (Figure 6.8) [83]. As vaginal and bladder epithelial cells are part of urogenital tract these data suggested that a common signalling mechanism may operate. However, the RT4 data presented here, particularly the evidence using pervanadate (2 mM or 5 mM) a well-known activator of Syk phosphorylation [168], did not support this. In fact these data argued, strongly, that zymosan treatment does not promote Syk phosphorylation in RT4 bladder cells. To address this enigma the original data ie the immunoblot from 2013 was retrieved and reviewed. Re-analyses of the western blot established that the blot data had been misinterpreted. In fact the sizes of the phospho-Syk bands detected were smaller, approx. 55 kDa, than the actual expected size of 72kDa.

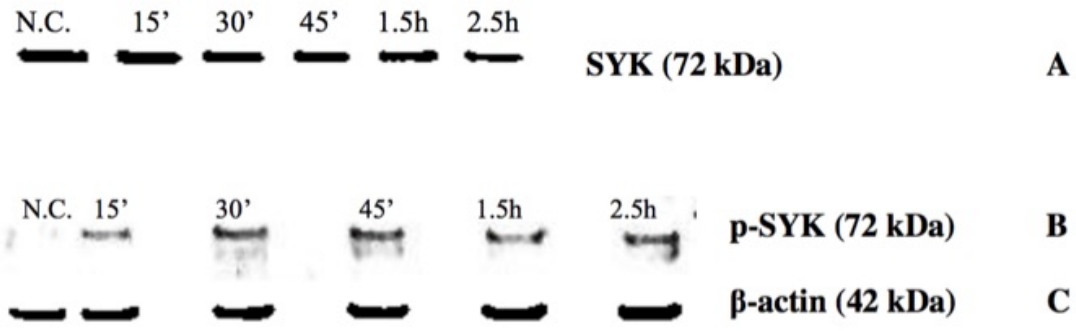

Figure 6.8 Immunoblot of phosphorylated Syk in VK2 cells challenged with zymosan [83].
The size of phospho-Syk bands presented in the blot was misinterpreted and was actually 55 kDa (p-Syk is 72kDa).

Re-analysing these data therefore helped to confirm that Dectin-1R activation and signalling in RT4 bladder (and presumably VK2 E6/E7 vaginal) epithelial cells does not involve Syk phosphorylation. Moreover, these new data indicated that the non-canonical signalling pathway functions in uro-genital epithelial cells in response to a zymosan (fungal) challenge.

Searches of the literature did not reveal many reports of Raf-1 signalling during fungal infections, although one paper was of interest. This paper reported research involving Candida and β-1-3 glucans challenges of human primary

mononuclear cells [177]. The authors concluded that such treatments can function to prime these cells, with priming leading to enhanced cytokine production when the cells are further stimulated with TLR ligands, LPS and lipopeptides eg Pam_3Cys_4, and intestinal bacterial commensals including *Bacteroides fragilis*, *Staphylococcus aureus* and *E.coli* ATCC 35218. It is significant that priming involves the Dectin-1R and is facilitated by the non-canonical pathway involving Raf-1. However, the data actually supporting the involvement of the Raf-1 pathway is weak as the experimental information mentions only that a Raf-1 inhibitor was used, but does not actually name the inhibitor. This raises serious questions relating to inhibitor specificity. Still these data, while focussed on TLR2/4 ligands and myeloid derived cells, are comparable to the results reported in this thesis using epithelial cells and flagellin. However, the key difference is that Dectin-1R signalling in response to β-1-3 glucan in RT4 bladder epithelial cells appears purely Raf-1 dependent.

Interestingly, data published by Trinath et al. (2014), suggests that activation of Dectin-1R and TLR pathways in fungal infected macrophages can result in the inflammatory responses being inhibited [178]. The authors propose a mechanism involving Syk and WNT5A pathways, and suggest that such pathways can be exploited by virulent fungi to limit and therefore overcome the host responses to infection.

More recent work although again focussed on dendritic cells has shown Dectin-1R stimulation by curdlan to involve Syk, Raf-1 and NF-κB signalling, and result in factors TNFSF15 and OX40L that function as agonists and promote differentiation of naïve CD4 T cells into anti-tumour Th9 cells [127]. These authors suggest a role for the Dectin-1Rs in triggering anti-tumour activity although the use of dendritic cells suggests this property may be unique to such cells.

Another C-type lectin receptor, DC-SIGN, has been shown to stimulate Raf-1 phosphorylation via Ras protein activation as part of the innate defences [95]. As in this pathway NF-κB is activated by phosphorylation and acetylation of p65

subunit it would be interesting to explore potential roles for Ras protein activation in the RT4 zymosan/Dectin-1R signalling cascade.

Issues linked to confirming Syk phosphorylation in the RT4 bladder cells challenged with zymosan meant that further analyses exploring the signalling events relating to Dectin-1R/ TLR5 co-operation were not explored. Future experiments are needed to examine these events. For example, data reported by Lanz [83] showed that Dectin-1R activation stimulated NF-κB activity. In the canonical NF-κB activation pathway IkBa is phosphorylated to allow translocation of NF-κB from cytoplasm into the nucleus to activate DNA transcription. Western blot data presented in this chapter confirmed that zymosan stimulation of the Dectin-1R in RT4 bladder cells promoted phosphorylation and degradation of IkBa. However, these data conflict with the data linked to dendritic cells, which showed that Raf-1 dependant NF-κB activation was due to acetylation of its p65 subunit [111]. These data suggest the functioning of different Dectin-1R intracellular signalling pathways in antigen presenting and epithelial cells, probably related to the different functions of the cells the defence of the host, and which need to be unravelled.

In summary the data presented in this chapter suggests a novel signalling cascade functioning following zymosan activation of the Dectin-1R in RT4 bladder epithelial cells. To date this cascade appears to be Syk independent and involves the protein kinase Raf-1, IkBa phosphorylation and NF-κB signalling (Figure 6.9).

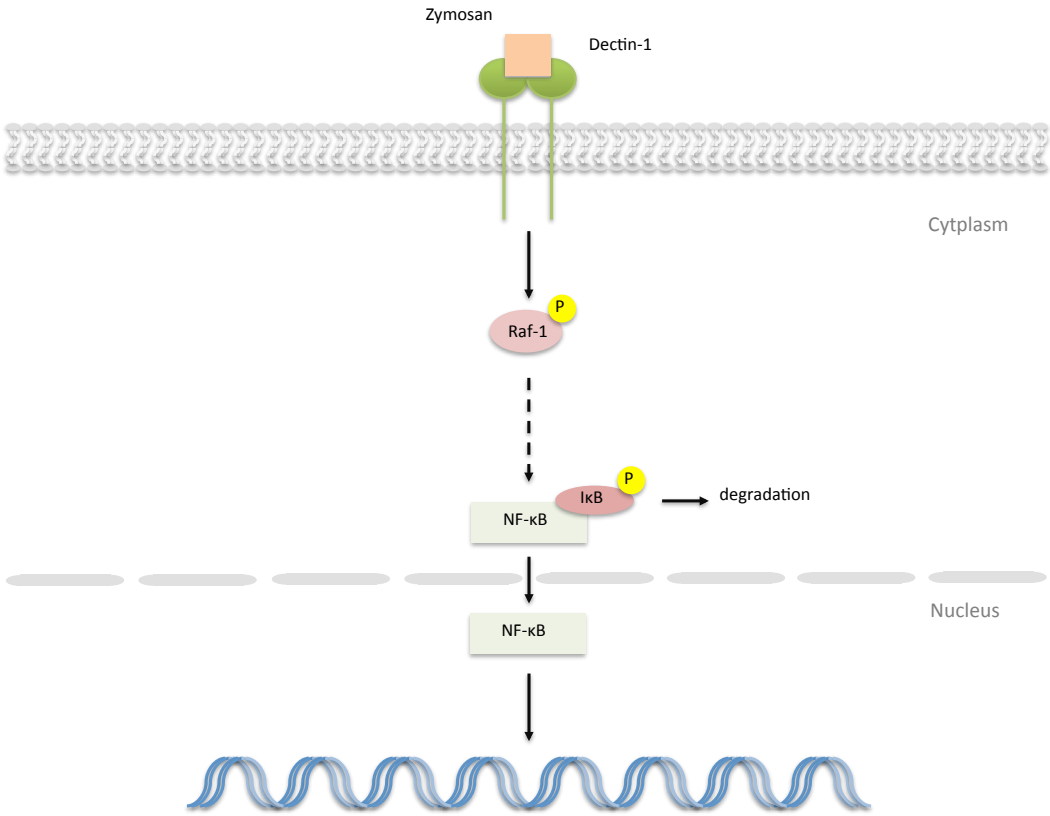

Figure 6.9 Dectin-1R signalling in bladder epithelial cells is Raf-1 dependent.
Dectin-1R upon triggering with zymosan activates Raf-1, which initiates IκBα phosphorylation and degradation. This allows NF-κB to translocate into nucleus and initiate transcription of defence molecules.

Chapter 7. Summary and Final Discussion

Approximately 25 to 50% of women will suffer an urinary tract infection (UTI) during their life-time and many of these, especially in their post-menopausal years, will experience recurrent infections. These infections are often treated with prophylactic antibiotics, but this raises significant clinical and environmental issues due to the development of antibiotic resistant strains. As a result there have been significant efforts to understand bacterial infections of the human urinary tract with much research centred on understanding the virulence factors that enable uropathogenic *E. coli* (UPEC) to ascend the urinary tract and cause disease. The arguments supporting such research are that knowledge of bacterial virulence allows the development of novel antimicrobial therapies. While research has also focussed on dissecting the relationship between host urothelial cells and UPEC the use of the mouse model has complicated the story. Data from mice work suggest TLR4 to be the key receptor in detecting UPEC [80-82] while work using human cells strongly suggests TLR5, which recognises flagellin, to be the key pathogen detector operating in lower urinary tract [83, 84].

The importance of TLR5 is supported by clinical studies that show patients carrying the TLR5 SNP C1174T synthesise a truncated receptor that cannot signal and are more susceptible to recurrent (r)UTIs [40, 86]. In fact, because of the truncated receptor the innate defences of such patients are reduced which helps to explain their increased susceptibility to rUTIs. One therapeutic option for such patients is to try and boost their own bladder innate defences, and one potential mechanism in females involves use of a topical hyaluronic acid treatment [155].

Previous work in our laboratory suggested that urothelial cells cultured *in vitro* expressed the *CLEC7A* gene encoding the Dectin-1(R) receptor, which binds β-glucans, a component of fungal cell wall. This was interesting as most of the published Dectin-1R literature relates to studies performed using myeloid derived cells including monocytes, macrophages and dendritic cells [98, 120, 129]. At present only a handful of published papers reporting on this receptor in

epithelial cells exist, and which relate to the lung, gut and corneal tissues [90, 130, 179]. Work in the laboratory also hinted at a co-operative relationship between the Dectin-1 and TLR5 receptors in the bladder that enhanced the innate response of the urothelial cells to a fungal challenge. This observation therefore suggested that the innate response of rUTI patients could be boosted using novel β-glucan based therapies that specifically targeted the Dectin-1R. To explore this further the expression and function of the Dectin-1R in bladder cells were investigated *in vitro* using the immortalised RT4 bladder cell line.

Data presented in chapter 3, analysed *CLEC7A* gene expression and Dectin-1R synthesis initially using a human bladder biopsy and then in immortalised RT4 bladder epithelial cells. These data revealed the synthesis of two Dectin-1R isoforms in the bladder biopsy, known as isoform 1 and isoform 2. Interestingly in the RT4 cells three isoforms 1, 2 and 4 were detected. The roles of isoform 4 in fungal defence are not known although work using myeloid derived cells suggests that only isoforms 1 and 2 are able to bind ligands [102]. Closer inspection of the isoform 4 sequence suggested that it encoded a smaller carbohydrate binding domain and a shorter signalling intracellular motif compared to the isoforms 1 and 2. Experiments attempting to explore the potential roles of isoform 4 in the innate response were designed and reported in chapter Chapter 5.

Data from the biopsy and *in vitro* work suggested that the RT4 bladder cells were an appropriate model of the human urothelium and were used in subsequent analyses. Dectin-1R activation used zymosan, a yeast cell wall preparation, and essentially this mimicked a fungal infection. The immune response was explored by measuring gene expression and synthesis of an array host defence peptides and proteins. The challenge data clearly showed that such molecules to be increased in the challenged cells, and this finding mirrored results reported in myeloid cells [124, 130, 131, 179]. These results, together with previous work in our laboratory and *CLEC7A* gene knockdown data presented in chapter 4, demonstrated that activation of the Dectin-1R could evoke an immune response in bladder epithelial cells. Importantly these data also suggested that targeting

the bladder Dectin-1R, for example, with agents mimicking β-glucans could potentially boost the bladder innate defences and be exploited as a new non-antibiotic based therapy to help treat recurrent UTIs.

However, exploitation of the Dectin-1R in rUTI therapy for all rUTI patients remains questionable because of data suggesting co-operation between the Dectin-1 and TLR5 receptors [83]. This co-operation was confirmed in chapter 4 using gene knock-down and proximity ligation assay techniques. Scientifically these data are novel as previous studies in macrophages and dendritic cells demonstrated Dectin-1R co-operation with TLR2 and TLR4 receptors, but not TLR5 [129, 180]. However, clinically these data suggest that knockdown or blocking of TLR5 decreases the potency of the Dectin-1R immune response. Therefore in patients carrying the TLR5 SNP C1174T it can be argued that treating with a β-glucan therapeutic to help boost the host innate response will probably have a reduced effect.

The proximity ligation assay data demonstrated that the Dectin-1R and TLR5 receptors interacted physically in zymosan challenged RT4 epithelial cells. It is reported that TLR5 receptors bind flagellin and function by forming homodimers [78, 79] so the idea of TLR5 forming a 'heterodimer' with the Dectin-1R is novel. It is known that TLR1, TLR2, TLR4 and TLR6 can form heterodimers in stimulated macrophages [181], and that Dectin-1 receptors form heterodimers with TLR2 in macrophages following a fungal challenge [182]. The outcome of this co-operation is still debatable, but is known to potentiate the host response. For example Dectin-1R co-operation with TLR2 results in an amplified immune response in curdlan challenged dendritic cells [111]. The Dectin-1 and TLR5 receptors were also observed to cluster (Figure 4.9). Dectin-1R/TLR2 clusters have been shown to have a role in the formation of a phagocytic synapse in macrophages [182]. However, as bladder epithelial cells do not have a phagocytic function clustering must play a different role.

It is possible that clustering increases the affinity and sensitivity of ligand binding and is needed to initiate a signalling cascade as was shown with T-cell receptors in T cells [183, 184]. However, clustering may relate to the fungal

infection *per se*. Fungi such as yeasts can colonise tissues without causing infection and in such conditions the β-glucan of the fungal cell wall is masked by mannan (Figure 1.8, B). During infection hyphae are produced that expose the β-glucan of the fungal cell wall, which is detected by the Dectin-1 receptors and triggers an innate defence response. It can be hypothesised that the concentrations of β-glucan during the initial infection stages are low therefore activated Dectin-1 receptors clustering with TLR5 receptors, which are major TLR receptors on the bladder epithelium, would amplify the signalling cascade significantly. This in turn would result in a very strong host defence response that rapidly clears the infecting fungi (Figure 7.1). Interestingly, molecular analyses of RT4 bladder cell RNA did not identify the expression of the *CLEC4N* gene, encoding Dectin-2 receptors, even following a α-mannan challenge (data not shown).

Experiments to explore this idea further, in addition to investigating the individual roles of Dectin-1 receptor isoforms 1, 2 and 4 in the co-operation/signalling events, were designed and presented in chapter Chapter 5. These involved engineering a suite of cell lines each over-expressing the Dectin-1 receptor isoforms and either TLR5 full-length or TLR5 truncated receptors. However, the outcomes were disappointing as the over-expression approach appeared to stress the cells, resulting in the cell lines being selected and passaged that did not over-express the Dectin-1 and TLR5 receptors. This experimental approach used a vector that co-expressed the two different receptor genes simultaneously. It could be argued therefore that the increased number of receptors synthesised by the cell over-loaded the urothelial cell membranes causing gene silencing and/or cell death. Several other approaches have been discussed to continue this work involving either the use of different expression vector systems and/or the use of isoform specific knockdowns and isoform specific antibodies.

The final part of this project presented in chapter Chapter 6 was to investigate the Dectin-1R signalling pathway in RT4 epithelial cells in response to a zymosan challenge. Studies in monocytes, macrophages, dendritic cells and corneal epithelial cells all identified a Syk-dependent pathway as the canonical signalling

pathway [131] that activated NF-κB mediated gene transcription of host defence peptides and proteins. However, western analyses using anti-phospho-Syk antibodies, use of the Syk inhibitor piceatannol and *SYK* gene knock-down all suggested that the Syk canonical pathway did not mediate Dectin-1R signalling in RT4 bladder epithelial cells. Instead the data supported a non-canonical signalling pathway involving Raf-1 and similar to that reported in dendritic cells [111].

This result was not expected, but may reflect differences in bladder epithelial cells compared to myeloid derived cells. For example macrophages and dendritic cells are migratory, can perform phagocytosis and often bridge the innate and adaptive immune systems. In contrast epithelial cells are fixed and as a first defence mechanism need to synthesise and secrete host defence peptides and proteins that kill microbes directly and attract antigen presenting cells to the site of infection. It is therefore probable that the signalling cascade using Raf-1 is activated in direct response to fungal, β-glucan, ligands. The data in this study suggested that physical interaction of Dectin-1R with TLR5 enhances the response (Figure 7.1). However composition of Dectin-1R/TLR5 complex has not been revealed. Moreover although it has been shown that Dectin-1R physically interacts with other toll-like receptors [143], no data has been published demonstrating stoichiometry of the complexes. Interestingly, challenging the RT4 urothelial cells with pervanadate, which is associated with the production of reactive oxygen species (ROS), resulted in production Syk-P. It has been shown that ROS affect kinases and phosphorylation of various targets in the NF-κB signalling pathway [185]. Therefore these data suggest, potentially, that ROS produced during a fungal infection work independently of Dectin-1R/TLR5 complex and are detected via a Syk-P signalling pathway, which in turn helps to amplify the epithelial host defence response (Figure 7.1). Future experiments are needed to explore these hypotheses further.

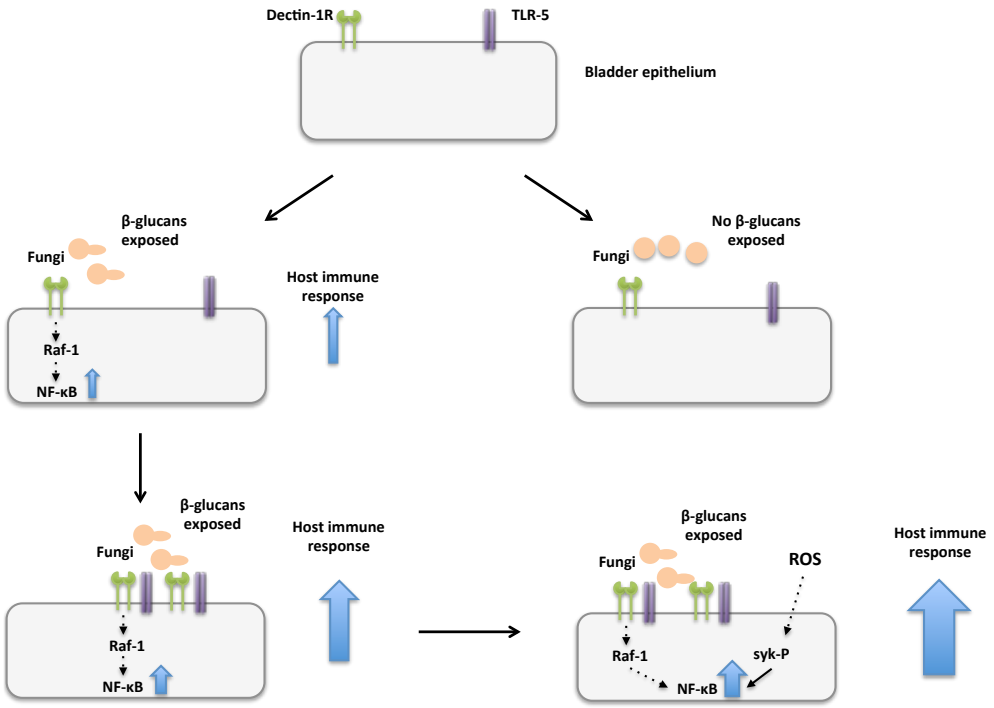

Figure 7.1 Dectin-1R in bladder epithelial cells.
β-glucans stimulate Dectin-1R and activate Raf-1 signalling pathway, which activates NF-κB to stimulate host immune response. Physical interaction of Dectin-1 with TLR5 strengthens the response. ROS activates Syk pathway independently of Dectin-1R and toll-like receptors and amplifies the response to a fungal infection.

In conclusion data presented in this thesis suggest that Dectin-1Rs are synthesised by urothelial cells and play a significant role in the defence of urothelium against fungal infection. Dectin-1R signalling involves a Raf-1 signalling cascade and the receptors appear to co-operate in the signalling process with TLR5 receptors.

These data are exciting, but further analyses of the Dectin-1 receptor isoforms synthesised by the bladder epithelia, their co-operation with TLR5 receptors and the signalling cascades that underpin the observed host responses are necessary to help unravel the roles these receptors play in defending the uro-genital tract from infection. These data also suggest that a future β-glucan based therapy might be successful in boosting the host defence response of patients suffering rUTIs, although it may be less effective in patients carrying the TLR5 SNP C1174T.

References

1. Hickling, D.R., T.T. Sun, and X.R. Wu, *Anatomy and Physiology of the Urinary Tract: Relation to Host Defense and Microbial Infection.* Microbiology Spectrum, 2015. **3**(4).
2. Riedel, I., et al., *Urothelial umbrella cells of human ureter are heterogeneous with respect to their uroplakin composition: different degrees of urothelial maturity in ureter and bladder?* European Journal of Cell Biology, 2005. **84**(2-3): p. 393-405.
3. Romih, R., et al., *Differentiation of epithelial cells in the urinary tract.* Cell and Tissue Research, 2005. **320**(2): p. 259-268.
4. Batourina, E., et al., *Apoptosis induced by vitamin A signaling is crucial for connecting the ureters to the bladder.* Nature Genetics, 2005. **37**(10): p. 1082-1089.
5. Oottamasathien, S., et al., *Bladder tissue formation from cultured bladder urothelium.* Developmental Dynamics, 2006. **235**(10): p. 2795-2801.
6. Wu, X.R., et al., *Uroplakins in urothelial biology, function, and disease.* Kidney International, 2009. **75**(11): p. 1153-1165.
7. Khandelwal, P., S.N. Abraham, and G. Apodaca, *Cell biology and physiology of the uroepithelium.* American Journal of Physiology-Renal Physiology, 2009. **297**(6): p. F1477-F1501.
8. Ramuta, T.Z. and M.E. Kreft, *Human Amniotic Membrane and Amniotic Membrane-Derived Cells: How Far Are We from Their Use in Regenerative and Reconstructive Urology?* Cell Transplantation, 2018. **27**(1): p. 77-92.
9. Wu, X.R., J.J. Medina, and T.T. Sun, *SELECTIVE INTERACTIONS OF UPIA AND UPIB, 2 MEMBERS OF THE TRANSMEMBRANE-4 SUPERFAMILY, WITH DISTINCT SINGLE TRANSMEMBRANE-DOMAINED PROTEINS IN DIFFERENTIATED UROTHELIAL CELLS.* Journal of Biological Chemistry, 1995. **270**(50): p. 29752-29759.
10. Hu, P., et al., *Ablation of uroplakin III gene results in small urothelial plaques, urothelial leakage, and vesicoureteral reflux.* Journal of Cell Biology, 2000. **151**(5): p. 961-971.
11. Kachar, B., et al., *Three-dimensional analysis of the 16 nm urothelial plaque particle: Luminal surface exposure, preferential head-to-head interaction, and hinge formation.* Journal of Molecular Biology, 1999. **285**(2): p. 595-608.
12. Arrighi, S., *The urothelium: Anatomy, review of the literature, perspectives for veterinary medicine.* Annals of Anatomy-Anatomischer Anzeiger, 2015. **198**: p. 73-82.
13. Hurst, R.E., *A deficit of proteoglycans on the bladder uroepithelium in interstitial cystitis.* European Urology Supplements, 2003. **2**(4): p. 10-13.
14. Bacakova, L., K. Novotna, and M. Parizek, *Polysaccharides as Cell Carriers for Tissue Engineering: the Use of Cellulose in Vascular Wall Reconstruction.* Physiological Research, 2014. **63**: p. S29-S47.
15. De Vita, D., H. Antell, and S. Giordano, *Effectiveness of intravesical hyaluronic acid with or without chondroitin sulfate for recurrent bacterial*

cystitis in adult women: a meta-analysis. International Urogynecology Journal, 2013. **24**(4): p. 545-552.
16. Nelson, D.E., et al., *Bacterial Communities of the Coronal Sulcus and Distal Urethra of Adolescent Males.* Plos One, 2012. **7**(5).
17. Siddiqui, H., et al., *Assessing diversity of the female urine microbiota by high throughput sequencing of 16S rDNA amplicons.* Bmc Microbiology, 2011. **11**.
18. Whiteside, S.A., et al., *The microbiome of the urinary tract-a role beyond infection.* Nature Reviews Urology, 2015. **12**(2): p. 81-90.
19. Delley, M., et al., *In vitro activity of commercial probiotic Lactobacillus strains against uropathogenic Escherichia coli.* Fems Microbiology Letters, 2015. **362**(13).
20. Liu, F.P., et al., *Characterization of the urinary microbiota of elderly women and the effects of type 2 diabetes and urinary tract infections on the microbiota.* Oncotarget, 2017. **8**(59): p. 100678-100690.
21. Ackerman, A.L. and D.M. Underhill, *The mycobiome of the human urinary tract: potential roles for fungi in urology.* Annals of Translational Medicine, 2017. **5**(2).
22. Foxman, B., *The epidemiology of urinary tract infection.* Nature Reviews Urology, 2010. **7**(12): p. 653-660.
23. Kawashima, A., et al., *Imaging of urethral disease: A pictorial review.* Radiographics, 2004. **24**: p. S195-S216.
24. Dason, S., J.T. Dason, and A. Kapoor, *Guidelines for the diagnosis and management of recurrent urinary tract infection in women.* Cuaj-Canadian Urological Association Journal, 2011. **5**(5): p. 316-322.
25. Dielubanza, E.J. and A.J. Schaeffer, *Urinary Tract Infections in Women.* Medical Clinics of North America, 2011. **95**(1): p. 27-+.
26. Ramakrishnan, K. and D.C. Scheid, *Diagnosis and management of acute pyelonephritis in adults.* American Family Physician, 2005. **71**(5): p. 933-942.
27. Lane, M.C., et al., *Expression of flagella is coincident with uropathogenic Escherichia coli ascension to the upper urinary tract.* Proceedings of the National Academy of Sciences of the United States of America, 2007. **104**(42): p. 16669-16674.
28. Flores-Mireles, A.L., et al., *Urinary tract infections: epidemiology, mechanisms of infection and treatment options.* Nature Reviews Microbiology, 2015. **13**(5): p. 269-284.
29. Robino, L., et al., *Intracellular Bacteria in the Pathogenesis of Escherichia coli Urinary Tract Infection in Children.* Clinical Infectious Diseases, 2014. **59**(11): p. E158-E164.
30. Rosen, D.A., et al., *Detection of intracellular bacterial communities in human urinary tract infection.* Plos Medicine, 2007. **4**(12): p. 1949-1958.
31. Farrell, D.J., et al., *A UK Multicentre study of the antimicrobial susceptibility of bacterial pathogens causing urinary tract infection.* Journal of Infection, 2003. **46**(2): p. 94-100.
32. Bergman, D.A., et al., *Practice parameter: The diagnosis, treatment, and evaluation of the initial urinary tract infection in febrile infants and young children.* Pediatrics, 1999. **103**(4): p. 843-852.

33. McMurdo, M.E.T., et al., *Cranberry or trimethoprim for the prevention of recurrent urinary tract infections? A randomized controlled trial in older women.* Journal of Antimicrobial Chemotherapy, 2009. **63**(2): p. 389-395.
34. Gupta, K., T.M. Hooton, and W.E. Stamm, *Increasing antimicrobial resistance and the management of uncomplicated community-acquired urinary tract infections.* Annals of Internal Medicine, 2001. **135**(1): p. 41-50.
35. Davies, S.C., *Reducing inappropriate prescribing of antibiotics in English primary care: evidence and outlook.* Journal of Antimicrobial Chemotherapy, 2018. **73**(4): p. 833-834.
36. Achkar, J.M. and B.C. Fries, *Candida Infections of the Genitourinary Tract.* Clinical Microbiology Reviews, 2010. **23**(2): p. 253-273.
37. Martins, N., et al., *Candidiasis: Predisposing Factors, Prevention, Diagnosis and Alternative Treatment.* Mycopathologia, 2014. **177**(5-6): p. 223-240.
38. Achkar, J.M. and B.C. Fries, *Candida infections of the genitourinary tract.* Clin Microbiol Rev, 2010. **23**(2): p. 253-73.
39. Kaper, J.B., J.P. Nataro, and H.L.T. Mobley, *Pathogenic Escherichia coli.* Nature Reviews Microbiology, 2004. **2**(2): p. 123-140.
40. Ali, A.S.M., et al., *Targeting Deficiencies in the TLR5 Mediated Vaginal Response to Treat Female Recurrent Urinary Tract Infection.* Scientific Reports, 2017. **7**.
41. Ali, A.S.M., et al., *Maintaining a Sterile Urinary Tract: The Role of Antimicrobial Peptides.* Journal of Urology, 2009. **182**(1): p. 21-28.
42. Engel, D., et al., *Tumor necrosis factor alpha- and inducible nitric oxide synthase-producing dendritic cells are rapidly recruited to the bladder in urinary tract infection but are dispensable for bacterial clearance.* Infection and Immunity, 2006. **74**(11): p. 6100-6107.
43. Engel, D.R., et al., *CCR2 mediates homeostatic and inflammatory release of Gr1(high) monocytes from the bone marrow, but is dispensable for bladder infiltration in bacterial urinary tract infection.* Journal of Immunology, 2008. **181**(8): p. 5579-5586.
44. Haraoka, M., et al., *Neutrophil recruitment and resistance to urinary tract infection.* Journal of Infectious Diseases, 1999. **180**(4): p. 1220-1229.
45. Schiwon, M., et al., *Crosstalk between Sentinel and Helper Macrophages Permits Neutrophil Migration into Infected Uroepithelium.* Cell, 2014. **156**(3): p. 456-468.
46. Schroeder, B.O., et al., *Reduction of disulphide bonds unmasks potent antimicrobial activity of human beta-defensin 1.* Nature, 2011. **469**(7330): p. 419-+.
47. Huang, G.T.J., et al., *A model for antimicrobial gene therapy: Demonstration of human beta-defensin 2 antimicrobial activities in vivo.* Human Gene Therapy, 2002. **13**(17): p. 2017-2025.
48. Joly, S., et al., *Human beta-defensins 2 and 3 demonstrate strain-selective activity against oral microorganisms.* Journal of Clinical Microbiology, 2004. **42**(3): p. 1024-1029.
49. Silva, P.M., S. Goncalves, and N.C. Santos, *Defensins: antifungal lessons from eukaryotes.* Frontiers in Microbiology, 2014. **5**.

50. Raj, P.A. and A.R. Dentino, *Current status of defensins and their role in innate and adaptive immunity.* Fems Microbiology Letters, 2002. **206**(1): p. 9-18.
51. Sahl, H.G., et al., *Mammalian defensins: structures and mechanism of antibiotic activity.* Journal of Leukocyte Biology, 2005. **77**(4): p. 466-475.
52. Schneider, J.J., et al., *Human defensins.* Journal of Molecular Medicine-Jmm, 2005. **83**(8): p. 587-595.
53. Pazgier, M., et al., *Human beta-defensins.* Cellular and Molecular Life Sciences, 2006. **63**(11): p. 1294-1313.
54. Ali, A.S.M., et al., *Release of the anti-microbial peptide beta-defensin 2 protects against attack by flagellated Escherichia coli in human urothelium.* European Urology Supplements, 2012. **11**(1): p. E183-U595.
55. Ali, A.S.M., et al., *Reduced innate beta-defensin-2 response in the bladder and vaginal epithelia increases suceptibility to flagellated E. coli infection.* Bju International, 2012. **109**: p. 44-44.
56. Ganz, T., *Defensins: Antimicrobial peptides of innate immunity.* Nature Reviews Immunology, 2003. **3**(9): p. 710-720.
57. Flo, T.H., et al., *Lipocalin 2 mediates an innate immune response to bacterial infection by sequestrating iron.* Nature, 2004. **432**(7019): p. 917-921.
58. Faraldo-Gomez, J.D. and M.S.P. Sansom, *Acquisition of siderophores in Gram-negative bacteria.* Nature Reviews Molecular Cell Biology, 2003. **4**(2): p. 105-116.
59. Ferreira, M.C., et al., *Interleukin-17-Induced Protein Lipocalin 2 Is Dispensable for Immunity to Oral Candidiasis.* Infection and Immunity, 2014. **82**(3): p. 1030-1035.
60. Saemann, M.D., W.H. Horl, and T. Weichhart, *Uncovering host defences in the urinary tract: cathelicidin and beyond.* Nephrology Dialysis Transplantation, 2007. **22**(2): p. 347-349.
61. Lopez-Garcia, B., et al., *Anti-fungal activity of cathelicidins and their potential role in Candida albicans skin infection.* Journal of Investigative Dermatology, 2005. **125**(1): p. 108-115.
62. Benincasa, M., et al., *Fungicidal activity of five cathelicidin peptides against clinically isolated yeasts.* Journal of Antimicrobial Chemotherapy, 2006. **58**(5): p. 950-959.
63. Xhindoli, D., et al., *The human cathelicidin LL-37 A pore-forming antibacterial peptide and host-cell modulator.* Biochimica Et Biophysica Acta-Biomembranes, 2016. **1858**(3): p. 546-566.
64. Ray, S., H.P.S. Dhaked, and D. Panda, *Antimicrobial Peptide CRAMP (16-33) Stalls Bacterial Cytokinesis by Inhibiting FtsZ Assembly.* Biochemistry, 2014. **53**(41): p. 6426-6429.
65. Y., L.E., L.M. W., and W.G. C.L., *Modulation of toll-like receptor signaling by antimicrobial peptides*. 2018, Semin Cell Dev Biol.
66. Chromek, M., et al., *The antimicrobial peptide cathelicidin protects the urinary tract against invasive bacterial infection.* Nature Medicine, 2006. **12**(6): p. 636-641.
67. Zasloff, M., *The antibacterial shield of the human urinary tract.* Kidney International, 2013. **83**(4): p. 548-550.

68. Huang, Y.C., et al., *The flexible and clustered lysine residues of human ribonuclease 7 are critical for membrane permeability and antimicrobial activity.* Journal of Biological Chemistry, 2007. **282**(7): p. 4626-4633.
69. Rosenberg, H.F., *RNase A ribonucleases and host defense: an evolving story.* Journal of Leukocyte Biology, 2008. **83**(5): p. 1079-1087.
70. Pak, J., et al., *Tamm-Horsfall protein binds to type 1 fimbriated Escherichia coli and prevents E. coli from binding to uroplakin Ia and Ib receptors.* Journal of Biological Chemistry, 2001. **276**(13): p. 9924-9930.
71. Takeuchi, O. and S. Akira, *Pattern Recognition Receptors and Inflammation.* Cell, 2010. **140**(6): p. 805-820.
72. Backhed, F., et al., *Induction of innate immune responses by Escherichia coli and purified lipopolysaccharide correlate with organ- and cell-specific expression of Toll-like receptors within the human urinary tract.* Cellular Microbiology, 2001. **3**(3): p. 153-158.
73. Thompson, M.R., et al., *Pattern Recognition Receptors and the Innate Immune Response to Viral Infection.* Viruses-Basel, 2011. **3**(6): p. 920-940.
74. Siednienko, J. and S.M. Miggin, *Expression analysis of the Toll-like receptors in human peripheral blood mononuclear cells.* Methods in molecular biology (Clifton, N.J.), 2009. **517**: p. 3-14.
75. Kawasaki, T. and T. Kawai, *Toll-like receptor signaling pathways.* Frontiers in Immunology, 2014. **5**.
76. Jin, M.S., et al., *Crystal structure of the TLR1-TLR2 heterodimer induced by binding of a tri-acylated lipopeptide.* Cell, 2007. **130**(6): p. 1071-1082.
77. Kang, J.Y., et al., *Recognition of Lipopeptide Patterns by Toll-like Receptor 2-Toll-like Receptor 6 Heterodimer.* Immunity, 2009. **31**(6): p. 873-884.
78. Zhou, K., et al., *Toll-like receptor 5 forms asymmetric dimers in the absence of flagellin.* Journal of Structural Biology, 2012. **177**(2): p. 402-409.
79. Yoon, S.I., et al., *Structural Basis of TLR5-Flagellin Recognition and Signaling.* Science, 2012. **335**(6070): p. 859-864.
80. Ashkar, A.A., et al., *FimH Adhesin of Type 1 Fimbriae Is a Potent Inducer of Innate Antimicrobial Responses Which Requires TLR4 and Type 1 Interferon Signalling.* Plos Pathogens, 2008. **4**(12).
81. Schilling, J.D., et al., *Bacterial invasion augments epithelial cytokine responses to Escherichia coli through a lipopolysaccharide-dependent mechanism.* Journal of Immunology, 2001. **166**(2): p. 1148-1155.
82. Song, J.M., et al., *TLR4-Initiated and cAMP-Mediated abrogation of bacterial invasion of the bladder.* Cell Host & Microbe, 2007. **1**(4): p. 287-298.
83. Lanz, M., *Investigations of the Innate Immune Defences in the Urogenital Tract*. 2013, Newcastle University.
84. Smith, N.J., et al., *Toll-Like Receptor Responses of Normal Human Urothelial Cells to Bacterial Flagellin and Lipopolysaccharide.* Journal of Urology, 2011. **186**(3): p. 1084-1092.
85. Hawn, T.R., et al., *A common dominant TLR5 stop codon polymorphism abolishes flagellin signaling and is associated with susceptibility to legionnaires' disease.* Journal of Experimental Medicine, 2003. **198**(10): p. 1563-1572.
86. Hawn, T.R., et al., *Toll-Like Receptor Polymorphisms and Susceptibility to Urinary Tract Infections in Adult Women.* Plos One, 2009. **4**(6).

87. Hardison, S.E. and G.D. Brown, *C-type lectin receptors orchestrate antifungal immunity.* Nature Immunology, 2012. **13**(9): p. 817-822.
88. InvivoGen. *C-Type Lectin Receptors Review*. 2012 [cited 2015 19 Jul]; Available from: http://www.invivogen.com/review-clr.
89. Rand, T.G., et al., *Dectin-1 and inflammation-associated gene transcription and expression in mouse lungs by a toxic (1,3)-beta-d glucan.* Archives of Toxicology, 2010. **84**(3): p. 205-220.
90. Li, C., et al., *Expression of dectin-1 during fungus infection in human corneal epithelial cells.* International Journal of Ophthalmology, 2014. **7**(1): p. 34-37.
91. Cohen-Kedar, S., et al., *Human intestinal epithelial cells respond to beta-glucans via Dectin-1 and Syk.* European Journal of Immunology, 2014. **44**(12): p. 3729-3740.
92. Kerscher, B., J.A. Willment, and G.D. Brown, *The Dectin-2 family of C-type lectin-like receptors: an update.* International Immunology, 2013. **25**(5): p. 271-277.
93. Behler, F., et al., *Macrophage-Inducible C-Type Lectin Mincle-Expressing Dendritic Cells Contribute to Control of Splenic Mycobacterium bovis BCG Infection in Mice.* Infection and Immunity, 2015. **83**(1): p. 184-196.
94. Garcia-Vallejo, J.J. and Y. van Kooyk, *The physiological role of DC-SIGN: A tale of mice and men.* Trends in Immunology, 2013. **34**(10): p. 482-486.
95. Gringhuis, S.I., et al., *C-type lectin DC-SIGN modulates toll-like receptor signaling via Raf-1 kinase-dependent acetylation of transcription factor NF-kappa B.* Immunity, 2007. **26**(5): p. 605-616.
96. Drickamer, K. and M.E. Taylor, *Recent insights into structures and functions of C-type lectins in the immune system.* Current Opinion in Structural Biology, 2015. **34**: p. 26-34.
97. Kerrigan, A.M. and G.D. Brown, *Syk-coupled C-type lectin receptors that mediate cellular activation via single tyrosine based activation motifs.* Immunological Reviews, 2010. **234**: p. 335-352.
98. Brown, G.D. and S. Gordon, *Immune recognition - A new receptor for beta-glucans.* Nature, 2001. **413**(6851): p. 36-37.
99. Hermanz-Falcon, P., et al., *Cloning of human DECTIN-1, a novel C-type lectin-like receptor gene expressed on dendritic cells.* Immunogenetics, 2001. **53**(4): p. 288-95.
100. Yokota, K., et al., *Identification of a human homologue of the dendritic cell-associated C-type lectin-1, dectin-1.* Gene, 2001. **272**(1-2): p. 51-60.
101. Heinsbroek, S.E.M., et al., *Expression of functionally different dectin-1 isoforms by murine macrophages.* Journal of Immunology, 2006. **176**(9): p. 5513-5518.
102. Willment, J.A., S. Gordon, and G.D. Brown, *Characterization of the human beta-glucan receptor and its alternatively spliced isoforms.* Journal of Biological Chemistry, 2001. **276**(47): p. 43818-43823.
103. Gantner, B.N., et al., *Collaborative induction of inflammatory responses by dectin-1 and toll-like receptor 2.* Journal of Experimental Medicine, 2003. **197**(9): p. 1107-1117.
104. Brown, G.D., et al., *Dectin-1 mediates the biological effects of beta-glucans.* Journal of Experimental Medicine, 2003. **197**(9): p. 1119-1124.

105. Rogers, N.C., et al., *Syk-dependent cytokine induction by Dectin-1 reveals a novel pattern recognition pathway for C type lectins.* Immunity, 2005. **22**(4): p. 507-517.
106. Steele, C., et al., *Alveolar macrophage-mediated killing of Pneumocystis carinii f. sp muris involves molecular recognition by the dectin-1 beta-glucan receptor.* Journal of Experimental Medicine, 2003. **198**(11): p. 1677-1688.
107. Plato, A., J.A. Willment, and G.D. Brown, *C-Type Lectin-Like Receptors of the Dectin-1 Cluster: Ligands and Signaling Pathways.* International Reviews of Immunology, 2013. **32**(2): p. 134-156.
108. Sun, S.C., *The noncanonical NF-kappa B pathway.* Immunological Reviews, 2012. **246**: p. 125-140.
109. McAllister-Lucas, L.M., M. Baens, and P.C. Lucas, *MALT1 Protease: A New Therapeutic Target in B Lymphoma and Beyond?* Clinical Cancer Research, 2011. **17**(21): p. 6623-6631.
110. Goodridge, H.S., R.M. Simmons, and D.M. Underhill, *Dectin-1 stimulation by Candida albicans yeast or zymosan triggers NFAT activation in macrophages and dendritic cells.* Journal of Immunology, 2007. **178**(5): p. 3107-3115.
111. Gringhuis, S.I., et al., *Dectin-1 directs T helper cell differentiation by controlling noncanonical NF-kappa B activation through Raf-1 and Syk.* Nature Immunology, 2009. **10**(2): p. 203-213.
112. Schmitz, M.L., et al., *Signal integration, crosstalk mechanisms and networks in the function of inflammatory cytokines.* Biochimica Et Biophysica Acta-Molecular Cell Research, 2011. **1813**(12): p. 2165-2175.
113. Yadav, M. and J.S. Schorey, *The beta-glucan receptor dectin-1 functions together with TLR2 to mediate macrophage activation by mycobacteria.* Blood, 2006. **108**(9): p. 3168-3175.
114. Netea, M.G., et al., *Immune sensing of Candida albicans requires cooperative recognition of mannans and glucans by lectin and Toll-like receptors.* Journal of Clinical Investigation, 2006. **116**(6): p. 1642-1650.
115. Chang, J., B.M. Kim, and C.-H. Chang, *Co-stimulation of TLR4 and Dectin-1 Induces the Production of Inflammatory Cytokines but not TGF-beta for Th17 Cell Differentiation.* Immune network, 2014. **14**(1): p. 30-7.
116. Ferwerda, G., et al., *Dectin-1 synergizes with TLR2 and TLR4 for cytokine production in human primary monocytes and macrophages.* Cellular Microbiology, 2008. **10**(10): p. 2058-2066.
117. Suchenko, A., *The Dectin-1 Receptor in the Urogenital Tract*. 2015, Newcastle University. p. 52.
118. Yoon, S.-i., et al., *Structural Basis of TLR5-Flagellin Recognition and Signaling.* Science, 2012. **335**(6070): p. 859-864.
119. Booth, C., et al., *Stromal and vascular invasion in an human in vitro bladder cancer model.* Laboratory Investigation, 1997. **76**(6): p. 843-857.
120. Romagnolo, A.G., et al., *Role of Dectin-1 receptor on cytokine production by human monocytes challenged with Paracoccidioides brasiliensis.* Mycoses, 2018. **61**(4): p. 222-230.
121. Abel, G. and J.K. Czop, *STIMULATION OF HUMAN MONOCYTE BETA-GLUCAN RECEPTORS BY GLUCAN PARTICLES INDUCES PRODUCTION OF*

TNF-ALPHA AND IL-1-BETA. International Journal of Immunopharmacology, 1992. **14**(8): p. 1363-&.
122. Au, B.T., T.J. Williams, and P.D. Collins, *ZYMOSAN-INDUCED IL-8 RELEASE FROM HUMAN NEUTROPHILS INVOLVES ACTIVATION VIA THE CD11B/CD18 RECEPTOR AND ENDOGENOUS PLATELET-ACTIVATING-FACTOR AS AN AUTOCRINE MODULATOR.* Journal of Immunology, 1994. **152**(11): p. 5411-5419.
123. Pivarcsi, A., et al., *Microbial compounds induce the expression of pro-inflammatory cytokines, chemokines and human beta-defensin-2 in vaginal epithelial cells.* Microbes and Infection, 2005. **7**(9-10): p. 1117-1127.
124. Noss, I., et al., *Comparison of the potency of a variety of beta-glucans to induce cytokine production in human whole blood.* Innate Immunity, 2013. **19**(1): p. 10-19.
125. Ali, M.F., et al., *beta-Glucan-Activated Human B Lymphocytes Participate in Innate Immune Responses by Releasing Proinflammatory Cytokines and Stimulating Neutrophil Chemotaxis.* Journal of Immunology, 2015. **195**(11): p. 5318-5326.
126. Hoover, D.M., et al., *The structure of human beta-defensin-2 shows evidence of higher order oligomerization.* Journal of Biological Chemistry, 2000. **275**(42): p. 32911-32918.
127. Zhao, Y.H., et al., *Dectin-1-activated dendritic cells trigger potent antitumour immunity through the induction of Th9 cells.* Nature Communications, 2016. **7**.
128. Esteban, A., et al., *Fungal recognition is mediated by the association of dectin-1 and galectin-3 in macrophages.* Proceedings of the National Academy of Sciences of the United States of America, 2011. **108**(34): p. 14270-14275.
129. Loures, F.V., et al., *TLR-4 cooperates with Dectin-1 and mannose receptor to expand Th17 and Tc17 cells induced by Paracoccidioides brasiliensis stimulated dendritic cells.* Frontiers in Microbiology, 2015. **6**.
130. Sun, W.K., et al., *Dectin-1 is inducible and plays a crucial role in Aspergillus-induced innate immune responses in human bronchial epithelial cells.* European Journal of Clinical Microbiology & Infectious Diseases, 2012. **31**(10): p. 2755-2764.
131. Kolar, S.S., H. Baidouri, and A.M. McDermott, *Role of Pattern Recognition Receptors in the Modulation of Antimicrobial Peptide Expression in the Corneal Epithelial Innate Response to F. solani.* Investigative Ophthalmology & Visual Science, 2017. **58**(5): p. 3463-3472.
132. Ariizumi, K., et al., *Identification of a novel, dendritic cell-associated molecule, dectin-1, by subtractive cDNA cloning.* Journal of Biological Chemistry, 2000. **275**(26): p. 20157-20167.
133. Kim, J., et al., *Human beta-defensin 2 plays a regulatory role in innate antiviral immunity and is capable of potentiating the induction of antigen-specific immunity.* Virology Journal, 2018. **15**.
134. Rohrl, J., et al., *Human beta-Defensin 2 and 3 and Their Mouse Orthologs Induce Chemotaxis through Interaction with CCR2.* Journal of Immunology, 2010. **184**(12): p. 6688-6694.
135. Bondeson, J., et al., *Selective regulation of cytokine induction by adenoviral gene transfer of I kappa B alpha into human macrophages:*

Lipopolysaccharide-induced, but not zymosan-induced, proinflammatory cytokines are inhibited, but IL-10 is nuclear Factor-kappa B independent. Journal of Immunology, 1999. **162**(5): p. 2939-2945.
136. Friedland, J.S., et al., *Regulation of interleukin-8 gene expression after phagocytosis of zymosan by human monocytic cells.* Journal of Leukocyte Biology, 2001. **70**(3): p. 447-454.
137. Malik, P., et al., *Zymosan-mediated inflammation impairs in vivo reverse cholesterol transport.* Journal of Lipid Research, 2011. **52**(5): p. 951-957.
138. Dillon, S., et al., *Yeast zymosan, a stimulus for TLR2 and dectin-1, induces regulatory antigen-presenting cells and immunological tolerance.* Journal of Clinical Investigation, 2006. **116**(4): p. 916-928.
139. Kataoka, K., et al., *Activation of macrophages by linear (1 -> 3)-beta-D-glucans - Implications for the recognition of fungi by innate immunity.* Journal of Biological Chemistry, 2002. **277**(39): p. 36825-36831.
140. Mueller, A., et al., *The influence of glucan polymer structure and solution conformation on binding to (1 -> 3)-beta-D-glucan receptors in a human monocyte-like cell line.* Glycobiology, 2000. **10**(4): p. 339-346.
141. Min, L., et al., *Synergism between Curdlan and GM-CSF Confers a Strong Inflammatory Signature to Dendritic Cells.* Journal of Immunology, 2012. **188**(4): p. 1789-1798.
142. Takeuchi, O., et al., *Differential roles of TLR2 and TLR4 in recognition of gram-negative and gram-positive bacterial cell wall components.* Immunity, 1999. **11**(4): p. 443-451.
143. Shin, D.-M., et al., *Mycobacterium abscessus activates the macrophage innate immune response via a physical and functional interaction between TLR2 and dectin-1.* Cellular Microbiology, 2008. **10**(8): p. 1608-1621.
144. Andersen-Nissen, E., et al., *A conserved surface on Toll-like receptor 5 recognizes bacterial flagellin.* Journal of Experimental Medicine, 2007. **204**(2): p. 393-403.
145. Gauthier, T., et al., *Proximity Ligation In situ Assay is a Powerful Tool to Monitor Specific ATG Protein Interactions following Autophagy Induction.* Plos One, 2015. **10**(6).
146. Hayashi, F., et al., *The innate immune response to bacterial flagellin is mediated by Toll-like receptor 5.* Nature, 2001. **410**(6832): p. 1099-1103.
147. Gewirtz, A.T., et al., *Cutting edge: Bacterial flagellin activates basolaterally expressed TLR5 to induce epithelial proinflammatory gene expression.* Journal of Immunology, 2001. **167**(4): p. 1882-1885.
148. Tallant, T., et al., *Flagellin acting via TLR5 is the major-activator of key signaling pathways leading to NF-kappa B and proinflammatory gene program activation in intestinal epithelial cells.* Bmc Microbiology, 2004. **4**.
149. Liu, X.W., et al., *Flagellin-induced expression of CXCL10 mediates direct fungal killing and recruitment of NK cells to the cornea in response to Candida albicans infection.* European Journal of Immunology, 2014. **44**(9): p. 2667-2679.
150. Kojima, K., et al., *Human conjunctival epithelial cells express functional Toll-like receptor 5.* British Journal of Ophthalmology, 2008. **92**(3): p. 411-416.
151. Yamada, K., et al., *Upregulation of Toll-like receptor 5 expression in the conjunctival epithelium of various human ocular surface diseases.* British Journal of Ophthalmology, 2014. **98**(8): p. 1116-1119.

152. Liu, Y., et al., *The role of Syk signaling in antifungal innate immunity of human corneal epithelial cells.* Bmc Ophthalmology, 2015. **15**.
153. Ernst, K.R.O., et al., *Toll like receptor 5 (TLR5) may be involved in the immunological response to Aspergillus fumigatus in vitro.* Medical Mycology, 2011. **49**(4): p. 375-379.
154. Yang, C.X., et al., *The High and Low Molecular Weight Forms of Hyaluronan Have Distinct Effects on CD44 Clustering.* Journal of Biological Chemistry, 2012. **287**(51): p. 43094-43107.
155. Mowbray, C.A., et al., *High molecular weight hyaluronic acid: a two-pronged protectant against infection of the urogenital tract?* Clinical & Translational Immunology, 2018. **7**(6).
156. Wheeler, R.T., et al., *Dynamic, Morphotype-Specific Candida albicans beta-Glucan Exposure during Infection and Drug Treatment.* Plos Pathogens, 2008. **4**(12).
157. Lanz, M., *Innate Host Defence in the Urinary Tract*. 2010.
158. Ferwerda, B., et al., *Human Dectin-1 Deficiency and Mucocutaneous Fungal Infections.* New England Journal of Medicine, 2009. **361**(18): p. 1760-1767.
159. Rosentul, D.C., et al., *Genetic Variation in the Dectin-1/CARD9 Recognition Pathway and Susceptibility to Candidemia.* Journal of Infectious Diseases, 2011. **204**(7): p. 1138-1145.
160. Taylor, P.R., et al., *Dectin-1 is required for beta-glucan recognition and control of fungal infection.* Nature Immunology, 2007. **8**(1): p. 31-38.
161. Saijo, S., et al., *Dectin-1 is required for host defense against Pneumocystis carinii but not against Candida albicans.* Nature Immunology, 2007. **8**(1): p. 39-46.
162. Grube, M., et al., *TLR5 stop codon polymorphism is associated with invasive aspergillosis after allogeneic stem cell transplantation.* Medical Mycology, 2013. **51**(8): p. 818-825.
163. Mizel, S.B., A.P. West, and R.R. Hantgan, *Identification of a sequence in human toll-like receptor 5 required for the binding of Gram-negative flagellin.* Journal of Biological Chemistry, 2003. **278**(26): p. 23624-23629.
164. Xiong, D., et al., *Molecular cloning and functional analysis of duck Toll-like receptor 5.* Research in Veterinary Science, 2014. **97**(1): p. 43-45.
165. Goodridge, H.S., A.J. Wolf, and D.M. Underhill, *beta-glucan recognition by the innate immune system.* Immunological Reviews, 2009. **230**: p. 38-50.
166. Reid, D.M., N.A.R. Gow, and G.D. Brown, *Pattern recognition: recent insights from Dectin-1.* Current Opinion in Immunology, 2009. **21**(1): p. 30-37.
167. Seow, C.J., S.C. Chue, and W.S.F. Wong, *Piceatannol, a Syk-selective tyrosine kinase inhibitor, attenuated antigen challenge of guinea pig airways in vitro.* European Journal of Pharmacology, 2002. **443**(1-3): p. 189-196.
168. Mahabeleshwar, G.H. and G.C. Kundu, *Syk, a protein-tyrosine kinase, suppresses the cell motility and nuclear factor kappa B-mediated secretion of urokinase type plasminogen activator by inhibiting the phosphatidylinositol 3'-kinase activity in breast cancer cells.* Journal of Biological Chemistry, 2003. **278**(8): p. 6209-6221.
169. Bijli, K.M., et al., *Activation of Syk by protein kinase C-delta regulates thrombin-induced intercellular adhesion molecule-1 expression in*

endothelial cells via tyrosine phosphorylation of RelA/p65. Journal of Biological Chemistry, 2008. **283**(21): p. 14674-14684.
170. Lee, C.K., et al., *Syk contributes to PDGF-BB-mediated migration of rat aortic smooth muscle cells via MAPK pathways.* Cardiovascular Research, 2007. **74**(1): p. 159-168.
171. Naldi, A., et al., *Reconstruction and signal propagation analysis of the Syk signaling network in breast cancer cells.* Plos Computational Biology, 2017. **13**(3).
172. Siebenlist, U., G. Franzoso, and K. Brown, *STRUCTURE, REGULATION AND FUNCTION OF NF-KAPPA-B.* Annual Review of Cell Biology, 1994. **10**: p. 405-455.
173. Baeuerle, P.A. and T. Henkel, *FUNCTION AMD ACTIVATION OF NF-KAPPA-B IN THE IMMUNE-SYSTEM.* Annual Review of Immunology, 1994. **12**: p. 141-179.
174. Chen, Z.J., et al., *SIGNAL-INDUCED SITE-SPECIFIC PHOSPHORYLATION TARGETS I-KAPPA-B-ALPHA TO THE UBIQUITIN-PROTEASOME PATHWAY.* Genes & Development, 1995. **9**(13): p. 1586-1597.
175. Scherer, D.C., et al., *SIGNAL-INDUCED DEGRADATION OF I-KAPPA-B-ALPHA REQUIRES SITE-SPECIFIC UBIQUITINATION.* Proceedings of the National Academy of Sciences of the United States of America, 1995. **92**(24): p. 11259-11263.
176. Simon, R. and C.E. Samuel, *Activation of NF-kappa B-dependent gene expression by Salmonella flagellins FliC and FljB.* Biochemical and Biophysical Research Communications, 2007. **355**(1): p. 280-285.
177. Ifrim, D.C., et al., *Candida albicans Primes TLR Cytokine Responses through a Dectin-1/Raf-1-Mediated Pathway.* Journal of Immunology, 2013. **190**(8): p. 4129-4135.
178. Trinath, J., et al., *The WNT Signaling Pathway Contributes to Dectin-1-Dependent Inhibition of Toll-Like Receptor-Induced Inflammatory Signature.* Molecular and Cellular Biology, 2014. **34**(23): p. 4301-4314.
179. Zhu, C.C., et al., *Dectin-1 agonist curdlan modulates innate immunity to Aspergillus fumigatus in human corneal epithelial cells.* International Journal of Ophthalmology, 2015. **8**(4): p. 690-696.
180. Dennehy, K.M., et al., *Syk kinase is required for collaborative cytokine production induced through Dectin-1 and Toll-like receptors.* European Journal of Immunology, 2008. **38**(2): p. 500-506.
181. Triantafilou, M., et al., *Membrane sorting of toll-like receptor (TLR)-2/6 and TLR2/1 heterodimers at the cell surface determines heterotypic associations with CD36 and intracellular targeting.* Journal of Biological Chemistry, 2006. **281**(41): p. 31002-31011.
182. Goodridge, H.S., et al., *Activation of the innate immune receptor Dectin-1 upon formation of a 'phagocytic synapse'.* Nature, 2011. **472**(7344): p. 471-U541.
183. Ma, Y.Q., et al., *An intermolecular FRET sensor detects the dynamics of T cell receptor clustering.* Nature Communications, 2017. **8**.
184. Care, B.R. and H.A. Soula, *Impact of receptor clustering on ligand binding.* Bmc Systems Biology, 2011. **5**.
185. Zhang, J.X., et al., *ROS and ROS-Mediated Cellular Signaling.* Oxidative Medicine and Cellular Longevity, 2016.